การกระตุ้นพันธะคาร์บอน-ไฮโดรเจนของโพรเพนบนตัวเร่งปฏิกิริยาโครเมียมแบบวิวิธพันธ์กัมมันต์เดี่ยว

(C-H activation of propane over
heterogeneous single-site chromium catalyst)

นายศุภณัฐ เกตานิรุจน์
Supanut Ketanirut

วิทยานิพนธ์นี้เป็นส่วนหนึ่งของการศึกษาตามหลักสูตร
ปริญญา วิทยาศาสตรมหาบัณฑิต สาขาวิชา ปิโตรเคมีและเคมีของไฮโดรคาร์บอน
ภาควิชาเคมี คณะวิทยาศาสตร์
สถาบันเทคโนโลยีพระจอมเกล้าเจ้าคุณทหารลาดกระบัง
พ.ศ.2560
KMITL-2017-SC-M-015-011

C-H ACTIVATION OF PROPANE OVER HETEROGENEOUS SINGLE-SITE CHROMIUM CATALYST

SUPANUT KETANIRUT

A THESIS SUBMITTED IN PARTIAL FULFILLMENT OF THE REQUIREMENT FOR THE DEGREE OF MASTER OF SCIENCE IN PETROCHEMICALS AND HYDROCARBON CHEMISTRY

DEPARTMENT OF CHEMISTRY

FACULTY OF SCIENCE

KING MONGKUT'S INSTITUTE OF TECHNOLOGY LADKRABANG

2017

KMITL-2017-SC-M-015-011

หัวข้อวิทยานิพนธ์	การกระตุ้นพันธะคาร์บอน-ไฮโดรเจนของโพรเพนโดยใช้ตัวเร่งปฏิกิริยาโครเมียมแบบวิวิธพันธ์กัมมันต์เดี่ยว
ชื่อนักศึกษา	นายศุภณัฐ เกตานิรุจน์
รหัสประจำตัว	58605035
ปริญญา	วิทยาศาสตรมหาบัณฑิต (ปิโตรเคมีและเคมีของไฮโดรคาร์บอน)
ภาควิชา	เคมี
พ.ศ.	2560
อาจารย์ที่ปรึกษาวิทยานิพนธ์	รศ.ดร.ตะวัน สุขน้อย
อาจารย์ที่ปรึกษาวิทยานิพนธ์ร่วม	ดร.กิตติศักดิ์ ชูจันทร์

บทคัดย่อ

กระบวนการขจัดไฮโดรเจนจากโพรเพนไปเป็นโพรพีลีนทางตรง มีความจำเพาะต่อการเลือกเกิดเป็นโพรพีลีนที่สูง อย่างไรก็ตามตัวเร่งปฏิกิริยาที่นิยมใช้ในกระบวนการผลิต โดยทั่วไปผลิตถ่านโค้กในระหว่างการเกิดปฏิกิริยา ส่งผลให้จำนวนของตำแหน่งก่อกัมมันต์ที่ใช้งานลดลงและทำให้เกิดการเสื่อมสภาพของตัวเร่งปฏิกิริยา ดังนั้นเพื่อที่จะลดการเสื่อมสภาพของตัวเร่งปฏิกิริยา ตัวเร่งปฏิกิริยาโลหะบนตัวรองรับแบบวิวิธพันธ์กัมมันต์เดี่ยวจึงเป็นที่น่าสนใจ ดังนั้นงานวิจัยนี้จึงศึกษาปฏิกิริยาการขจัดไฮโดรเจนจากโพรเพนโดยใช้ตัวเร่งปฏิกิริยาโครเมียมแบบวิวิธพันธ์กัมมันต์เดี่ยว โดยเตรียมจากเทคนิคการดูดซับแบบสตรองอิเล็กโตรสแตติกด้วยกรดโครมิก เปรียบเทียบกับเทคนิคการฝังเคลือบแบบเปียกด้วยโครเมียมไนเทรตโนนะไฮเดรต โดยพิสูจน์เอกลักษณ์ของตัวเร่งปฏิกิริยาด้วยเทคนิคการดูดกลืนรังสีเอกซ์ เทคนิคการโปรแกรมอุณหภูมิเพื่อทดสอบการรีดักชันด้วยแก๊สไฮโดรเจน เทคนิคอัลตราไวโอเลตและวิสิเบิลสเปกโทรสโคปีและเทคนิคอินดักทีฟลีคัพเพิลพลาสม่าแมสสเปคโตรสโคปี พบว่าปริมาณโครเมียมแบบวิวิธพันธ์กัมมันต์เดี่ยวเป็นดังนี้ [ADS] Cr/SiO_2 >>> [IM] Cr/SiO_2 1% > [IM] Cr/SiO_2 2% > [IM] Cr/SiO_2 5% > [IM] Cr/SiO_2 10% wt. จากนั้นนำตัวเร่งปฏิกิริยามาทดสอบประสิทธิภาพในเครื่องปฏิกรณ์แบบเบดคงที่ พบว่าค่าความสามารถในการทำปฏิกิริยาของตัวเร่งปฏิกิริยา (TOF) มีความสัมพันธ์โดยตรงกับปริมาณของโครเมียมแบบวิวิธพันธ์กัมมันต์เดี่ยวข้างต้น นอกจากนี้ตัวเร่งปฏิกิริยาโครเมียมแบบวิวิธพันธ์กัมมันต์เดี่ยวมีประสิทธิภาพในการเร่งปฏิกิริยาที่สูงว่าตัวเร่งปฏิกิริยาโคบอลล์แบบวิวิธพันธ์กัมมันต์เดี่ยวสูงถึง 6 เท่า เนื่องจากความเป็นกรดลิวอิส (Lewis acidity) ของโครเมียมไอออน (3+) ที่สูงกว่าโคบอลล์ไอออน (2+)

คำสำคัญ : ตัวเร่งปฏิกิริยาโครเมียมแบบวิวิธพันธ์กัมมันต์เดี่ยว การขจัดไฮโดรเจนจากโพรเพน การแตกพันธะคาร์บอน-ไฮโดรเจน

Thesis Title	C-H activation of propane over heterogeneous single-site chromium catalyst
Student Name	Supanut Ketanirut
Student ID	58605035
Degree	Master of Science (Petrochemicals and hydrocarbon chemistry)
Department	Chemistry
Year	2017
Thesis Advisor	Assoc. Prof. Dr. Tawan Sooknoi
Thesis Co-advisor	Dr. Kittisak Choojun

Abstract

The direct dehydrogenation of propane produces propylene with high selectivity. However, these catalysts generally produce coke during the reaction, which reduces the number of active sites and causes deactivation of the catalyst. In order to reduce the deactivation of catalysts, the concept of heterolytic C-H cleavage by single-site metal on support is introduced. In this research, the dehydrogenation of propane was investigated using single-site Cr/SiO_2 and non-single-site Cr/SiO_2 as a catalyst. The catalysts were prepared by strong electronic adsorption [ADS] and wetness impregnation [IM] using CrO_3 and $Cr(NO_3)_3.9H_2O$ as a precursor, respectively. All catalysts were characterized by X-ray absorption near edge structure (XANES), temperature-programmed reduction (TPR), UV-vis spectroscopy (DR-UV) and inductively coupled plasma mass spectrometry (ICP-MS). The amount of single-site Cr over silica is in the order of; [ADS] Cr/SiO_2 >>> [IM] Cr/SiO_2 1% > [IM] Cr/SiO_2 2% > [IM] Cr/SiO_2 5% > [IM] Cr/SiO_2 10% wt. The catalytic performance was investigated in fixed-bed reactor showing the TOF corresponded to the single-site Cr species. Furthermore, single-site Cr/SiO_2 shows relatively six times higher activity than single-site Co/SiO_2 prepared by a similar method due to the higher Lewis acidity of Cr^{3+} species compared with Co^{2+} species.

Keywords : Chromium, Single-site Catalyst, Propane dehydrogenation, C-H activation.

ACKNOWLEDGEMENTS

The author takes this opportunity to acknowledge advisors Assoc. Prof. Dr. Tawan Sooknoi and Dr. Kittisak Choojun for knowledge in catalysis, skill coaching, helpful suggestion, experimental instrument and encouragement throughout this research. In addition, I would like to sincere appreciate chairperson and committee member, Asst. Prof. Dr. Sutha Sutthiruanwong, Assoc. Prof. Dr. Siriporn Jongpatiwut and Dr. Amnat Permsubscul, repectively, for judgment and valuable comments.

The special thanks to SCG Chemical Company Limited and Thailand Research Fund and by National Research Council of Thailand for financial support. I am appreciated the supports from the Department of Chemistry, Faculty of Science, King Mongkut's Institute of Technology Ladkrabang for the equipment, chemicals and facilities.

I sincerely thank Synchrotron Light Research Institute (Public Organization) and Scientific and Technological Research Equipment Centre, Department of Chemistry, Chulalongkorn University for the characterization of catalyst.

I sincerely thank Mr. Thanakhom Sothaisong for his glassware equipment.

Special appreciation would distribute to a kindness of Catalytic Chemistry Research Unit members for their contribution of ideas and facilities and most importantly their support.

Finally, we deeply appreciate and thank my parent and family for their love and supports.

Mr. Supanut Ketanirut

LIST OF CONTENTS

Page

LIST OF CONTENTS (Continued)

Page

LIST OF CONTENTS (Continued)

Page

LIST OF TABLES

Table Page

LIST OF FIGURES

Figure **Page**

Chapter2

Chapter3

Chapter4

LIST OF FIGURES (Continued)

Figure Page

LIST OF FIGURES (Continued)

Figure Page

LIST OF FIGURES (Continued)

Figure Page

CHAPTER 1
INTRODUCTION

1.1 Motivation

The global demand for light hydrocarbon has been increasing steadily because of their various applications. For instance, propylene is the most demand light hydrocarbons for polymer and fiber productions [1]. Propylene is typically produced from the cracking and pyrolysis from high molecular weight hydrocarbons [2]. Alternative processes are thermal or catalytic dehydrogenation of propane. The catalytic dehydrogenation of propane can be classified in two main processes namely direct and indirect strategy [3]. The indirect strategy, known as oxidative dehydrogenation, usually involved CO, CO_2, O_2 or halogens as an auxiliary component to facile C-H bond activation at relatively low temperature [4]. However, this route competes with the combustion of propane and gives low propylene selectivity [5]. In sharp contrast, the direct dehydrogenation of propane produces propylene with high selectivity. The catalysts for the direct dehydrogenation of propane are mostly metal loaded on various supports [6]. The examples are Cr/Al_2O_3, Cr/ZrO_2, [3], Pt/Al_2O_3 and $Pt\text{-}Sn/Al_2O_3$ [7]. However, these catalysts generally produce coke during the reaction, which reduces the number of active sites and causes deactivation of the catalyst.

In order to reduce the deactivation of catalysts, the idea of single-site metal on support is introduced. The term single-site heterogeneous catalysts is the combination of homogeneous and heterogeneous catalysts leading to highly metal dispersion with the well-define pocket site and resulting the high activity and selectivity. Recently, single-site Co^{2+} [8] and single-site Zn^{2+} [9] on silica heterogeneous catalysts had been reported to activate C-H and H–H bond. They also showed the better activity, high selectivity for propylene and less coke production that leads to higher catalyst stability.

Since chromium shows C-H bond activation [10] and it is considered as an inexpensive metal, we, thus, reason to study the use of single-site Cr on silica support for dehydrogenation of propane. The single-site Cr catalysts will be synthesized by strong electrostatic adsorption (SEA) using chromic acid as a precursor and compared with the wetness impregnation of chromium nitrate nonahydrate on silica support. The catalysts will be characterized by X-ray absorption near edge structure (XANES), Temperature-programmed reduction (TPR), and inductively coupled plasma mass spectrometry (ICP-MS). The catalytic performance will be investigated for the effect of temperature, contact time, method of catalyst preparation on the silica support, on the selectivity, and stability.

1.2 Objectives

1.2.1 To obtain high selectivity of propylene and minimal coke formation form

propane dehydrogenation over single-site Cr heterogeneous catalysts

1.2.2 To understand the reaction pathway for propane dehydrogenation over single-site Cr heterogeneous catalysts

1.2.3 To understand the effect of temperature, contact time, carrier gas and catalyst preparation on silica support

1.2.4 To improve the stability of the prepared catalysts

1.3 Scope of this study

1.3.1 Catalyst preparation by strong electrostatic adsorption methodology preparation single-site Cr heterogeneous on silica support using chromic acid and the wetness impregnation of chromium nitrate nonhydrate on silica support

1.3.2 Characterization of catalysts by X-ray absorption (XAS), X-ray Fluorescence (XRF), Inductively coupled plasma mass spectrometry (ICP-MS), Temperature-programmed reduction (TPR), UV-vis spectroscopy(DR-UV), Thermogravimetic Analysis (TGA) and Surface area analysis

1.3.3 Testing on propane over various catalysts in a continuous fixed-bed reactor

1.3.4 Investigation on the effect of temperature (450, 500, 550, 600 and 650 °C), contact time (10, 21, and 31 g.h/mol), carrier gas (N_2 and H_2), reduction temperature and method of catalyst preparation

1.3.5 Analysis and quantification of gas products by online gas chromatography with flame ionization detector (GC-FID)

1.4 Expected results

New technology for the production of propylene from propane could be obtained. This technology could be an alternative process with the high selectivity of propylene and stability. Moreover, the knowledge of understanding dehydrogenation of propane could be applied to other processes.

CHAPTER 2
LITERATURE REVIEWS AND THEORY

2.1 Propane

2.1.1 Propane production [11]

Propane is a three-carbon alkane with the molecular formula C_3H_8. Propane is produced as a by-product of two processes, natural gas processing and petroleum refining. The processing of natural gas involves the removal of butane, propane, and large amounts of ethane from the raw gas, in order to prevent condensation of these volatiles in natural gas pipelines. Moreover, oil refineries produce some propane as a by-product from cracking petroleum into gasoline or heating oil. Propane is a more reactive paraffin than ethane and methane. This is due to the presence of two secondary hydrogens that could be easily substituted.

2.1.2 Propane application [11]

Propane is primarily used as a chemical intermediate in the production of propylene, which is then used mainly to make polypropylene and adiponitrile, respectively. Both of these are typically used to produce industrial materials, such as, plastic and other synthetic resins. In addition, liquid propane is a selective hydrocarbon solvent used to separate paraffinic constituents in lube oil base stocks from harmful asphaltic materials. It is also a refrigerant for liquefying natural gas and used for the recovery of condensable hydrocarbons from natural gas.

2.2 Propylene Production

Propylene, "the crown prince of petrochemicals", is an important chemical intermediate. Its most consumption is for the production of polypropylene, which is used for making plastic films, synthetic fibers and packing [11]. Currently, the industrial demand for propylene is increasing. The method development of propylene production is of great commercial interest. Normally, propylene can be produced from thermal process and catalytic processes via propane dehydrogenation.

2.2.1 Thermal process [12]

Thermal cracking is a chemical process in which organic molecules are decomposed into lower molecular weight products. For example, the decomposition of propane at 625 °C, the main products of the thermal cracking of propane are propylene, ethylene, methane, and hydrogen [12]. These products may be considered to be formed by two parallel decomposition reactions of propane. Ethane, butenes, butadiene, and aromatics are also formed as the reaction path is shown in **Figure 2.1**.

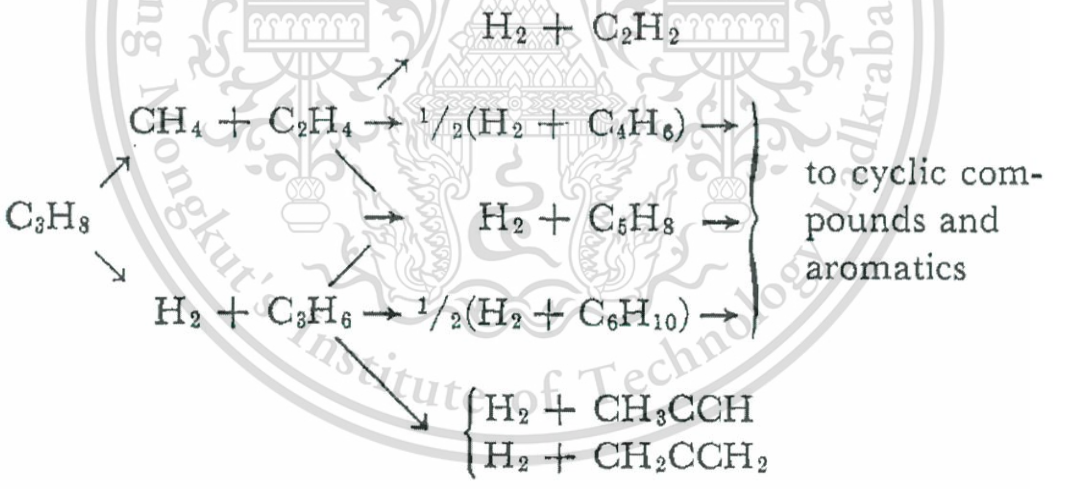

Figure 2.1 Reaction pathways of thermal cracking of propane [12]

2.2.2 Catalytic process [7, 8, 9, 13, 14, 15]

Catalytic cracking is a chemical processes that use a catalyst in chemical reactions to reduce the activation energy resulting the increase of reaction rate. For propane dehydrogenation, mostly these catalysts are considered to be the heterogeneous catalyst.

2.2.2.1 Heterogeneous catalysts [16, 17, 18, 19, 20]

Heterogeneous catalysis involves the use of a catalyst in a different phase from the reactants. Typically, heterogeneous catalysts are solids that react with substrates in a liquid or gaseous reaction mixture. The diverse mechanisms for reactions on surfaces are known, depending on how the adsorption taking place. The dispersion of solid has the important effect on the reaction rate. If diffusion rates are not considered, the reaction rates for various reactions on surfaces depend merely on the rate constants and reactant concentrations. In addition, the total surface area of solid is critical since it determines the availability of catalytic sites. The smaller the catalyst particle size the larger the surface area for a given mass of particle. The advantages of heterogeneous catalysts are easy and inexpensive for catalyst's recovery and good thermal stability. While, the main disadvantages in this catalyst is the selectivity which is depending on multiple active sites.

2.2.2.2 Single-site heterogeneous catalysts [21]

The single-site heterogeneous catalysts are classified as a type of heterogeneous catalysts. However, it also behaves like homogeneous catalyst where the pocket site of the active site can be controlled by the environmentally surrounding on a support. The "single site" (catalytically active center) may consist of one or more atoms. Such single sites are spatially isolated from one another with no other cross-link between such sites. The example of single-site heterogeneous catalyst is a monometallic linked to support by having tetrahedral structure. This catalyst has a discrete active site which is believed to be significant for their low coke formation and greater selectivity to the desired products than those observed over non-single-site heterogeneous catalysts of the similar composition.

For example, the single-site heterogeneous supported on silica catalysts are single-site Fe^{2+} [22], single-site Zr [23], single-site Co^{2+} [8] and single-site Zn^{2+} [9]. The preparation of single-site heterogeneous catalysts typically requires controlled synthetic techniques. Some of them need to use the semi-stable compound as a reactant which requires the inert atmosphere environment. One interesting technique called strong electrostatic adsorption methodology (SEA) is much easier to handle to prepare the single-site heterogeneous catalyst [24].

2.3 Route to Propylene by Catalytic Process

The catalytic dehydrogenation of propane is the commercial method to produce propylene. They have been investigated both indirect and direct conversion of propane.

2.3.1 Oxidative dehydrogenation (Indirect Route)

Oxidative dehydrogenation is a chemical reaction that uses oxygen in reaction. It is an alternative routine to obtain propylene as shown in **Equation 2.1.**

(Equation 2.1)

Propane oxidative dehydrogenation has the advantages of using a low temperature during the process. The catalysts in this reaction are metal oxide, such as, NbO_x/CeO_2 [25], VO_x/γ-Al_2O_3 [26] and Cr_xO_x/SiO_2 [5]. For example, Sameer's group reports the use of VO_x/γ-Al_2O_3 catalyst for propane oxidative dehydrogenation. They showed low conversion (11.73%) at low temperature (475 °C) [26]. The main drawback of producing propylene from oxidative dehydrogenation of propane is low propylene selectivity and it produces significant amounts of CO_x and H_2O. Thus, it is not favorable for industry point of view.

2.3.2 Dehydrogenation (Direct Route)

This process requires the removal of the H_2 as a by-product to increase the yield of propylene. The general catalysts are noble metal catalysts. Due to the excellent activity, selectivity and stability, noble metals, such as, Palladium (Pd), Platinum (Pt), Gold (Au) , and Ruthenium (Ru) are used as catalysts in many heterogeneous catalytic reactions. However, these noble metals are expensive. Dehydrogenation is a chemical reaction using catalysts for the removal of hydrogen from a reactant shown in **Equation 2.2**. It is the reverse process of hydrogenation.

(Equation 2.2)

Cr/Al_2O_3, Cr/SiO_2, [3], Pt/Al_2O_3 and $Pt\text{-}Sn/Al_2O_3$ [7] had been used for dehydrogenation of propylene. Prior starting the reaction, the catalyst must be reduced. Alternatively, single-site Cr heterogeneous catalysts can activate C-H and H–H bond. It had been also shown that the reaction occur via a non-redox mechanism as representing in **Figure 2.4**. This reaction is initiated by C-H bond cleavage to form chromium three propylidene intermediate (intermediate 3). So, the metal stabilizes alkylidene species and the oxygen on the surface stabilizes the proton. After that, the chromium propylidene will have a β-H elimination to form chromium propene hydride (intermediate 4) and subsequently releasing propene forming the chromium hydride species (intermediate 5). Finally, the chromium hydride then reacts with the neighboring hydroxyl proton to generate hydrogen by protons transfer, which desorbs to regenerate the initial Cr–O resting state [10].

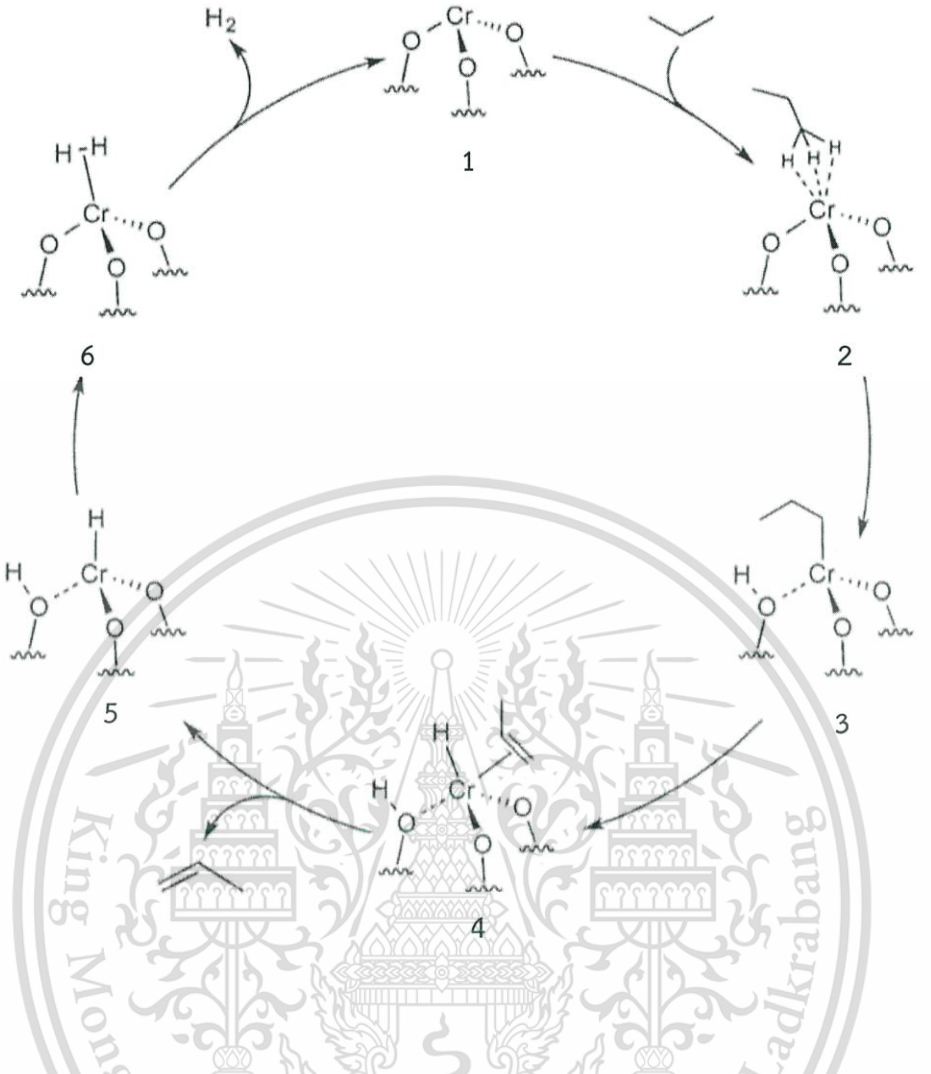

Figure 2.2 Catalytic Cycle reaction pathway for propane dehydrogenation on single-site chromium heterogeneous catalysts [10].

On the contrary, inexpensive metals that can activate C-H bond are Cobalt (Co), Zinc (Zn) and Chromium (Cr). Recently, single-site Co^{2+} and single-site Zn^{2+} on silica heterogeneous catalysts had been reported to activate C-H and H–H bond. They also showed the better activity, high selectivity for propylene and less coke production that leads to higher catalyst stability. Therefore, we are interested in single-site Cr heterogeneous catalysts prepared by using strong electrostatic adsorption (SEA).

2.4 Strong Electrostatic Adsorption [24, 27]

The idea of strong electrostatic adsorption (SEA), is to control the pH of the excess liquid so as to arrive at the optimal pH where metal complex–surface interaction is strongest. This method uses charge balance to bind a cation complex to a negatively charged silica surface in basic solution or an anion complex to a positively charged silica surface in acidic solution. Components of an electrostatic adsorption mechanism are illustrated in **Figure 2.3**. An oxide surface contains terminal hydroxyl groups that are protonated or deprotonated depending of the acidity of the impregnating solution. The pH at which the hydroxyl groups overall are neutral is termed the point of zero charge (PZC).

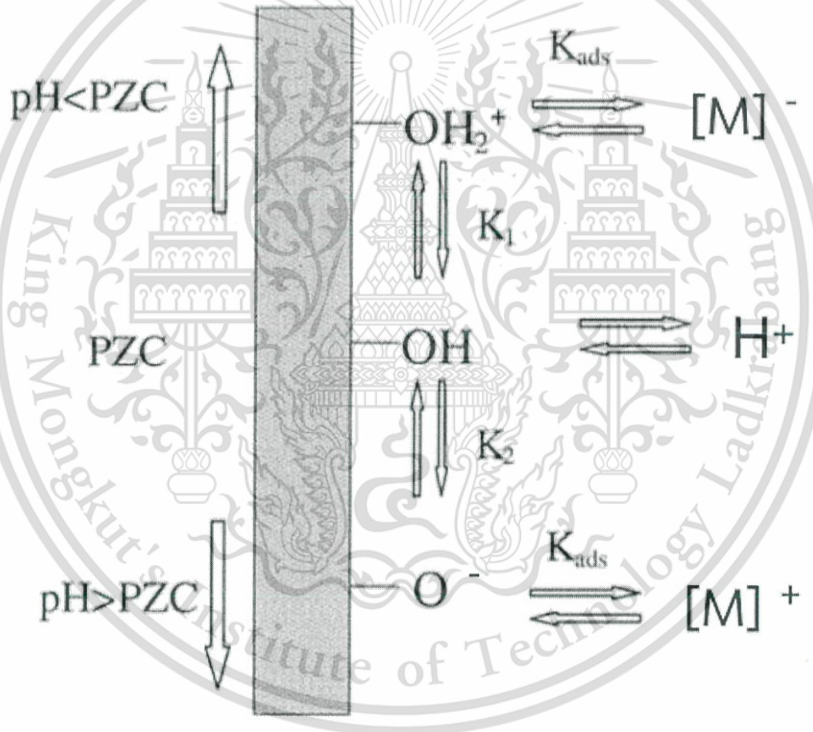

Figure 2.3 Components of an electrostatic adsorption mechanism: surface charging, metal adsorption, and proton transfer. $[M]^+$= Cationic metal complex, $[M]^-$= Anionic metal complex [24].

Below this pH (pH<PZC), the hydroxyl groups are protonated and become positively charge, and this positively surface can adsorb anionic metal complexes; on the other hand, above the PZC (pH>PZC), the hydroxyl groups are deprotonated and become negatively charge, and the surface can adsorb cationic metal complexes.

The PZCs and suitable metal complexes for common supports are shown in **Figure 2.4.**

Support	PZC	Complex
MoO_3	<1	Cations
Nb_2O_5	2–2.5	Cations
SiO_2	4	Cations
Oxidized carbon black	2–4	Cations
Oxidized activated carbon	2–4	Cations
Graphitic carbon	4–5	Cations
TiO_2	4–6	Cations (or anions)
CeO_2	7	Cations or anions
ZrO_2	8	Cations or anions
Co_3O_4	7–9	Cations or anions
Al_2O_3	8.5	(Cations or) anions
Activated carbon	8–10	Anions
Carbon black	8–10	Anions

Figure 2.4 PZCs and suitable metal complexes for common supports [24].

2.5 Literature reviews

The catalytic dehydrogenation of propane has an important commercial interest for industry. Therefore, this reaction has been studied by a lot of scientists over 50 years. Nowadays, the dehydrogenation of propane (PDH) is commercially available. In this case, the feed gas is composed by propane, hydrogen and an inert gas. Some processes used for this reaction can be quoted, such as ABB/Catofin, UOP Oleflex, PDH (Linde), Phillips STAR [28].

Most of those catalysts generally produce coke during the reaction in which reduces the number of active sites and causes the deactivation of catalysts. In 2011, SHIN's group reports indicated the role of tin in coke formation. The increasing of tin loading on a Pt-Al_2O_3 catalyst has an effect on the electronic properties of Pt allowing better coke tolerance and a catalytic performance. However, the use of the noble metals is expensive [7, 29, 30].

In 1907, Sabatier., et. al., found some catalytic dehydrogenation processes. They studied various oxides which were able to catalyze this reaction [31]. And finally, in 1940's, Vladimir, et. al., found a reforming process with platinum as catalyst to produce a high octane gasoline from naphtha (for Universal Oil Product Company) [32]. Platinum was particularly studied, because it has a high activity for activating C-H bonds, and a relatively low activity for the cracking of C-C bounds. However, Pt-catalysts need to be improved because they suffer from rapid deactivation, or poor selectivity, depending on experimental conditions [7].

In 1996, Bert M. Weckhuysen., et. al., studied surface chemistry and spectroscopy of chromium in inorganic oxides. The results showed that Chromium oxide is also a really good metal for catalytic dehydrogenation of propane. This is because it represents to obtain unsaturated hydrocarbons from feedstocks of low-cost saturated hydrocarbons. [33]

In 2004, Xin Ge., et. al., studied propane dehydrogenation with carbon dioxide over a different-supported chromium oxide catalyst. The results showed that Cr/SiO_2 catalyst can activated propane to propylene. This suggests that chromium is active toward the C-H bond for the dehydrogenation of alkanes. However, this routine exhibits low propylene selectivity and produces significant amounts of CO_x. [5].

In 2002, Xuezheng Zhang., et al., studied chromium oxide in different inner supported as a catalyst for the propane dehydrogenation. The results showed that chromium oxide on SBA-15 support exhibited the excellent performance with 59.3% propane conversion at 550°C. However, after running the reaction using chromium oxide on this support for six hours, the conversion of propane dehydrogenation was decreased [3]. This means that the catalyst is deactivated even though, the support is inert. So, the bulk lewis metal catalyst does not solve the coke formation problem.

Single-site catalyst has, on the other hand, been shown the absence or low formation of coke. Furthermore, it shows relatively high activity and selectivity to light olefin. Single site iron (Fe) catalyst on silica is an example [22]. Guo, X., et. al., (2014) studied single-site iron (Fe) catalyst on silica support. The activity of this catalyst for ethane conversion to ethylene, aromatics, and hydrogen reached 48.1% with the absence of coke formation even at 1363 K. Moreover, there is no deactivation during a 60-hour test. It also shows a relative high activity and selectivity towards light olefins [22].

Recently, the single-site Co^{2+} and Zn^{2+} heterogeneous catalysts had been reported that they can activate C-H and H-H bond form propane by Hu and Schweitzer [8, 9]. Schweitzer, N.M., et al., (2014) , studied about the selective dehydrogenation of propane to propylene. The catalyst is a single-site Zn^{2+} on heterogeneous catalysts silica support prepared via electrostatic adsorption methodology. The catalytic performance was studied at 550 and 650 °C. They found out that the single-site Zn^{2+} heterogeneous catalysts on silica support have highly selective dehydrogenation of propane to propylene (>95%) [8]. Hu, B., et al., (2015), reported the study of the propylene selectivity via dehydrogenation of propane over single-site Co^{2+} heterogeneous catalysts on silica support. The catalysts were prepared by two cobalt precursors, hexaamminecobalt (III) chloride ($[Co(NH_3)_6]Cl_3$) and cobalt(II) nitrate hexahydrate ($Co(NO_3)_2.6H_2O$), with the loadings of 0.125 or 5.00 g of cobalt precursors in 20 g of silica. The catalytic performance was investigated at 550 and 650 °C. The result showed that the single-site Co^{2+} heterogeneous catalysts on silica support has selectivities more than 95% at 550 °C and more than 90% at 650 °C with stable activity over 24 hours [9].

These catalysts have a discrete active site which is believed to be significant for their low coke formation and greater selectivity to the desired products than those observed over non-single-site heterogeneous catalysts of the similar composition. Therefore, the single-site heterogeneous catalyst is of interest to be studied.

CHAPTER 3

EXPERIMENTAL DETAILS

3.1 Chemicals and substrates

Table 3.1. Representing the chemical used in this study

Chemical reagents	Grade of purity	Manufacturers
1. Silicon dioxide (SiO_2)	99.00%	CARLO ERBA
2. 30% Ammonium hydroxide	29.50%	CARLO ERBA
solution (NH_4OH)		CARLO ERBA
3. Ammonium chloride (NH_4Cl)	99.00%	LABORATORY REAGENT
4. Cobalt(II) nitrate hexahydrate	98.00%	(RANKEM)
($Co(NO_3)_2.6H_2O$)		
5. Chromium(III) nitrate nonahydrate	97.00%	FLUKA
($Cr(NO_3)_3.9H_2O$)		
6. Chromium(IV) oxide	98.00%	SIGMA-ALDRICH
(CrO_3)		
7. Hydrogen peroxide 30%	29.50%	CARLO ERBA
(H_2O_2)		
8. Acetone ($(CH_3)_2CO$)	99.00%	FISHER SCIENTIFIC
9. 37% Hydrochloric acid (HCl)	36.90%	CARLO ERBA
10. 70% Nitric acid (HNO_3)	69.90%	CARLO ERBA
11. Deionized water		
12. Gas mixture (C_1-C_6), 5190-0519		AGILENT TECHNOLOGIES
13. Propane gas	99.95%	LINDE
14. Air zero gas, zero grade		PRAXAIR
15. Hydrogen gas, high purity	99.99%	PRAXAIR
16. Nitrogen gas, ultra-high purity	99.999%	PRAXAIR

3.2 Apparatus and instruments

1. Mass flow controller
   (BROOKS INSTRUMENT LLC, Model SLA5350SB1AB1B2A1D3N4AA)
2. Tube furnace with a programmed temperature controller
   (UTSAKAN, Model VIF)
3. Tube furnace with a programmed temperature controller
   (VECSTAR, Model VCTF4)
4. Muffle furnace with a programmed temperature controller
   (WISETHEM, Model FHP-05)
5. Hot air oven (FISHER SCIENTIFIC, Model ISOTEMP)
6. Moisture Trap (AGILENT TECHNOLOGIES, Model MT-120)
7. Oxygen Trap (AGILENT TECHNOLOGIES, Model 5182-9401)
8. Gas chromatograph (SHIMADZU, Model GC-2010)
9. Gas adsorption analysis (Autosorb-1C, Quantachrome)
10. Capillary column (RESTEK, Model RT-Q-BOND)
11. Sieve (U.S.A standard sieve, Model AASHO N-92)
12. Centrifuge (UNIVERSAL, Model 320)
13. pH conductivity meter (OHAUS, S Model TARTER3100)
14. Ultra sonicator (WISECLEAN, Model WUC.B02)
15. Digital Round-Top Stirring Hot Plate (IKA, Model 3810001)
16. Temperature programmed reduction (TPR, Model TCD2-NIFED)
17. Transmission electron microscopy (TEM, Model JEM-2100)
18. Thermogravimetic analyzer (Perkin-Elmer, Scientific Instrument Service Center, KMITL)
19. Inductively coupled plasma mass spectrometry (ICP-MS, Model iCAP Qc)
20. X-ray powder diffractometer (XRD, Bruker AG, Model D8 Advance)
21. X-ray fluorescence spectrometer (Wavelength Dispersive, Philips, Model PW2400) and (Energy Dispersive, Oxford, Model ED-2000,)
22. X-ray absorption (XAS, Synchrotron radiation with fluorescence mode detector, Hamamatzu)

3.3 Synthesis and preparation of catalysts

3.3.1 Preparation of catalysts

3.3.1.1 Silica support (SiO_2)

Silica was calcined in muffle oven by ramping to 650 °C for 1 hour with a heating rate of 10 °C/min.

3.3.1.2 Preparation of single-site Co^{2+} heterogeneous catalysts on silica support ([ADS] Co/SiO_2)

The [ADS] Co/SiO_2 was prepared by strong electrostatic adsorption method from the previous reported literature [8]. In a typical synthesis, silica were suspended in deionized water. The pH of the solution was adjusted to 11 using concentrated ammonium hydroxide (NH_4OH). Another, $[Co(NH_3)_6]Cl_3$ was dissolved in deionized water. The pH of the solution was adjusted to 11 with NH_4OH. The cobalt solution was rapidly added to the silica and stirred at room temperature. The solid was allowed to settle. The resulting wet powder was vacuum filtered continued with for rinsed several times with deionized water, and dried at room temperature, followed by drying in air at 125 °C for. After that, the catalyst was calcined in muffle furnace.

3.3.1.3 Preparation of single-site Cr^{3+} heterogeneous catalysts on silica support ([ADS] Cr/SiO_2)

The [ADS] Cr/SiO_2 was prepared by strong electrostatic adsorption method using chromium (IV) oxide (CrO_3) as a precursor. First, 4.76 g of silica were suspended in approximately 50.00 mL of deionized water. In a separate flask, 0.49 g of chromium (IV) oxide was dissolved in 50.00 mL of deionized water. The pH of the solution was 1.76. Then, chromium solution was rapidly added to the silica and stirred for 60 minutes at room temperature. The solid was allowed to settle for 5 minutes. The resulting wet powder was vacuum filtered continued with for rinsed several times with deionized water at pH 1.76., and dried at room temperature for 8 hours, followed by drying in air at 125 °C for 8 hours. Afterward, the catalyst was calcined horizontal tube furnace under a flow of air zero (60 mL/min) at 650 °C for 3 hours with a heating rate at 2 °C/min.

3.3.1.4 Preparation of chromium oxide on silica catalysts ([IM] Cr/SiO_2)

Chromium oxide supported silica ([IM] Cr/SiO_2) with the loading of 1, 2, 5, and 10%wt. was prepared by wetness impregnation method using chromium nitrate nonahydrate ($Cr(NO_3)_3 \cdot 9H_2O$) as a precursor shown in **Table 3.2**. Then, the solid was dried in oven at 70 °C for 24 hours. The dried catalyst was calcined in a horizontal tube furnace under a flow of air zero (60 ml/min) at 650 °C for 3 hours with a heating rate at 10 °C/min.

Table 3.2 Preparation of Chromium Loading on Silica

Catalysts	Metal precursor	Mass of Precursor (g)	Volume of Deionized Water (mL)	Mass of SiO_2 (g)
[IM] Cr/SiO_2 1%	$Cr(NO_3)_3 \cdot 9H_2O$	0.7826	7.60	9.92
[IM] Cr/SiO_2 2%	$Cr(NO_3)_3 \cdot 9H_2O$	1.5640	15.20	9.84
[IM] Cr/SiO_2 5%	$Cr(NO_3)_3 \cdot 9H_2O$	5.7835	14.40	14.35
[IM] Cr/SiO_2 10%	$Cr(NO_3)_3 \cdot 9H_2O$	7.7215	19.20	9.02

3.4 Characterization of catalysts

3.4.1 X-ray Absorption (XAS)

The energy of the X-ray absorption was used to determine the oxidation state of the metal species and coordination environment of the catalyst [34]. X-ray absorption were measured at SLRI (Synchrotron Light Research Institute, Public Organization) using a Ge (220) double crystal monochromator. The storage ring was operated at 1.2 GeV. Data were collected in the transmission mode on self-supporting sample wafers using gas-filled ionization chambers as detectors.

3.4.2 Temperature-programmed reduction (TPR)

Temperature-programmed reduction (TPR) provides information on the active site species of the catalysts by monitoring their reducibility and determine the % metal loading of the catalysts [35]. Temperature programmed reduction was measured using thermal conductivity detector (TCD). The sample weighed 300 mg was placed into a quartz tube reactor, which was located inside a temperature-regulated furnace. Prior to the H_2-TPR, each sample was heated to its activations temperature in air zero (30 mL/min) for 1 hours with 10 °C /min and was cooled down to below 40 °C in N_2 zero (30 mL/min). After that, the heating rate of 10 °C/min, 20 mL/min of 10% H_2 in Ar was applied for TPR analysis. Water production during the reduction process was removed in a U-shape tube trap before entering the TCD.

3.4.3 Inductively Coupled Plasma Mass Spectrometry (ICP-MS)

Inductively coupled plasma mass spectrometry (ICP-MS) was used to determine the metal loading amount. ICP-MS was performed on a Thermo Scientific iCAP Qc ICP-MS. An accurate 100 mg of sample was weighed and then digested with aqua regia solution [36]. Then, sample solvents were evaporated and the organic components were removed by heating at 625 °C for several hours and analyzed by ICP-MS. The flow rate on the instrument was 1 mL/min and dual detector mode was employed. A blank was subtracted after internal standard correction and the value reported are an average of three reading.

3.4.4 X-ray Fluorescence (XRF)

The conventional technique to check the chemical composition of catalyst is by X-ray fluorescence spectroscopy [37]. This technique can be done according to the following procedure: the catalyst sample was weighed about 0.5 g and boric acid was weighted about 4.5 g, then sample and boric acid were mixed together, and compressed into alumina pan before bring into the XRF sample holder in XRF instrument.

3.4.5 Transmission Electron Microscopy (TEM)

Transmission electron microscope (TEM) is the commonly applied for studying supported catalysts. It is used to investigate the morphology, structure, surface of the catalyst, and dispersion of metal, which are important aspects in catalysis [38]. TEM uses a beam of highly energetic electron (voltage 80-120 kV) and signals from TEM depending on the sample density and thickness. Electrons that passes through the sample without energy loss it show bright filed image and electrons are diffracted (scattered) by particles obtain dark-field images at magnification of 100,000 – 120,000x.

3.4.6 Thermogravimetic Analysis (TGA)

The coke deposit of samples was determined from the mass loss after being heated to high temperature [39], as measured by a Perkin-Elmer thermogravimetric analyzer (Pyris 1). Approximately 15 mg of samples was loaded to the platinum plan, after which the exact mass was recorded by the instrument. The sample was then heated from room temperature to 900 °C at the heating rate of 10 °C/min under the flow of Air Zero atmosphere (50 mL/min).

3.4.7 Surface area analysis

Surface area of the catalyst was determined by gas adsorption analyzer [40]. The sample was prepared by weighing approximately 40-50 mg of sample and loaded into a cleaned and dried sample cell. After that, the sample was degassed at the out-gas station at 300°C for 24 hours. The sample cell was then removed from the out-gassing station after nitrogen was filled and was attached to the analysis station. The adsorption isotherm was measured in a pressure range of 0.05-0.30 P/P0 at -196°C.

3.5 Catalytic testing

Catalytic conversion of propane was investigated at atmospheric pressure in a continuous fixed-bed reactor made with quartz tube (8.0 mm O.D.). The catalyst bed was packed in the middle of the reactor, topped and bottomed with quartz wool and quartz beads. The reactor was then installed inside a temperature-controlled electrical furnace. The gas flows were controlled by the mass flow controllers and checked by bubble flow meter. Before the testing, the catalyst was activated by heating rate at 10 °C/min to its calcinations temperature at 650 °C and was hold at that temperature for 1 hour under the stream of air zero (30 mL/min), then cooled down to room temperature under stream of nitrogen (30 mL/min). Next, following TPR results, the catalyst was reduced by heating from room temperature to the chosen reduction temperature (10 °C/min), held at the final temperature for 3 hours) under the stream of hydrogen (100 mL/min). Then, 99.95% propane was fed into the reactor by a mass flow controller at a flow rate of 600 mL/h. The catalytic testing will be conducted for a total time on stream (TOS) of 6 hours. Finally, the product effluents will be analyzed using an online gas chromatograph. Schematic of the catalytic testing reactor is shown in Figure 3.1.

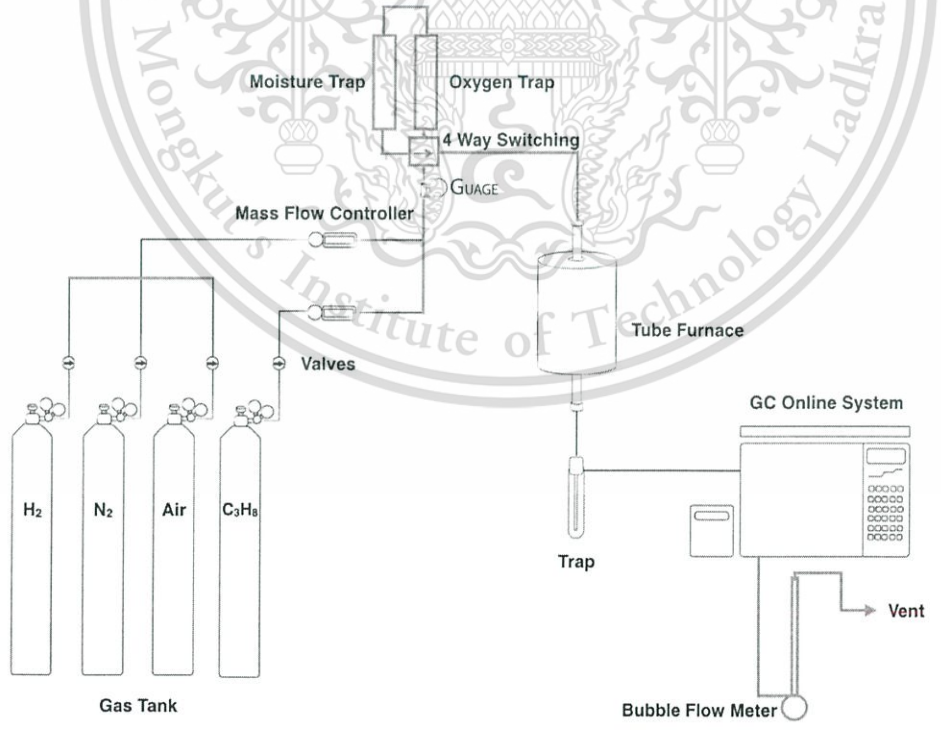

Figure 3.1 Schematic of the catalytic testing reactor

The reacted gaseous mixture was flowed out of the reactor and passed through a gas sampling loop. In order to prevent condensation of products, the line after reactor was heated by heating rods. Description of the reactor set up and the reaction conditions are summarized in **Table 3.3.**

Table 3.3 Description of the reactor set up and reaction condition

Parameters	Value
Reactor outside diameter (mm)	8
Bed length (mm)	12-92
Total flow (mL/min)	60
Catalyst weight (g)	0.2-1.0
Contact time (g.h/mol)	10-30
Catalyst activation (before reaction)	Heating rate: 10 °C/min Calcination temperature: 650 °C Gas: Air Zero (30 mL/min)
Reaction temperature	450-650 °C
Reaction total pressure	Atmospheric pressure (1 atm)

3.6 Analysis products

Propane and product gas were analysed by gas chromatography (GC) (SHIMADZU GC 2010 series) equipped with Rt®-Q-BOND capillary column (length, 30 m; internal diameter, 0.53 mm; film thickness, 0.20 μm) and a flame ionization detector (FID). The initial column temperature was 30°C hold for 7 min, often then ramp at 20°C/min to 85°C hold for 4 min, then ramp at 20°C/min to 140°C hold 3 min, finally then ramp at 15°C/min to 225°C and hold at this temperature for 6.83 min. The temperature of the injection port and FID was kept constant at 250 °C during analysis.N_2 gas was used as a carrier gas. Each component was separated as they pass though the column with an inert carrier N_2 gas and their presence in the effluent were recorded as a chromatogram. Each peak areas from the chromatogram was measured and calculated. Then each peak was identified by comparing with standard and the composition of each product was determined by calibration of standard.

CHAPTER 4
RESULTS AND DISCUSSION

4.1 Catalyst characterization

4.1.1 Elemental analysis and gas adsorption

The elemental composition, specific surface area, and H_2 consumption of each catalyst were determined by inductively coupled plasma mass spectrometry (ICP-MS), X-ray fluorescence spectroscopy (XRF), N_2-BET measurement, temperature programmed reduction (TPR) and the physicochemical properties of all catalysts obtained are shown in **Table 4.1**.

Table 4.1 The physicochemical properties of the catalysts.

Catalysts	Support calcination temperature (°C)	S_{BET} [a] (m^2/g)	% Metal loading	H_2 consumption [d] (mmol/g)	% Reducible metal [d]
SiO_2	650	319	-	-	-
[IM] Cr/SiO_2 1% wt.	650	231	1.05[b]	0.04	0.20
[IM] Cr/SiO_2 2% wt.	650	225	1.83[b]	0.08	0.43
[IM] Cr/SiO_2 5% wt.	650	218	4.89[b] (5.18)[c]	0.16	0.83
[IM] Cr/SiO_2 10% wt.	650	206	9.58[c]	0.11	0.59
[ADS] Cr/SiO_2	650	263	0.20[b]	0.12	0.64
[ADS] Co/SiO_2	550	206	1.67[b]	0.27	1.14

[a] Determined by BET [b] Determined by ICP-MS [c] Determined by XRF [d] Determined by H_2-TPR

It is found that SiO_2 support possesses relatively high surface area of 319 m^2/g. However, the surface area of all metal supported catalysts is obviously decreased upon metal loading. Although, the surface areas of all catalysts prepared by wetness impregnation (IM) and adsorption method (ADS) of metal precursors are lower than that of the SiO_2, their surface areas are considered relatively high surface catalyst. From ICP-MS and XRF results, it can be seen that metal content in the impregnated catalysts [IM] is similar to the expected values. For the catalysts prepared by adsorption method [ADS], chromium and cobalt loading investigated by ICP-MS were 0.20% wt. and 1.67% wt., respectively. The lower the Cr loading, comparing with Co loading on silica support, could be attributed to the lower number of silanol group on the silica surface upon calcination at higher temperature [41]. These silanol groups interact with the metal cationic or anionic complexes via electrostatic forces.

4.1.2 Reducibility of the catalyst

The reducibility of chromium catalysts was investigated by H_2-temperature programmed reduction (H_2-TPR). The H_2-TPR profiles of the catalysts prepared by wetness impregnation [IM] and adsorption [ADS] methods are shown in **Figure 4.1.** The hydrogen consumption (mmol.H_2/g) of all the catalysts is tabulated in **Table 4.1.**

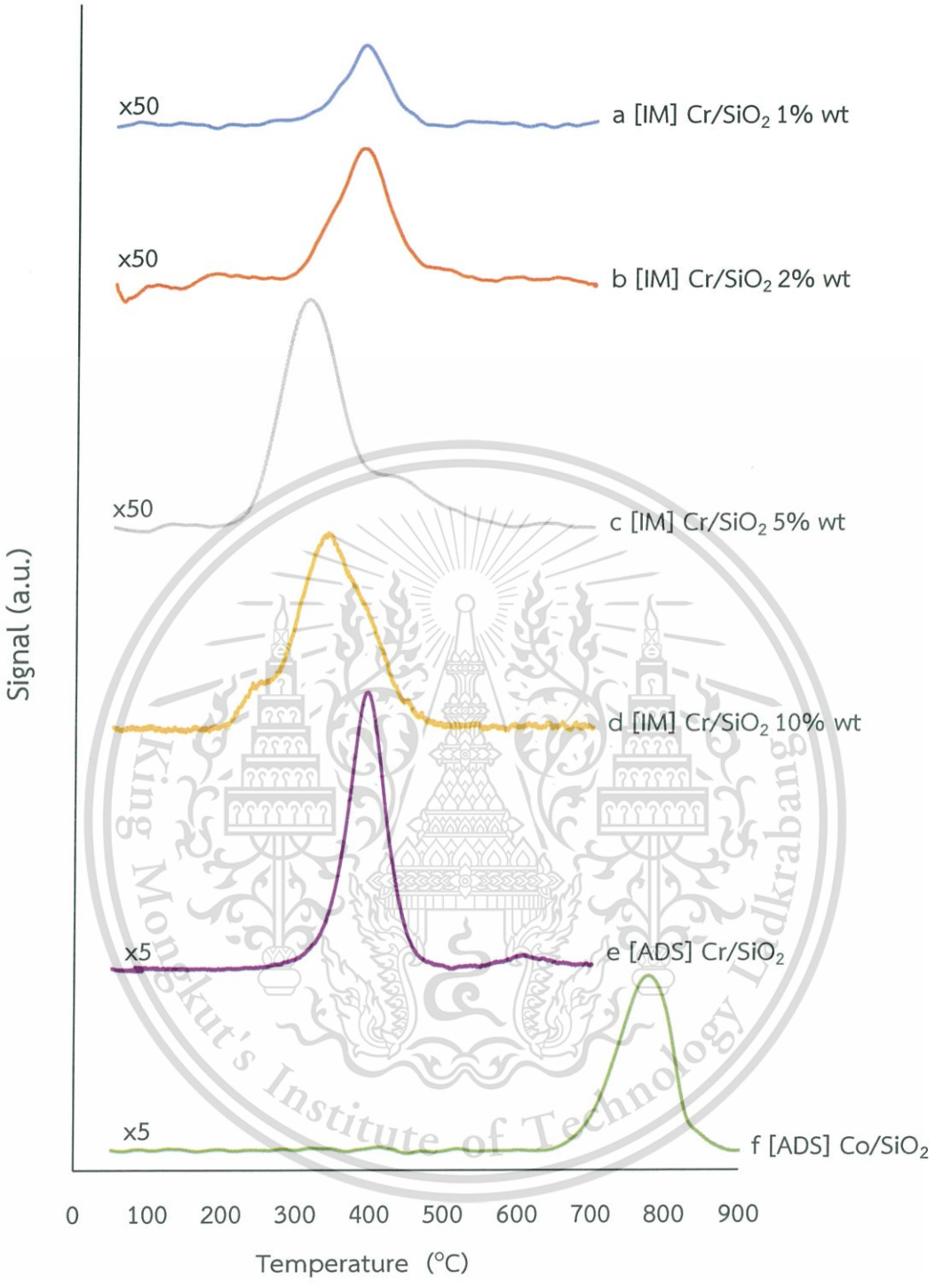

Figure 4.1 TPR profiles of (a) [IM] Cr/SiO_2 1% wt, (b) [IM] Cr/SiO_2 2% wt, (c) [IM] Cr/SiO_2 5% wt, (d) [IM] Cr/SiO_2 10% wt, (e) [ADS] Cr/SiO_2, and (f) [ADS] Co/SiO_2.

In general, chromium H_2-TPR profile exhibits a broad peak around 300-400 °C attributed to Cr^{6+} to Cr^{3+} reduction of, mono-oxo, di-oxo and polymeric oxide species. (**Figure 4.2**) [42,44].

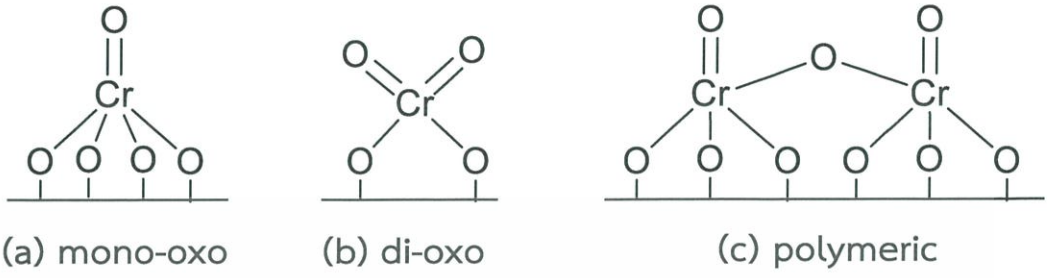

Figure 4.2 Schematic of molecular structures surface CrO_x sites on SiO_2 support (a) mono-oxo, (b) di-oxo, and (c) polymeric species [42,44]

As seen from **Figure 4.1**, [IM] Cr/SiO_2 1% and 2% wt catalysts possess only single reduction peak at ~398 °C. Upon increasing chromium loading to 5% and 10% wt. the reduction peak shifts to 328 °C and 348 °C, respectively. This suggests that the lower reduction temperature is the result of weak interaction of chromium and silica when chromium loading increased. [43]. This is presumably because at low chromium loading, chromium cation binds with oxygen on the silica surface (**Figure 4.2a** and **b**); while, at high chromium loading can form as a bulk polymeric Cr^{6+} as shown in **Figure 4.2c** [44]. The relatively high reduction temperature (398°C) at low metal loading suggests that chromium should be highly dispersed on the surface silica presumably as monomeric CrO_x species [44].

The H_2-consumption of impregnation catalyst shown in **Table 4.1** is increased upon the increment of chromium content. However, % reducible metal species formed in chromium catalysts is lower than the % metal loading characterized by ICP-MS, particularly at 10% wt loading. This suggests that the oxidation state of chromium species present in [IM] Cr/SiO_2 10% wt is mostly III (Cr^{3+}) and only small fraction of Cr^{6+} is retained. This is because Cr_2O_3 (Cr^{3+}) is the most stable oxide preferably formed at high chromium loading [45]. Reduction of this species requires high temperature (>500°C) [46]

For adsorption method [ADS], the reduction peak observed at 400°C is similar to the highly dispersed chromium species in [IM] Cr/SiO_2 1% and 2% wt catalysts. In addition, another reduction peak at ~600-700°C is observed for [ADS] Cr/SiO_2 catalyst, indicating the reduction of isolated Cr^{3+} to Cr^{2+} [46]. This is because at low loading, the migration of highly dispersed chromium oxide species to form Cr_2O_3 clusters is more difficult. Therefore, the Cr^{3+} species formed upon reduction at 400°C, can be reduced further to Cr^{2+} at 600-700 °C [45, 46]. This suggests that the higher fraction of monomeric Cr^{6+} is present in the catalyst prepared by adsorption, as compared with the wetness impregnation. In line with this view, it is observed that the H_2-consumption of [ADS] Cr/SiO_2 catalyst is higher than that of [IM] Cr/SiO_2 samples.

In the case of [ADS] Co/SiO_2 catalyst, the peak between 650-850 °C represents the reduction of isolated Co^{2+} to metallic Co. The reduction temperature of [ADS] Co/SiO_2 catalyst is higher than reduction temperature of bulk cobalt oxide which is approximately 300-400 °C [47]. This suggests that cobalt species present in the cobalt catalyst prepared by adsorption is highly dispersed single-site Co^{2+} species [8].

4.1.3 Oxidation state and coordination geometry of the catalysts

4.1.3.1 Chromium catalysts prepared by impregnation method

X-ray absorption spectroscopy was used for the determination of the oxidation state and coordination environment of the catalysts [48]. The XANES of CrO_3 standard, Cr_2O_3 standard and [IM] Cr/SiO_2 1% wt. are shown in **Figure 4.3.**

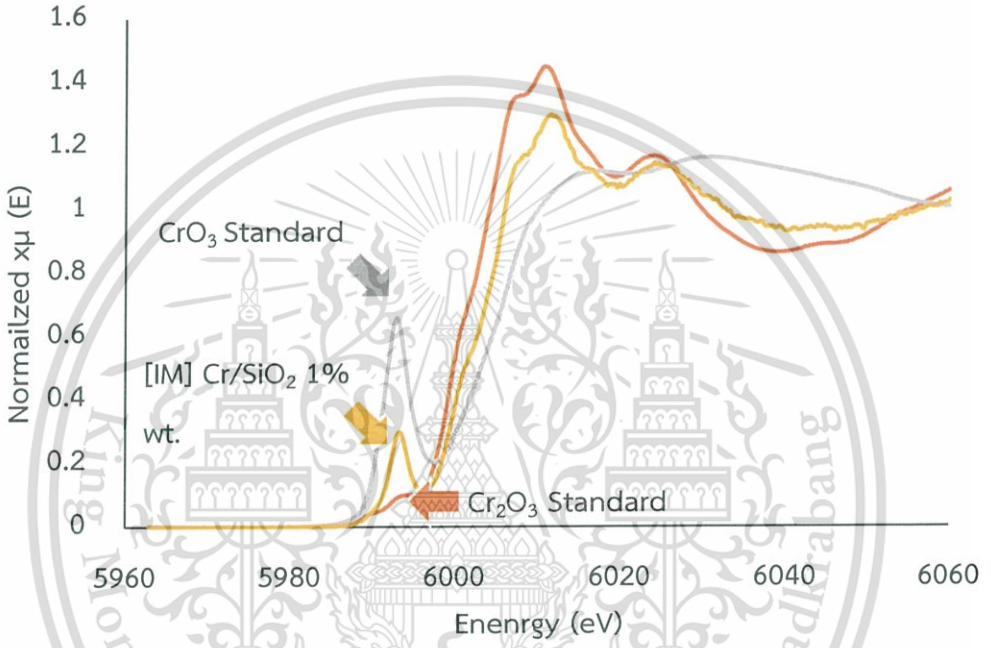

Figure 4.3 XANES spectra of chromium catalysts: Cr_2O_3 (orange line), CrO_3 (gray line) and [IM] Cr/SiO_2 1% wt. (yellow line) catalysts.

It can be seen that CrO_3 standard (Cr^{6+}), which is composed of chains of tetrahedral coordinated chromium oxide, shows the pre-edge peak at 5995 keV and the edge adsorption at 6005.21 keV attributed to Cr^{6+} oxidation state. On the other hand, Cr^{3+} in octahedral environment like Cr_2O_3 shows the edge adsorption peak around 5999.26 keV. Considering the impregnation catalyst ([IM] Cr/SiO_2 1% wt), its edge adsorption at 5999.64 keV is in a position between that of Cr^{3+} and Cr^{6+}, indicating a mixture of both species. Moreover, the [IM] Cr/SiO_2 1% wt catalyst possesses a pre-edge peak which indicates the presence of chromium in tetrahedral environment in a manner similar to CrO_3 (Cr^{6+}).

Upon increasing % loading, the edge adsorption is shifted towards Cr^{3+} species as shown in **Figure 4.4**. In consistence with H_2-TPR results (**Figure 4.1**), the majority of chromium species at high loading are non-reducible, i.e, Cr^{3+} species in bulk phase.

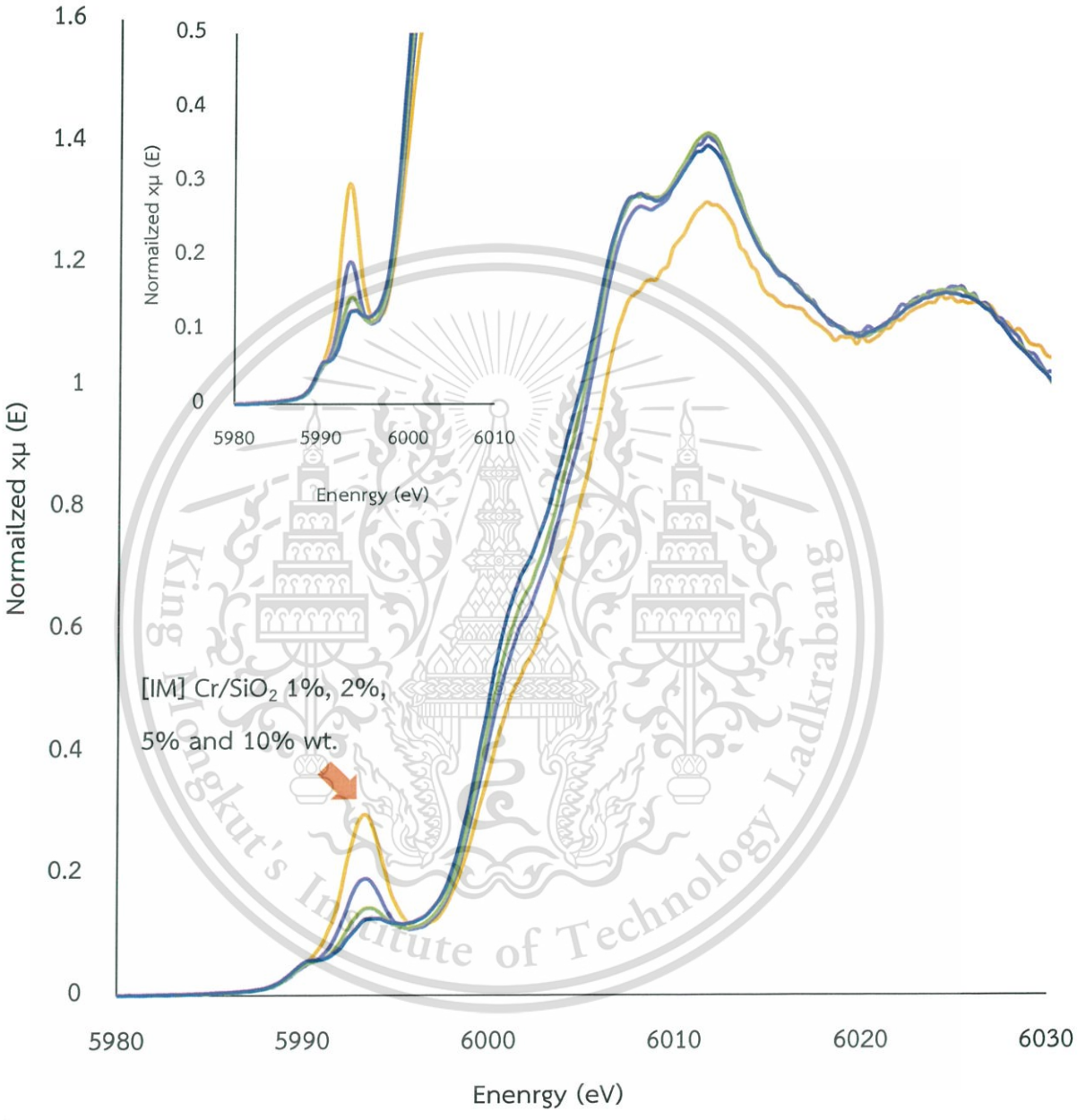

Figure 4.4 XANES spectra of chromium catalysts: [IM] Cr/SiO_2 1% wt. (yellow line), [IM] Cr/SiO_2 2% wt. (blue line), [IM] Cr/SiO_2 5% wt. (green line) and [IM] Cr/SiO_2 (dark blue line) catalysts

Accordingly, the intensity of pre-edge peak represents tetrahedral Cr^{6+} species is inversely proportional to the % loading for the catalyst prepared by impregnation method. This indicates that for the impregnate catalysts, octahedral Cr^{3+} species are formed favorably at high chromium loading presumably as bulk Cr_2O_3. Since Cr_2O_3 possesses weak interaction with silica support, as suggested by lower reduction temperature in the H_2-TPR profile. In line with this view, TEM (**Figure 4.5**) shows that [IM] Cr/SiO_2 5% wt (B) possesses chromium particles larger than that of [IM] Cr/SiO_2 1% wt (A).

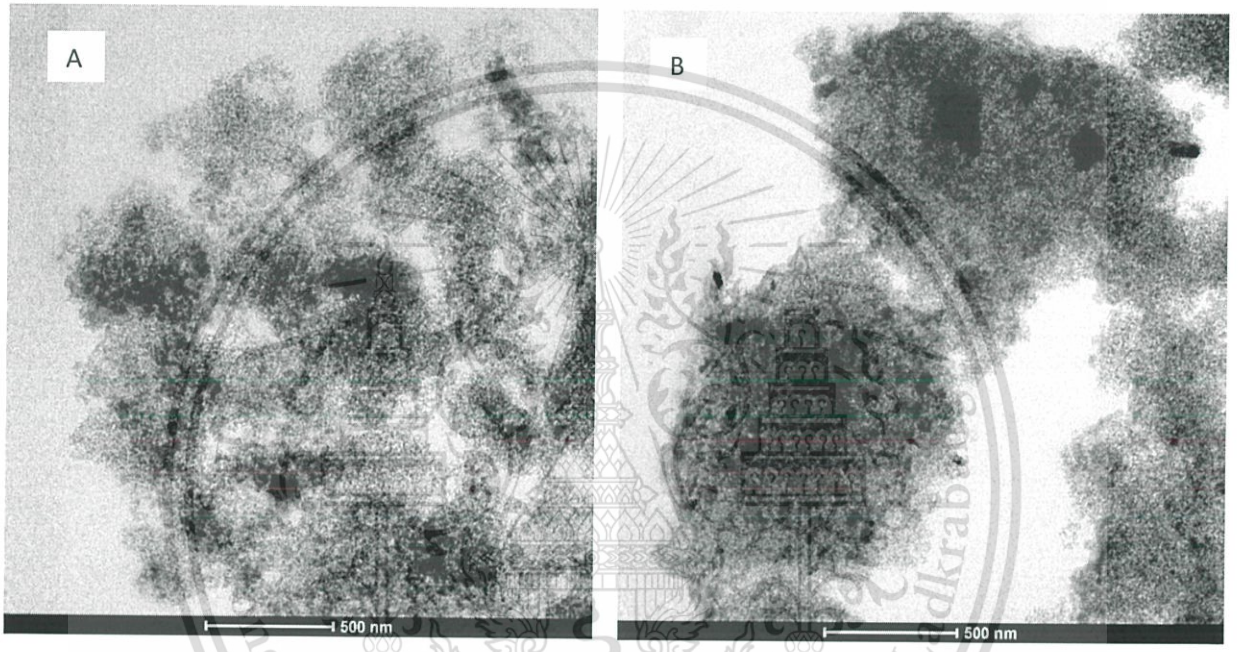

Figure 4.5 TEM images of fresh catalyst: (A) [IM] Cr/SiO_2 1% and (B) [IM] Cr/SiO_2 5% wt

In addition to XANE, EXAFS validates the coordination of chromium species in [IM] Cr/SiO_2 1% wt catalyst, as shown in **Figure 4.6**.

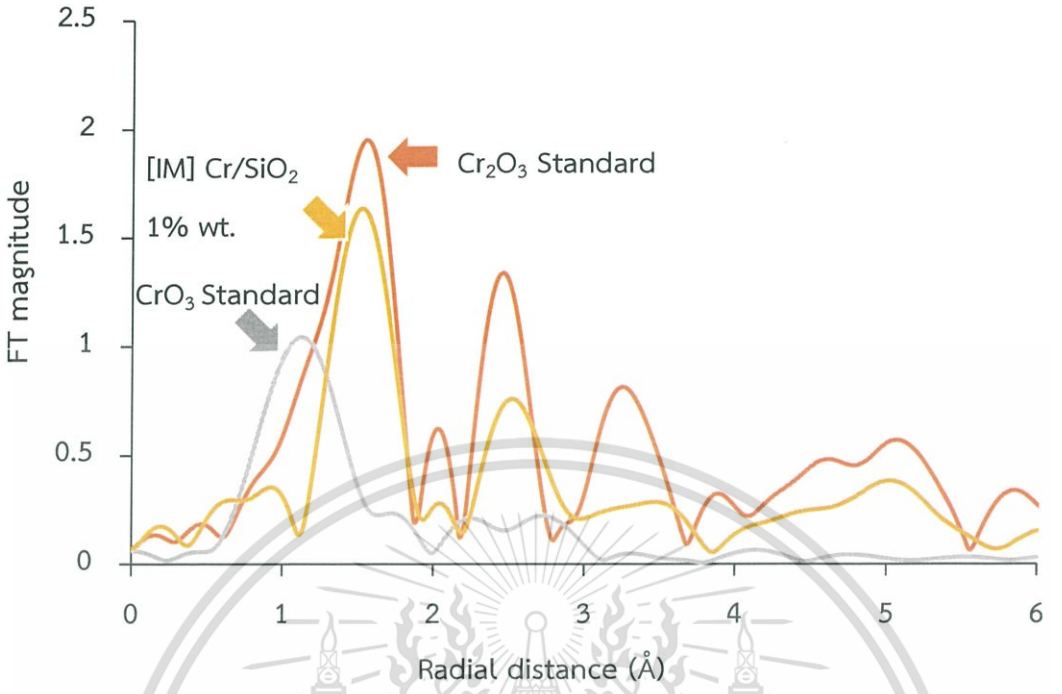

Figure 4.6 FT-EXAFS spectra of chromium catalysts: Cr_2O_3 (orange line), CrO_3 (gray line) and [IM] Cr/SiO_2 1% wt (yellow line) catalysts.

From the FT-EXAFS spectra of Cr_2O_3 (Cr^{3+}) standard, a peak at 1.61 Å corresponded to Cr–O distance while the peaks at 2.45 Å and 3.31 Å are corresponded to Cr–O–Cr and Cr–Cr distance, respectively. (**Table 4.2**) These Cr–O–Cr (2.45 Å) and Cr–Cr (3.31 Å) coordination suggest that chromium is present in an octahedral environment. While, only 1.17 Å of Cr=O distance would be observed for CrO_3 in which chromium is located in tetrahedral environment.

Table 4.2 Metal formal oxidation state and nearest-neighbor distance from XANES and EXAFS.

Catalysts	*Edge-adsorption Energy (eV)	*Oxidation State	**Nearest-neighbor distance (Å)					
			Cr=O, Cr-O	Cr-O-Cr	Cr-Cr	Co-O	Co-N	Co-O-Co
Cr Foil	5989.31	(Calibration)	-	-	-	-	-	-
Cr_2O_3	5999.26	+3	1.62	2.45	3.31	-	-	-
CrO_3	6005.21	+6	1.17	-	-	-	-	-
[IM] Cr/SiO_2 1% wt.	5999.64	+3, +6	1.56	2.51	-	-	-	-
[IM] Cr/SiO_2 2% wt.	5999.60	+3, +6	-	-	-	-	-	-
[IM] Cr/SiO_2 5% wt.	5999.57	+3, +6	1.59	2.51	-	-	-	-
[IM] Cr/SiO_2 10% wt.	5999.55	+3, +6	-	-	-	-	-	-
[ADS] Cr/SiO_2	6005.20	+6	1.22	-	-	-	-	-
Co Foil	7709.19	(Calibration)	-	-	-	-	-	-
CoO	7717.95	+2	-	-	-	1.66	-	2.58
$Co(NH_3)_6Cl_3$	7721.01	+3	-	-	-	-	1.47	-
[ADS] Co/SiO_2	7718.43	+2	-	-	-	1.44	-	-

* Determined by XANES ** Determined by FT-EXAFS

From **Figure 4.6** and **Table 4.2**, EXAFS spectrum of [IM] Cr/SiO_2 1% wt, shows only two distances, 1.56 Å (Cr-O distance) and 2.45 Å (Cr-O-Cr distance), indicating that this catalyst consists of octahedral chromium species. The lack of Cr-Cr peak (3.31 Å) generally found in bulk oxide in **Figure 4.7a**. suggests that the octahedral chromium species in the impregnation catalyst is present in a 2-dimensional structure, presumably polymeric chromium oxide sheet on the silica surface as shown in **Figure 4.7b** [44,46,51,52,53].

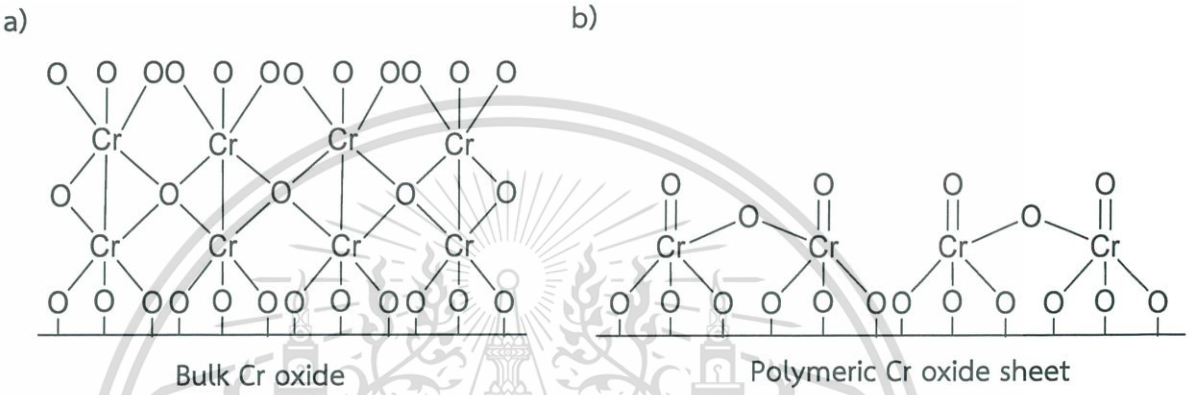

Figure 4.7 Schematic of molecular structures surface of bulk CrO_x sites on SiO_2 support (a) bulk Cr oxide and (b) polymeric Cr oxide sheet [44,46]

DR-UV Spectroscopy was also employed to investigate the chromium species in [IM] Cr/SiO_2 1% wt. catalyst as shown in **Figure 4.8.**

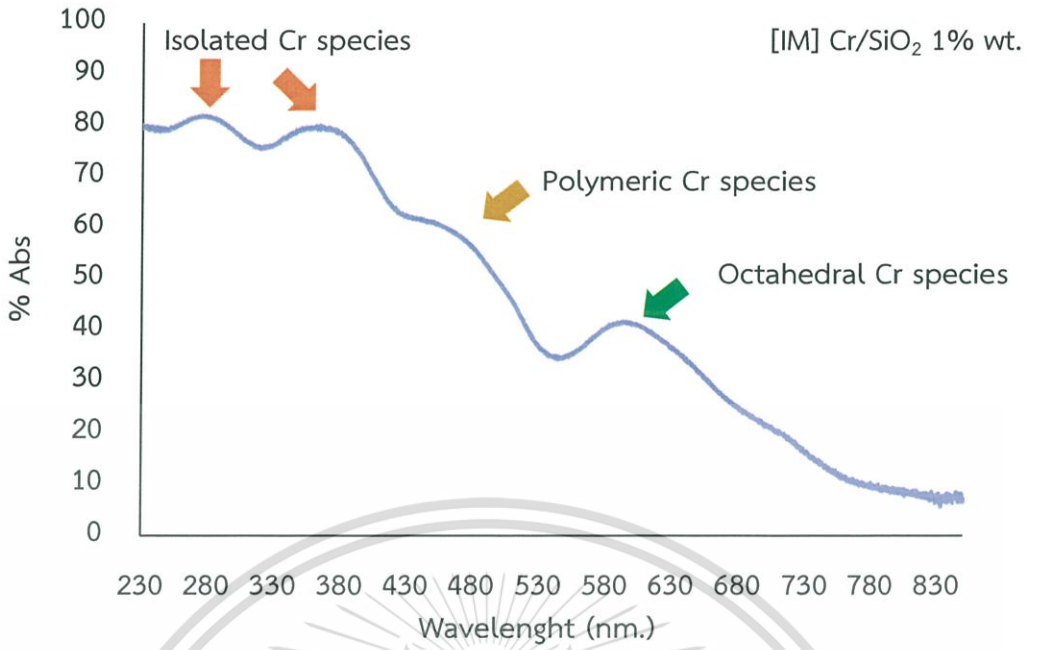

Figure 4.8 DR-UV reflectance spectra of [IM] Cr/SiO_2 1% wt. catalyst.

From **Figure 4.8.**, the sample shows reflectance peaks at 280, 375, 450 and 596 nm. According to the standard experiments by Edward L. Lee *et. al.*, the peaks at 280 and 375 nm correspond to isolated chromium tetrahedral species. While peak at 450 nm corresponds to polymeric chromium species and peak at 596 nm corresponds to Cr^{3+} in octahedral environment including Cr_2O_3 species [54]. The results confirm that the chromium species in the [IM] Cr/SiO_2 1% wt were consisted that of (i,ii)highly disperse tetrahedral chromium oxide, (iii) polymeric chromium oxide sheet and (iv) bulk octahedral chromium oxide (**Figure 4.9**) in consistent with XANES and EXAFS results.

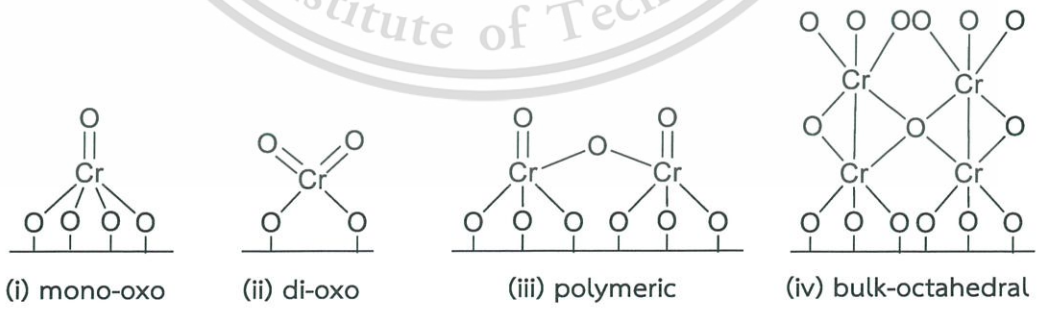

Figure 4.9 Schematic of molecular structures surface chromium species in [IM] Cr/SiO_2 1% wt. catalyst (i) mono-oxo, (ii) di-oxo, (iii) polymeric and (iv) bulk-octahedral chromium oxide [42,44]

4.1.3.2 Chromium catalyst prepare by strong electrostatic adsorption

The XANES of CrO_3 standard, Cr_2O_3 standard, and [ADS] Cr/SiO_2 are shown in **Figure 4.10.**

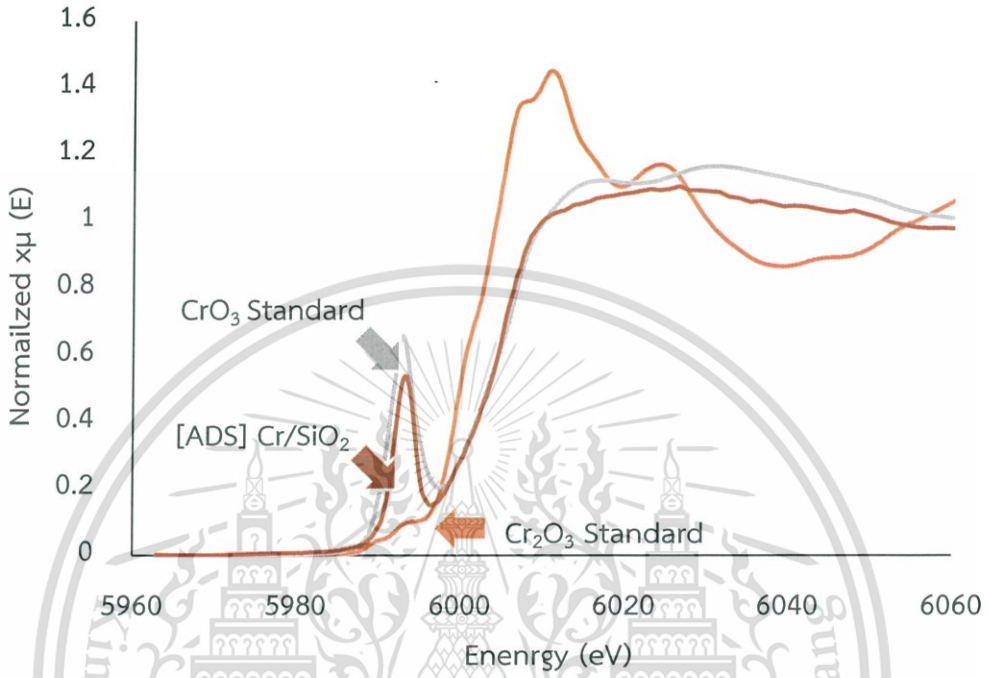

Figure 4.10 XANES spectra of chromium catalysts: Cr_2O_3 (orange line), CrO_3 (gray line) and [ADS] Cr/SiO_2 (brown line) catalysts.

In contrast to the impregnation catalyst, the edge adsorption of chromium species in the catalyst prepared by adsorption, ([ADS] Cr/SiO_2) are well matched with the CrO_3 standard. This indicates the presence of Cr^{6+} species virtually in this catalyst. Moreover, the pre-edge peak of chromium at ~6000 keV represents the Cr^{6+} in tetrahedral environment were notably observed [48]. This is in line with the single-site chromium species, reported in literature [49].

The Fourier transforms (FT) of the EXAFS spectra also confirms the presence of tetrahedral chromium species in [ADS] Cr/SiO_2 catalyst as shown in **Figure 4.11.**

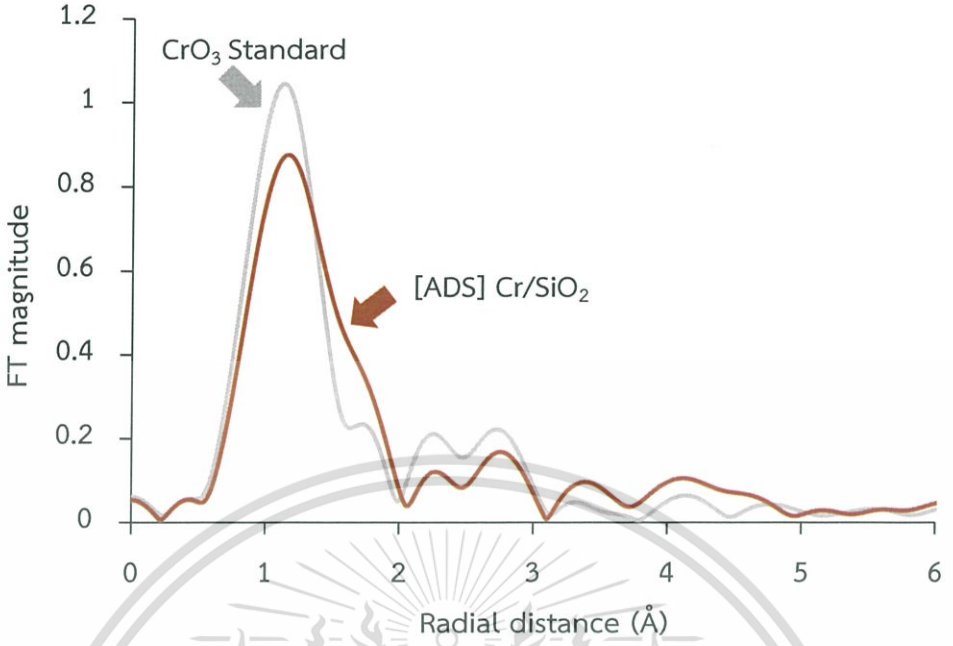

Figure 4.11 FT-EXAFS spectra of chromium catalysts: CrO_3 (gray line) and [ADS] Cr/SiO_2 1% wt. (brown line) catalysts.

From **Figure 4.11**, it was observed that the FT-EXAFS spectra pattern of [ADS] Cr/SiO_2 is somewhat identical to that of CrO_3 standard. The main peak at 1.22 Å, coincides with the Cr=O bond distance of a Cr^{6+} in a tetrahedral environment. It is important to note that, only a single peak due to the neighboring oxygen atoms (Cr=O) can be observed in [ADS] Cr/SiO_2 catalyst. This suggests that chromium ions are highly dispersed on the silica surface. In consistence with H_2-TPR, such monomeric tetrahedral Cr^{6+} species are reduced at relatively high temperature (~400°C). In line with this view, DR-UV spectra of [ADS] Cr/SiO_2, shows only two reflectance peaks at 280 and 375 nm as shown in **Figure 4.12**.

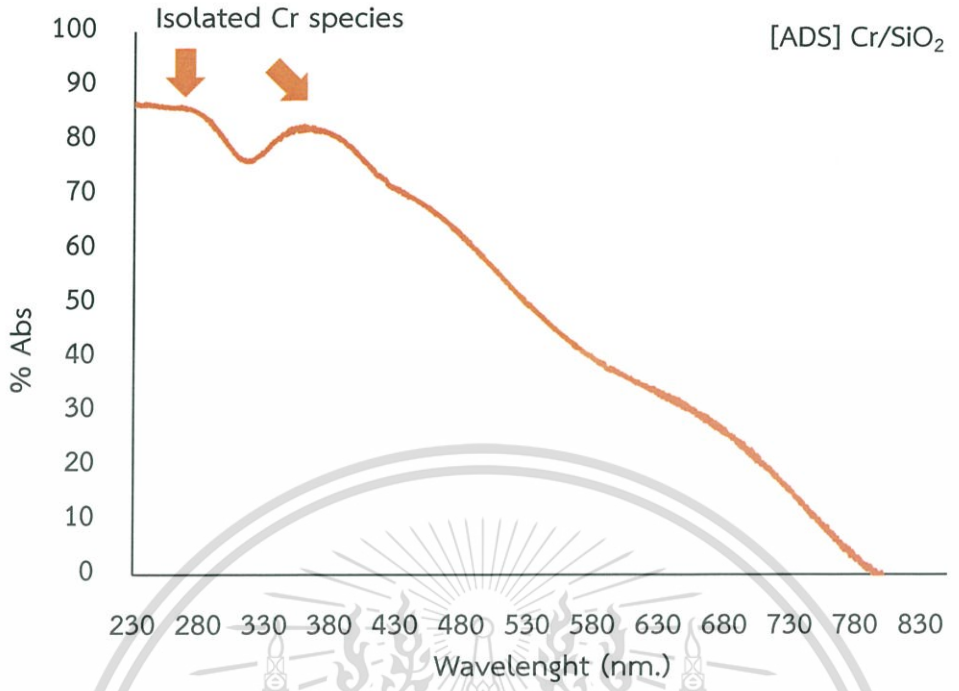

Figure 4.12 DR-UV reflectance spectra of [ADS] Cr/SiO_2 catalyst.

As discussed earlier, peak is at 280 and 375 nm correspond to the isolated tetrahedral chromium species [54]. Hence, it can be concluded at this stage that the strong electrostatic adsorption method yields selectively of tetrahedral chromium species that are highly dispersed as isolated chromium oxide on silica surface as shown in **Figure 4.13** [50].

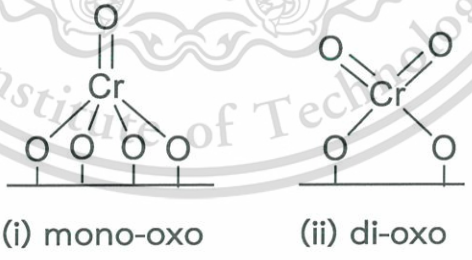

Figure 4.13 Schematic of molecular structures surface isolated chromium species in [ADS] Cr/SiO_2 catalyst (i) mono-oxo and (ii) di-oxo [42,44]

4.1.3.3 Cobalt catalyst prepared by strong electrostatic adsorption.

In the case of single-site Co^{2+}/SiO_2 catalyst, XANES spectra of [ADS] Co/SiO_2 and Co standard are shown in **Figure 4.14**.

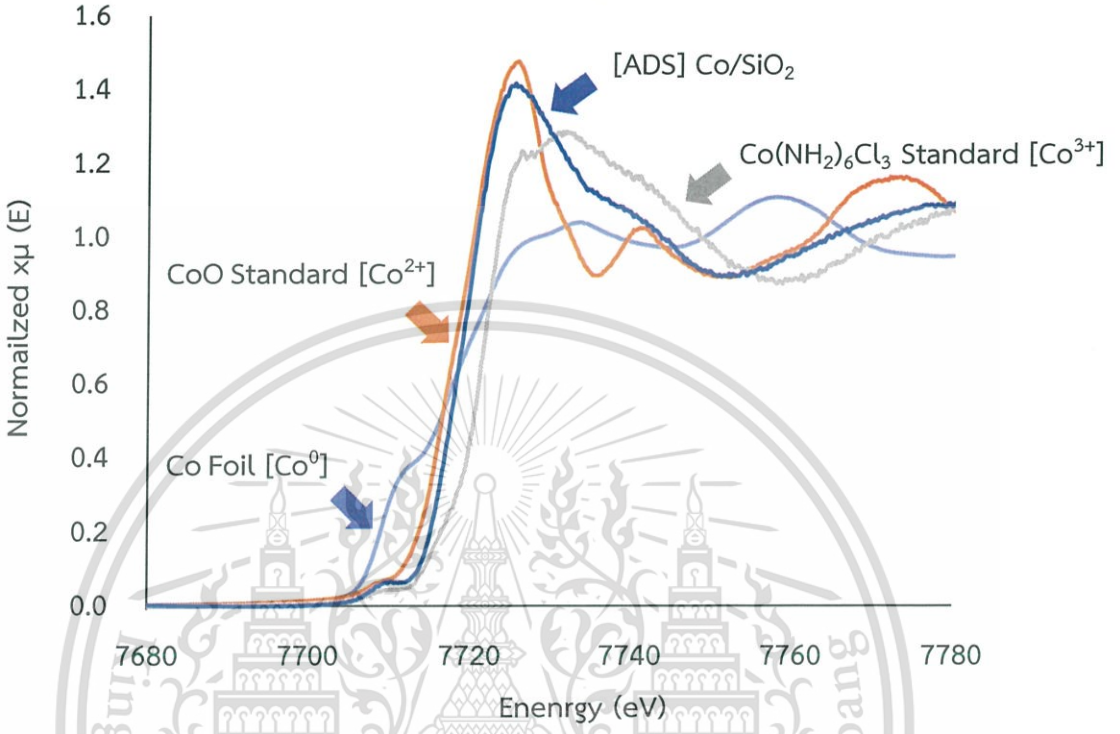

Figure 4.14 XANES spectra of cobalt catalysts:, Co Foil (light blue line), CoO standard (orange line), $Co(NH_3)_6Cl_3$ standard (gray line) and [ADS] Co/SiO_2 (dark blue line) catalysts.

As seen from **Figure 4.14**, Co foil spectra exhibits the edge adsorption peak at 7709.19 eV corresponding to metallic cobalt. CoO standard (Co^{2+}) shows the edge adsorption peak at 7717.95 eV. In the case of $Co(NH_3)_6Cl_3$ standard, the edge adsorption peak at 7721.01 eV is consistent with octahedral coordination Co^{3+}. From XANES spectra, it can be seen that the edge adsorption of [ADS] Co/SiO_2 at 7718.43 eV is similar to that of CoO standard (Co^{2+}). This indicates that the Co^{2+} is present in the cobalt catalyst prepared by strong electrostatic adsorption. However, EXAFS spectra of [ADS] Co/SiO_2 is not well matched with CoO standard (Co^{2+}) as shown in **Figure 4.15**.

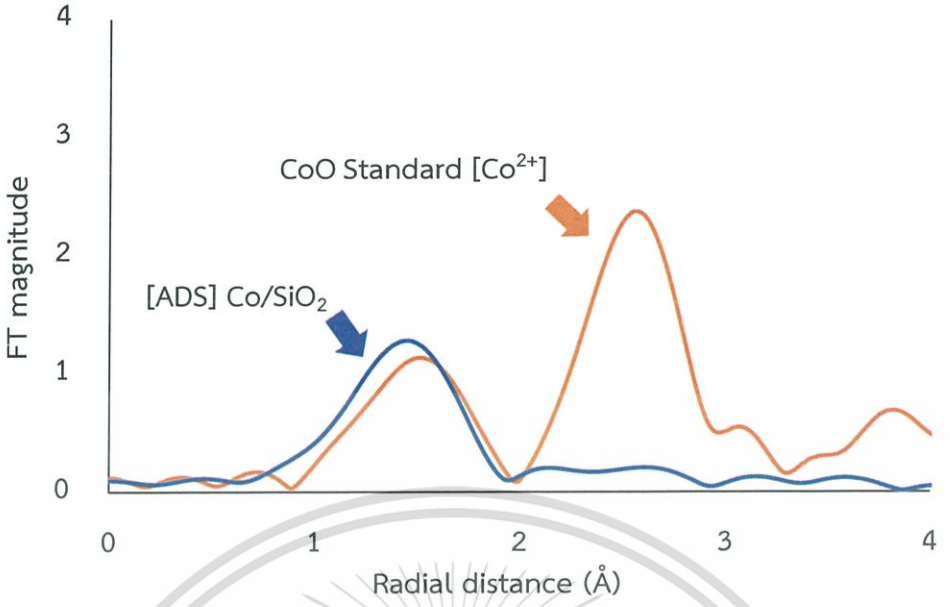

Figure 4.15 FT-EXAFS spectra of cobalt catalysts, CoO standard (orange line) and [ADS] Co/SiO_2 (dark blue line) catalysts.

It was observed that bulk CoO standard (Co^{2+}) shows the peak at 1.66 Å, attributed to Co–O distance, and the peak at 2.58 Å attributed to Co–O–Co distance. This Co–O–Co contribution refers to octahedral cobalt species in bulk CoO particles [55]. While [ADS] Co/SiO_2 catalyst shows only single peak at 1.44 Å, corresponded to Co-O distance, no-two adjacent cobalt coordination (Co-O-Co distance) was observed. This suggests that cobalt species prepared by strong electrostatic adsorption is present as single-site cobalt species bond with silica surface (**Figure 4.16**). This cobalt single-site species has been widely reported by the literatures to be a tetrahedral cobalt oxide [8].

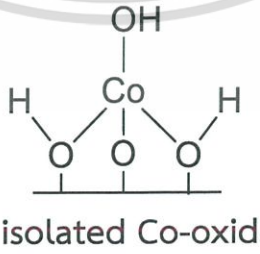

Figure 4.16 Schematic of molecular structures surface isolated cobalt species in [ADS] Co/SiO_2 catalyst [8].

4.2 Catalytic Testing

4.2.1 Effect of temperature

The effect of temperature from 450–650 °C of propane activation using SiO_2 and [IM] Cr/SiO_2 2% wt. as a catalyst are shown in **Figure 4.17**.

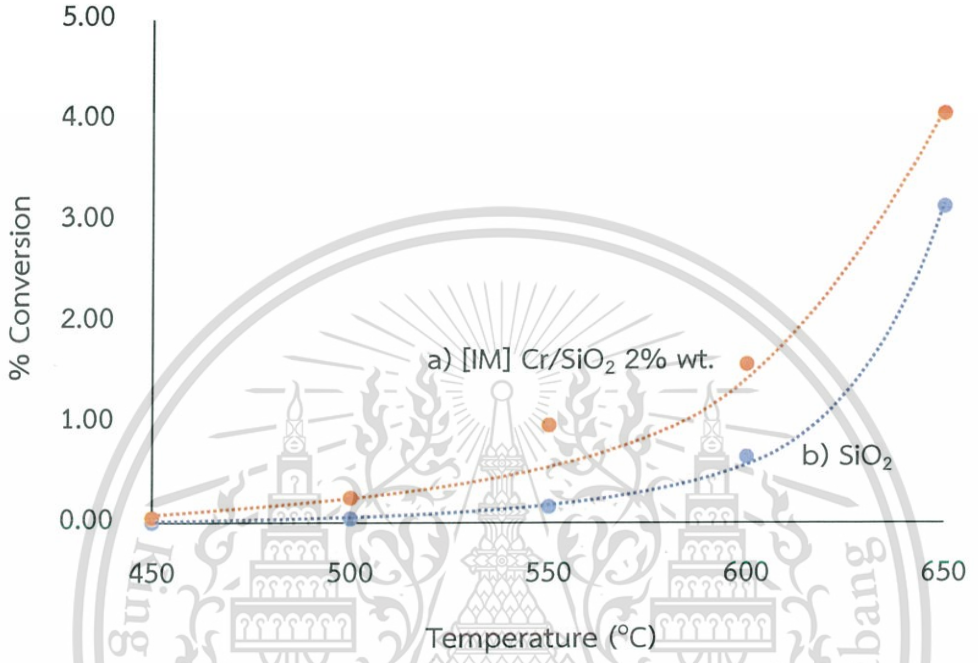

Figure 4.17 The Comparison of Scanning Temperature Propane Conversion (a) [IM] Cr/SiO_2 2% wt, (b) SiO_2 Catalysts *(Reaction temperature: 450 – 650 °C, 0.0258 mol/h of propane (99.95%), and 50 mL/min nitrogen, W/F;* (A) 7.1869 *g.h/mol*, (B) 7.1129 *g.h/mol)*

Figure 4.17 shows that increasing of temperature results in the higher reaction rate, particularly at 650 °C. In the presence of chromium over silica, a higher overall activity (~4%) was obtained, in addition to thermal activity observed over the SiO_2 support. It is noted that the equilibrium conversion for propane dehydrogenation at 450-650 °C is 6-45% [56]. The results indicate that C-H bond activation of propane required a temperature at least 500 °C. The main product was propylene at all temperatures as shown in **Table 4.3**.

Table 4.3 Product selectivity at various reaction temperatures.

Catalyst	Temperature (°C)	% Conversion	% Selectivity					
			Methane	Ethane	Ethylene	Propylene	C_4	$+C_5$
SiO_2	450	0.00	0.0	0.0	0.0	0.00	0.0	0.0
	500	0.04	0.0	0.0	0.0	100.0	0.0	0.0
	550	0.16	14.1	0.0	25.3	60.6	0.0	0.0
	600	0.65	13.9	0.0	25.7	60.4	0.0	0.0
	650	3.14	15.6	0.5	28.6	55.3	0.0	0.0
[IM] Cr/SiO_2 2% wt.	450	0.04	0.0	0.0	0.0	100.0	0.0	0.0
	500	0.24	0.0	0.0	0.0	100.0	0.0	0.0
	550	0.97	3.0	1.0	4.6	88.7	2.7	0.0
	600	1.58	5.2	0.0	9.0	84.5	1.3	0.0
	650	4.06	10.9	0.3	19.6	68.7	0.5	0.0

(Reaction temperature: 450–650 °C, 0.0258 mol/h of propane (99.95%), and 50 mL/min nitrogen, W/F; (SiO_2) 7.1869 g.h/mol, ([IM] Cr/SiO_2 2% wt.) 7.1129 g.h/mol)

Considering the reaction at 450-500 °C, only propane dehydrogenation was observed with 100% yield of propylene. In contrast, at 550 °C and above, there are additional products including propylene, ethylene, ethane and methane and these products increase as the temperature raises. For methane and ethylene, they were products from the thermal cracking of propane. Ethane would be yielded from the hydrogenation of ethylene. C_4 product would be obtained from the coupling of ethylene, which was only observed using chromium as the catalyst. This is because chromium possesses Lewis acidity that can promote ethylene oligomerization. As higher selectivity of ethylene and methane can be observed at high temperature (>550 °C), the temperature at 550 °C was chosen for further investigation.

4.2.2 The effect of % chromium loading

The comparative studies of propane dehydrogenation using all the impregnation catalysts at 550 °C with same contact time are shown **in Table 4.4**.

Table 4.4 Product selectivity over various catalysts at the same contact time.

Catalysts	Conversion (%)	Selectivity of products (%)						
		Methane	Ethane	Ethylene	Propylene	C_4	C_5	C_6+
SiO_2	0.21	16.9	-	31.2	51.9	-	-	-
[IM] Cr/SiO_2 1% wt.	1.72	4.0	1.4	5.3	88.1	1.2	-	-
[IM] Cr/SiO_2 2% wt.	1.76	2.5	1.0	3.5	91.4	1.6	-	-
[IM] Cr/SiO_2 5% wt.	1.81	2.8	1.3	3.9	92.0	-	-	-
[IM] Cr/SiO_2 10% wt.	2.09	4.1	1.4	5.8	88.7	-	-	-

(Reaction temperature: 550 °C, 0.0258 mol/h of propane (99.95%), and 50 mL/min nitrogen, W/F; 10 g.h/mol, Time on stream; 45 minutes)

As seen from **Table 4.4**, the conversion of propane and selectivity to propylene is increased when chromium was loaded in SiO_2 catalyst. This suggests that chromium promoted C-H cracking rather than C-C cracking. In addition, it was observed that no significant difference in the propylene selectivity, when chromium content is increased. Nevertheless, light hydrocarbons, such as C_4, was slightly observed over 1% and 2% Cr/SiO_2 catalysts, presumably due to the oligomerization of ethylene. As XANES results indicate that the catalyst with lower chromium loading ([IM] Cr/SiO_2 1% and 2% wt.) possesses higher tetrahedral chromium species, these single-site chromium species acts as Lewis acid site that can promote for ethylene oligomerization. In the mechanistic point of view, the ethylene would be coordinated to electrophilic Lewis center. The coordinated ethylenes can be coupled bearing C_4 olefins as products (**Figure 4.18**).

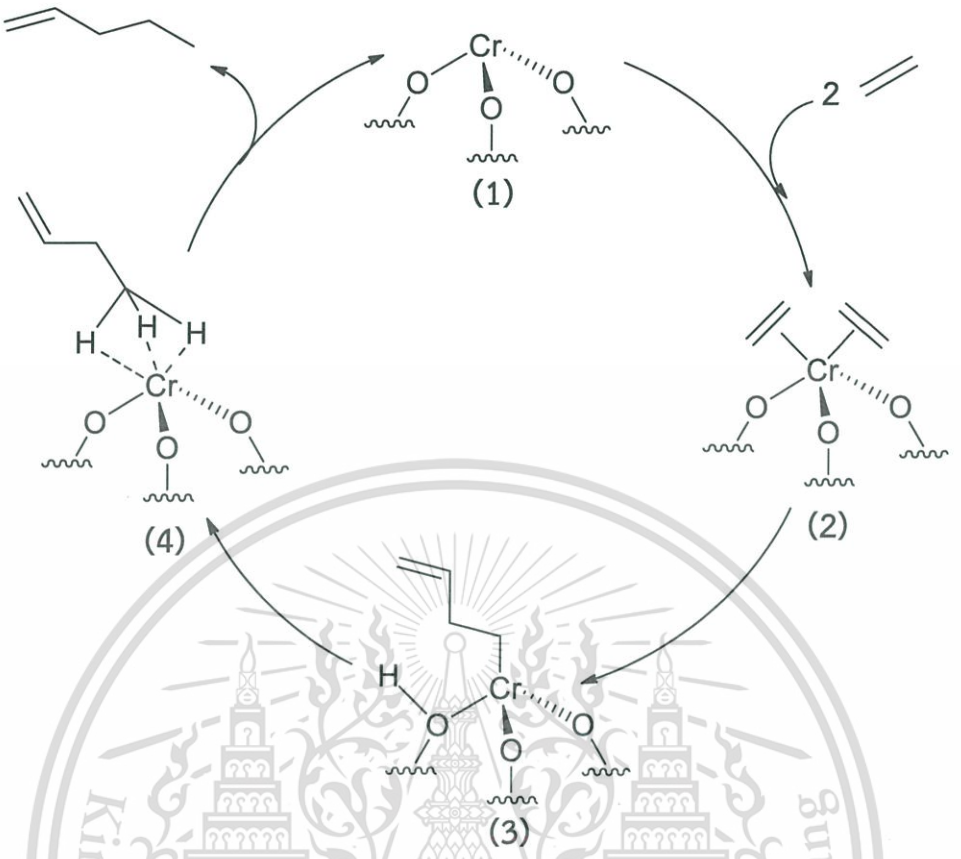

Figure 4.18 Catalytic cycle reaction pathway for ethylene oligomerization on chromium heterogeneous catalysts [10].

However, the conversion of propane is not proportionally increased with chromium loading. This suggests that the active site for propane dehydrogenation is not a function of chromium loading. This can be seen by the decrease in turnover frequency (TOF) of [IM] Cr/SiO_2 catalysts when chromium loading is increased as shown in **Figure 4.19**.

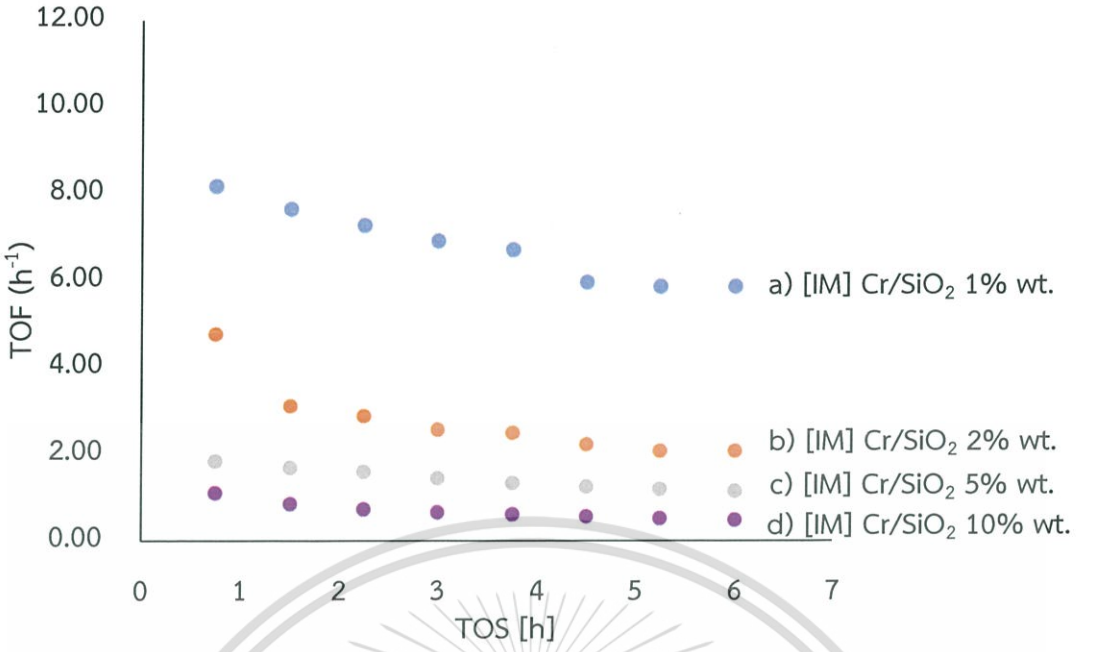

Figure 4.19 Turn over frequency (TOF) of [IM] Cr/SiO_2 for propane dehydrogenation (a) [IM] Cr/SiO_2 1% wt., (b) [IM] Cr/SiO_2 2% wt., (c) [IM] Cr/SiO_2 5% wt. and (d) [IM] Cr/SiO_2 10% wt. catalyst. *(Reaction temperature: 550 °C, 0.0258 mol/h of propane (99.95%), and 50 mL/min nitrogen, W/F; 10 g.h/mol.)*

It can be seen that turnover frequency (TOF) of the chromium catalysts for propane dehydrogenation are in the order of; IM1% >>>> IM2% > IM5% > IM10%. According to H_2-TPR, XANES and EXAFS results, the impregnation chromium consists of a mixture of tetrahedral and octahedral coordinated chromium oxide species. The chromium tetrahedral (single-site species) are formed favorably in the catalyst with lower loading ([IM] Cr/SiO_2 1% wt). Since more chromium bulk species were observed at high chromium loading, this indicates that the tetrahedral chromium species, i.e. single-site chromium species, possesses higher activity, as compared to the chromium species in bulk Cr_2O_3. As the concentration of chromium single-site can be related to the pre-edge absorption intensity in XANES, the turnover frequency (TOF) is linearly increased with the intensity of pre-edge absorption as observed in **Figure 4.20**.

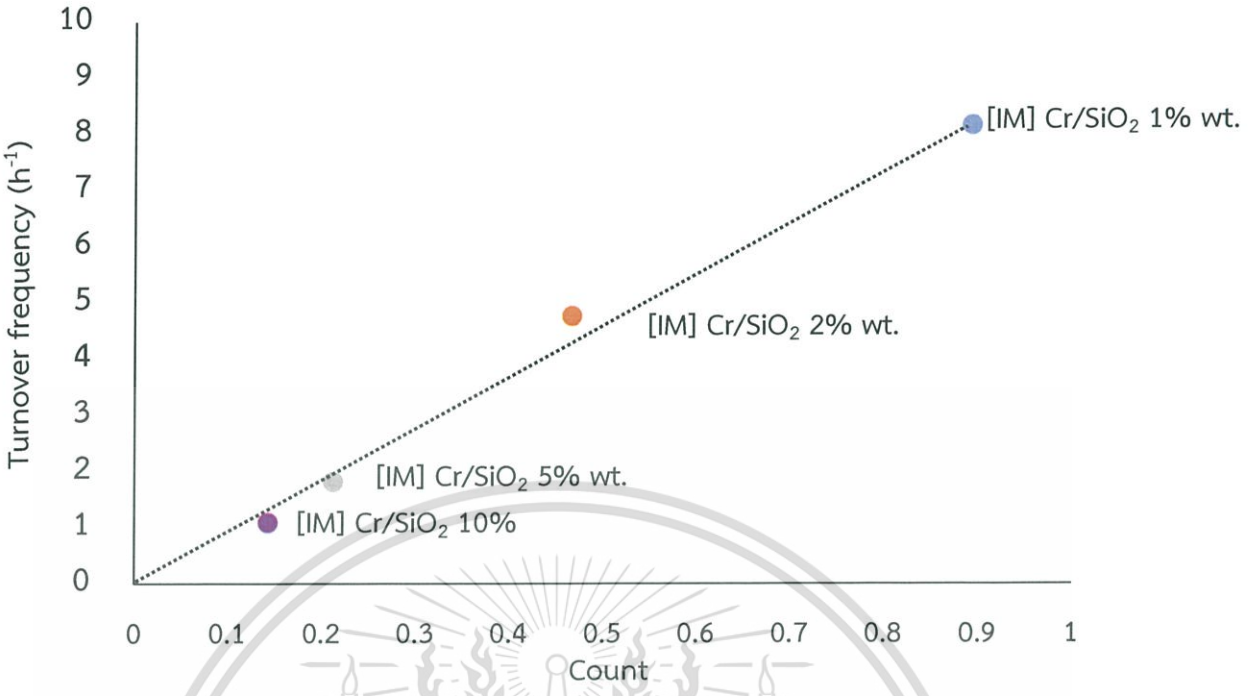

Figure 4.20 Relationship between the intensity of pre-edge absorption by XANES spectra of [IM] Cr/SiO_2 catalysts (Count) and turnover frequency (TOF).

This clearly indicates that the single-site chromium species are the active species for propane dehydrogenation over the Cr/SiO_2 catalysts.

However, TOF of all catalyst decreased overtime. It is suggested that the catalyst is deactivated presumably due to the coke formation as shown by TGA in **Table 4.5.**

Table4.5 TGA analysis under Air Zero of [IM] Cr/SiO_2 1% and 10% wt.

Catalyst	Low Temperature	High Temperature
[IM] Cr/SiO_2 1% wt	250 °C (0.5% wt.)	725 °C (0.5% wt.)
[IM] Cr/SiO_2 10% wt	250 °C (0.5% wt.)	750 °C (1.9% wt.)

The TGA of the spent chromium catalyst shows weight loss of water around 250 °C and hard coke at ~750 °C. It was also observed that the spent [IM] Cr/SiO_2 10% wt. retrains higher carbon deposit (1.9% wt.), as compared to [IM] Cr/SiO_2 1% wt (0.5% wt.). This result suggests that when increasing chromium bulk species, the C-C coupling can be promoted leading to formation of higher MW products and hence coke formation.

4.2.3 The effect of catalyst preparation method

The comparative studies between [ADS] Cr/SiO_2 and [IM] Cr/SiO_2 1% wt. at the same contact time at 550 °C are presented in **Figure 4.20**

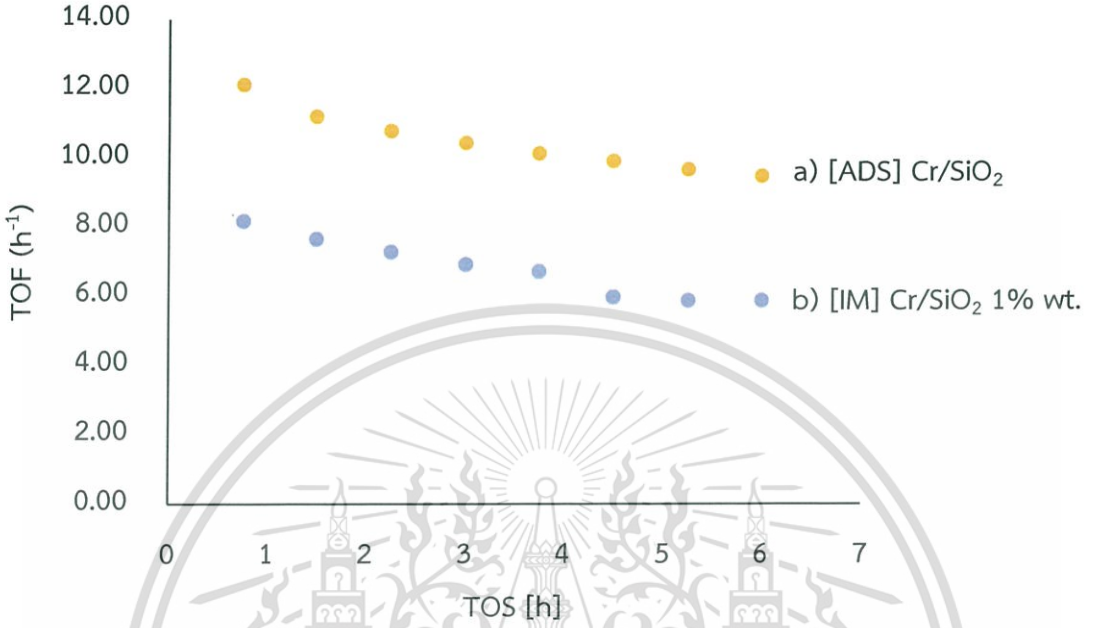

Figure 4.21 Turn over frequency (TOF) for propane dehydrogenation (a) [ADS] Cr/SiO_2 and (b) [IM] Cr/SiO_2 1% wt. catalyst. (Reaction temperature: 550 °C, 0.0258 mol/h of propane (99.95%), and 50 mL/min nitrogen, W/F; 10 g.h/mol.)

It can be clearly seen that chromium catalyst prepared by strong electrostatic adsorption ([ADS] Cr/SiO_2) shows a higher TOF, as compared to that by wetness impregnation. This suggests that the [ADS] Cr/SiO_2 is more active than [IM] Cr/SiO_2 1% wt catalyst likely due to the higher concentration of chromium single-site species as evidenced by H_2-TPR, XANES and EXAFS results. A high fraction of chromium single-site would provide a high number of active site, and hence higher propane dehydrogenation activity, as observed. In line with this view, the turnover frequency (TOF) is linearly increased with intensity of pre-edge absorption and the catalyst prepared by strong electronic adsorption method yields the highest rate as shown in **Figure 4.22.**

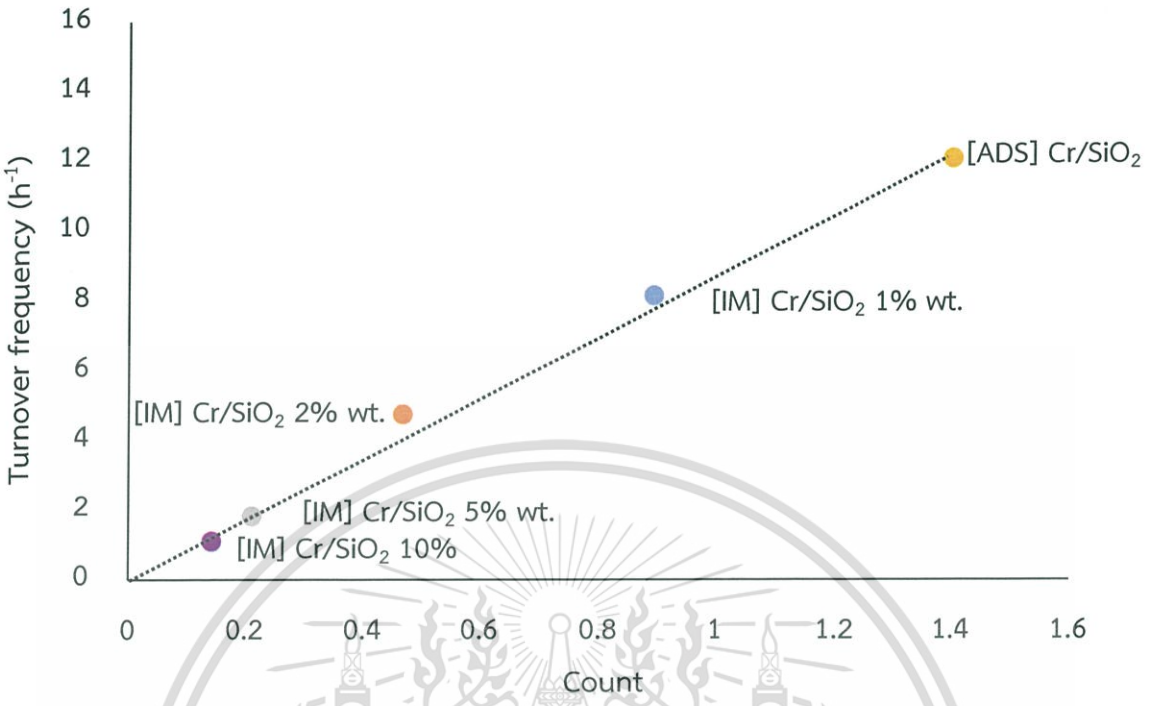

Figure 4.22 Relationship between the intensity of pre-edge absorption by XANES spectra of chromium catalysts (Count) and turnover frequency (TOF).

However, the deactivation of the catalyst was still observed despite that the coke formation is small (weight loss of carbon deposited <0.5% wt). This is because small fraction of chromium single-site is highly dispersed on silica surface. Such isolated Lewis acid center would be sensitive to strong adsorption of any high MW species formed. Accordingly, only small amount of carbon deposits would drastically deactivate the catalyst.

4.2.4 The effect of reduction temperature

From H_2-TPR profiles, the high temperature reduction (650 °C) corresponds to reduction of Cr^{3+} to Cr^{2+} species was observed over [ADS] Cr/SiO_2 catalyst [57]. In order to verify the propane activity over Cr^{3+} and Cr^{2+} species in this chromium catalyst, the effect of reduction temperature on propane dehydrogenation at 550 °C using [IM] Cr/SiO_2 1% wt and [ADS] Cr/SiO_2 catalysts with same contact time were investigated as shown in **Figure 4.23.**

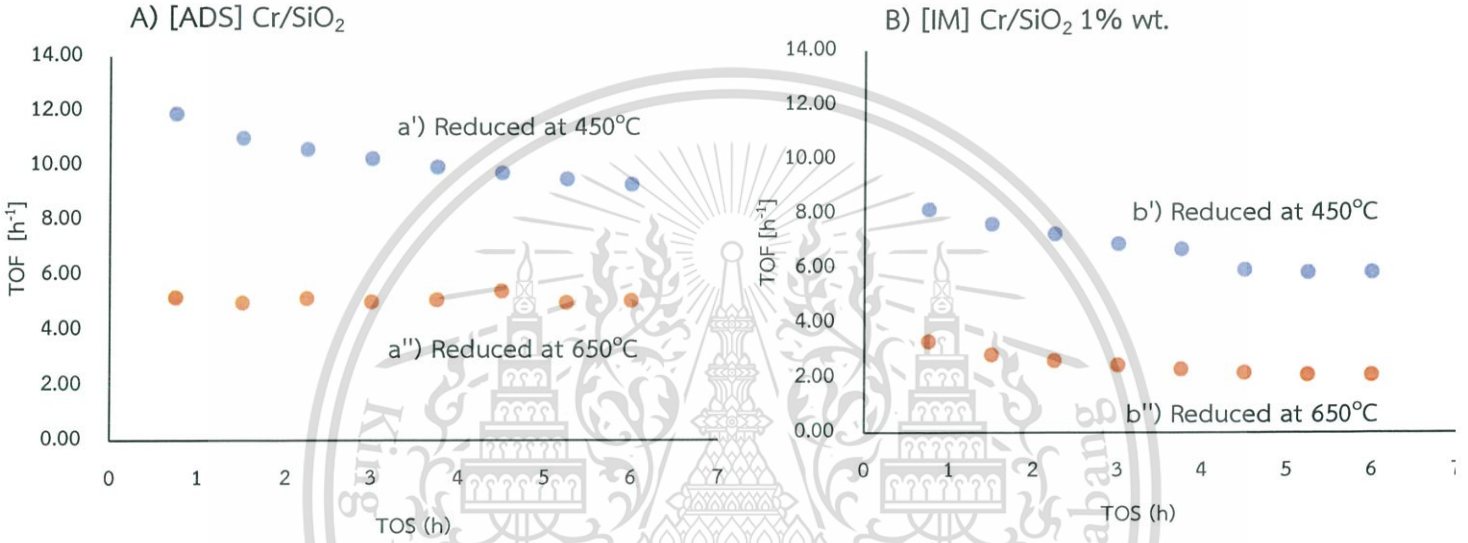

Figure 4.23 Turnover frequency of A)[ADS] Cr/SiO_2 and B) [IM] Cr/SiO_2 1% wt for propane dehydrogenation using reduction temperature at (a',b') 450 °C, (b) 650 °C (a'',b''). *(Reaction temperature: 550 °C, 0.0258mol/h of propane (99.95%), and 50 mL/min hydrogen or nitrogen, W/F; 10 g.h/mol.)*

According to **Figure 4.23**, it is clearly seen that upon reducing chromium at 650 °C, the TOF of both [ADS] Cr/SiO_2 and [IM] Cr/SiO_2 1% wt are decreased (from 11.9 to 5.1 h^{-1} and 8.1 to 3.3 h^{-1}), respectively. This suggests that the isolated Cr^{3+} species (formed upon reduction at ~398 °C) is more active than isolated Cr^{2+} species (formed upon reduction at ~650 °C). This is because Cr^{2+} species possesses lower Lewis acid character, as compared to Cr^{3+} species. As Cr^{3+} species is reduced to Cr^{2+}, electron density of chromium is increased. Hence, weaker interaction of propane with Cr^{2+} can be expected. This would also be the case for the hydride species, leading to lower H-transfer activity. Therefore, the chromium catalyst prepared by strong electrostatic adsorption is reduced at 450 °C ([ADS] Cr/SiO_2) and used for further study.

4.2.5 The effect of carrier gas

In order to study the effect of carrier gas, hydrogen or nitrogen was tested in propane conversion over [ADS] Cr/SiO_2 catalyst. The turnover frequency (TOF) of [ADS] Cr/SiO_2 under N_2 or H_2 atmosphere is shown in **Figure 4.24.**

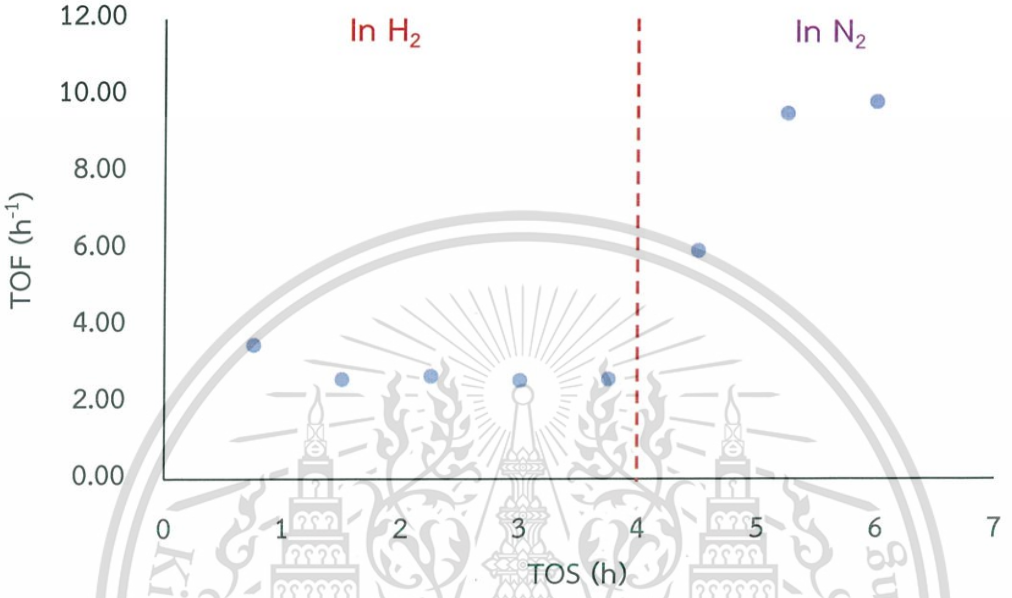

Figure 4.24 Turnover frequency (TOF) of [ADS] Cr/SiO_2 for propane dehydrogenation catalysts under N_2 and H_2 atmosphere.

(Reaction temperature: 550 °C, 0.0258 mol/h of propane (99.95%), and 50 mL/min hydrogen or nitrogen, W/F; 10.5117 g.h/mol,)

As seen from **Figure 4.24**, the turnover frequency (TOF) of [ADS] Cr/SiO_2 using H_2 as a carrier gas is lower than that using N_2 as a carrier gas (**Figure 4.21**). This is presumably due to high concentration of H_2 that promotes the hydrogenation of propylene, in a manner similar to the ethylene hydrogenation, as discussed in the section **4.2.6** (**Figure 4.28**)

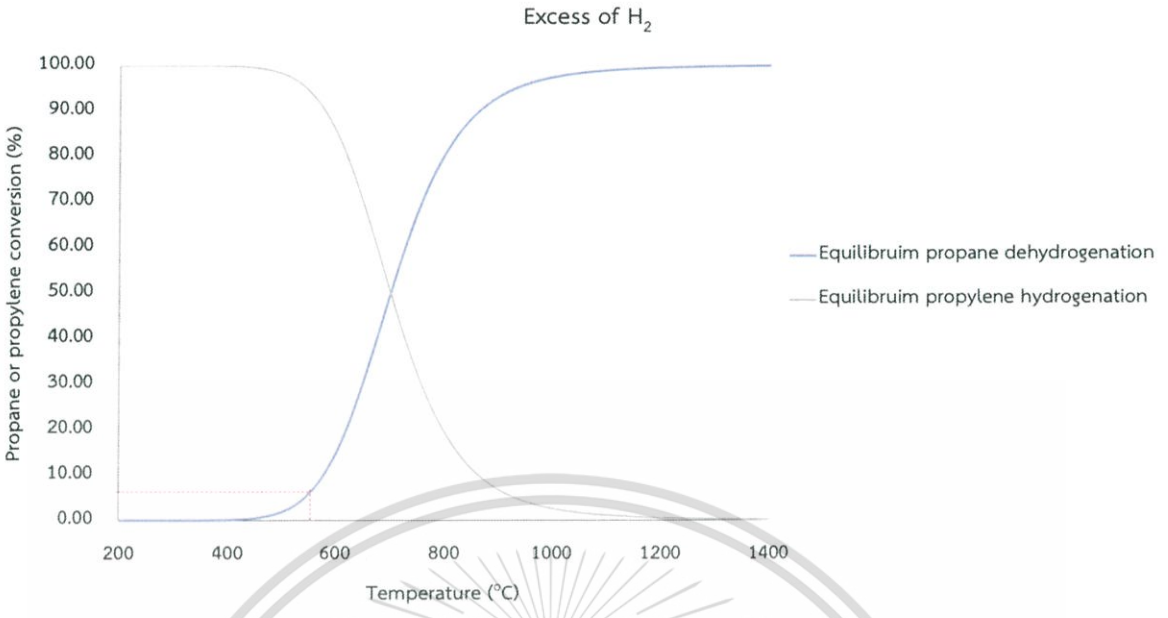

Figure 4.25 Relationship between equilibrium propane dehydrogenation, propylene hydrogenation and temperature under excess H_2 atmosphere.

According to the equilibrium conversion shown in **Figure 4.25**, propane can be readily dehydrogenated to propylene up to only 7 % at 550 °C. While, hydrogenation of propylene is distinctly enhanced at this temperature. Therefore, with excess hydrogen, the rate of propylene hydrogenation (k_2) would also be increased (**Scheme 4.1**) [58].

Scheme 4.1 Dehydrogenation and Hydrogenation of Propane.

Form **Figure 4.24**, it can be seen that when hydrogen was replaced by nitrogen, the turnover frequency (TOF) was gradually increased to the value of that in N_2 (TOF = 10 h^{-1}). This suggests that when concentration of H_2 is gradually decreased, k_2 would be reduced while rate constant, k_1, in **Scheme 4.1** would be enhanced, as observed.

4.2.6 The effect of contact time

In order to verify the reaction pathway for dehydrogenation of propane over different chromium species, the effect of contact time with [IM] Cr/SiO_2 1% wt. and [ADS] Cr/SiO_2 catalyst were investigated. The turnover number (TON) for products at various contact time is represented **in Figure 4.26**.

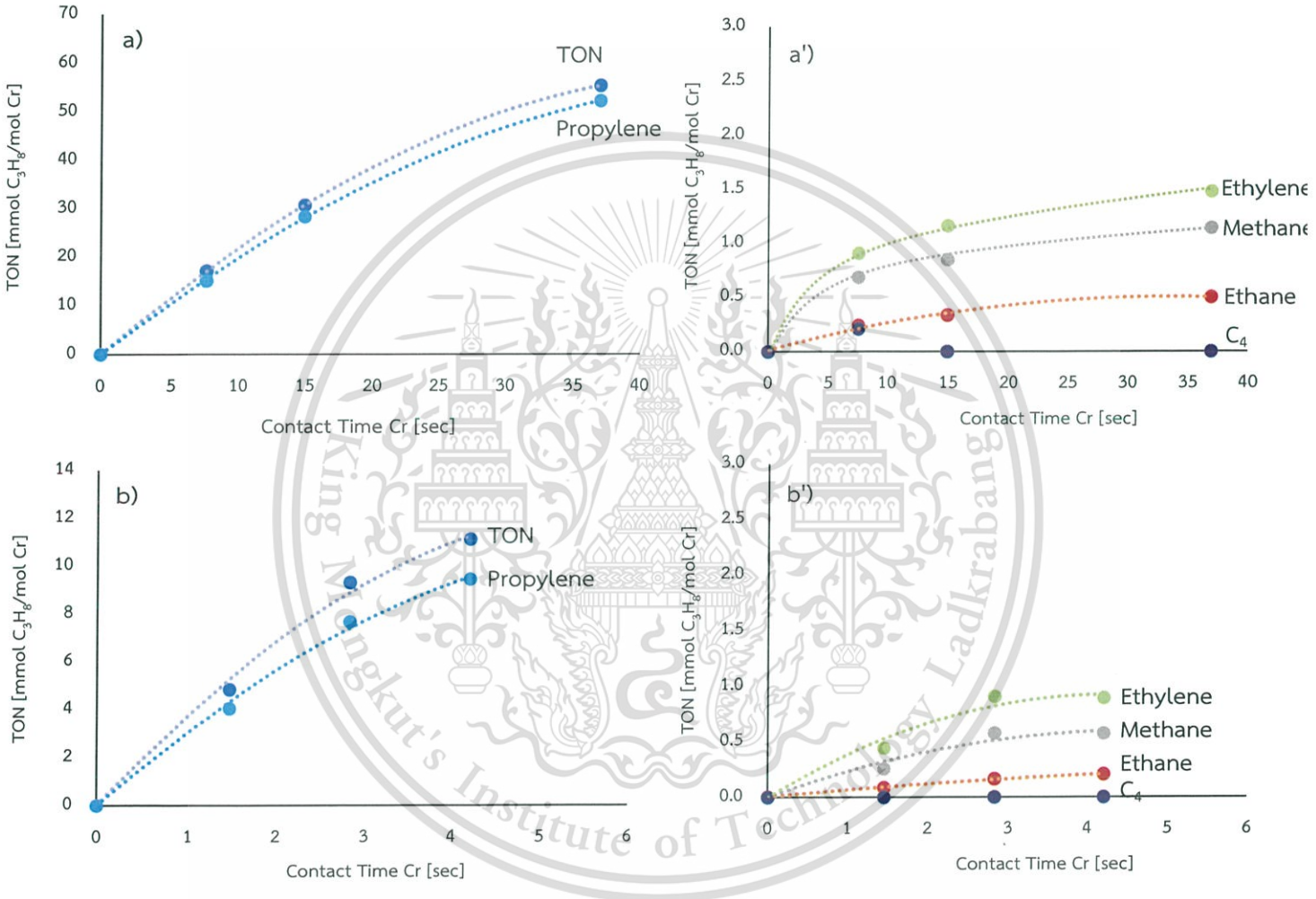

Figure 4.26 Turn over number (TON) by using various chromium catalysts; (a, a') [IM] Cr/SiO_2 1% wt., (b, b') [ADS] Cr/SiO_2 catalysts. (TON; is calculated from moles of desired product formed per Cr active site). *(Reaction temperature: 550 °C, Pressure 1 atm, Feed rate: 0.5819 g/h of Propane, W/F: 0-31 g.h.mol^{-1}, W/F of Chromium: 1-37 sec, Average results at 45 minutes of time on stream)*

It can be seen form **Figure 4.26** that the turnover number (TON) is increased with contact time. This is because increasing the contact time provides a better opportunity for the propane to interact with the active sites. Propylene is the major product (**Figure 4.26a, b**); while methane, ethane and ethylene are found as minor products (**Figure 4.26a', b'**). The propylene yield is initially increased with contact time (**Figure 4.26a**), suggesting that propane can be catalytic converted to propylene via dehydrogenation. In the mechanistic point of view, it was suggested by Matthew P., *et al.* [10] that the reaction is initiated by C-H bond cleavage to form chromium-propylidene intermediate as shown in **Figure 4.27** (intermediate 3). While the surface oxygen stabilizes the dissociated proton. The chromium propylidene can undergo a β-H elimination to form chromium propene hydride (intermediate 4). Propene is subsequently released bearing the chromium hydride species on the surface (intermediate 5). Finally, the chromium hydride can react with the neighboring hydroxyl proton to generate hydrogen that desorbs as H_2 gas [10]. The overall reaction pathway for propane dehydrogenation on chromium catalyst is represented **in Figure 4.27**.

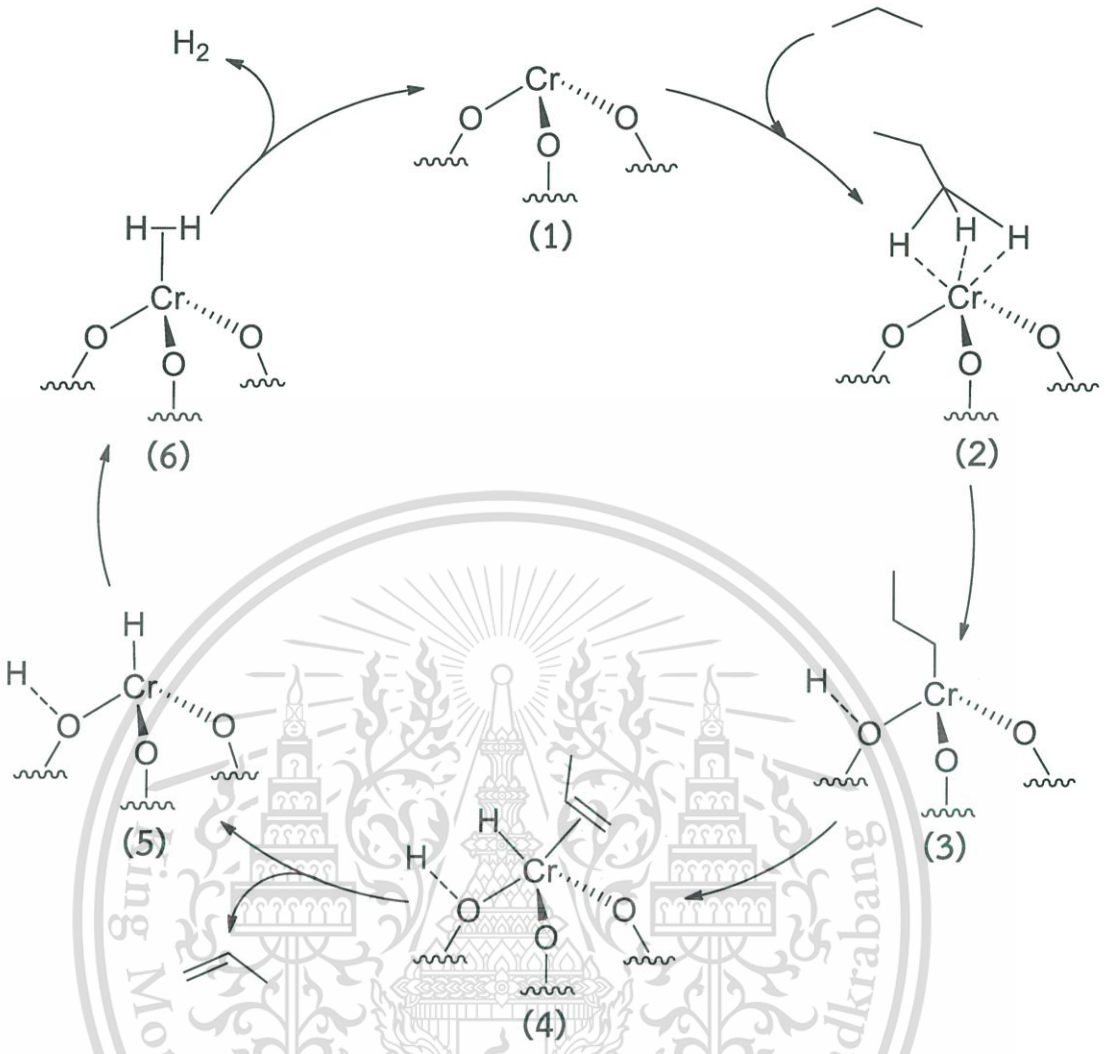

Figure 4.27 Catalytic cycle reaction pathway for propane dehydrogenation on chromium heterogeneous catalysts [10].

In a different manner (**Figure 4.26a', b'**), methane and ethylene is significantly increased at initial, but only slight increased, as the catalyst bed is increased. This suggests that methane and ethylene are produced in parallel by thermal cracking. As the catalyst bed is increased, the catalyst surface is also enhanced. Accordingly, the thermal distribution is improved and the thermal activity is enhanced. A small amount of ethane can also be obtained, presumably due to ethylene hydrogenation. It was also suggested by Matthew P., *et al.* [10] that ethylene hydrogenation can be thermodynamically activated. This reaction is initiated by coordination of ethylene, generated from the cracking of propane, to form the **π**-coordinated species as shown

in **Figure 4.28** (intermediate 3). Such species is inserted by chromium hydride to form the chromium ethyl complex (intermediate 4). Finally, the chromium ethyl complex reacts with the neighboring hydroxyl proton to generate ethane. The overall catalytic cycle for hydrogenation of ethylene over single-site chromium catalyst is represented **Figure 4.28**.

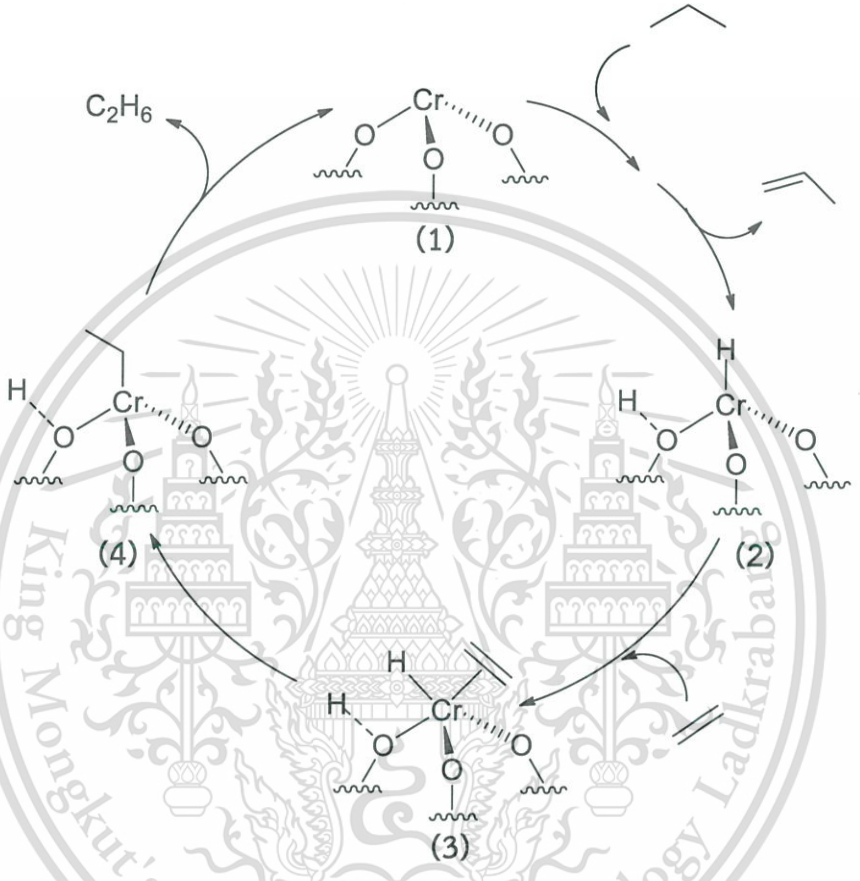

Figure 4.28 Catalytic cycle reaction pathway for hydrogenation of ethylene to ethane on chromium heterogeneous catalysts [10].

It can be concluded at this stage, propane can be dehydrogenated to form propylene and hydrogen. Propane can also thermally crack to methane and ethylene. While ethylene can be further hydrogenated to ethane. the overall reaction pathway can be proposed in **Scheme 4.2**.

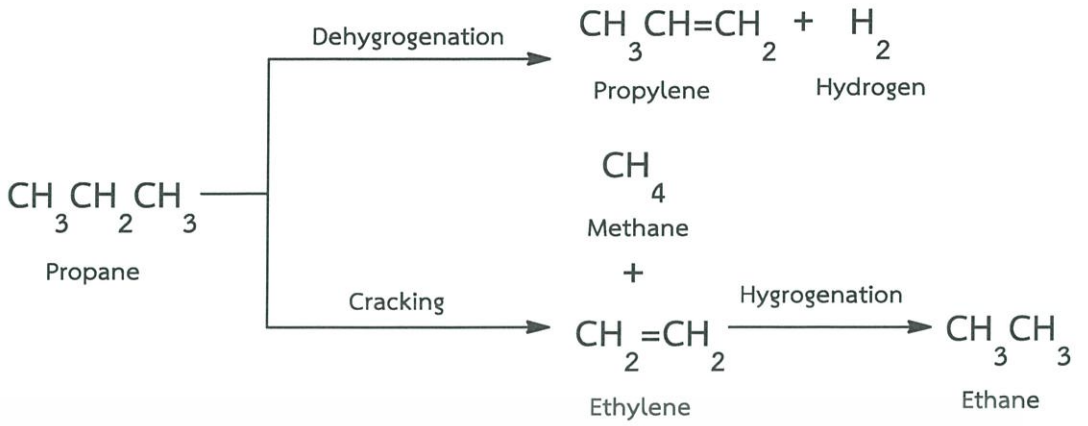

Scheme 4.2. Proposed reaction mechanism of propane conversion over chromium catalysts.

From **Figure 4.26**, it was observed that the reaction pathway of propane conversion over [ADS] Cr/SiO_2 catalyst is similar to [IM] Cr/SiO_2 catalyst. Nevertheless, the initial rate of propane dehydrogenation over [ADS] Cr/SiO_2 is relatively higher than that over [IM] Cr/SiO_2 catalyst as shown in **Figure 4.29**. This is again because of a higher fraction of single-site chromium in the catalyst prepared by strong electrostatic adsorption ([ADS] Cr/SiO_2), as discussed earlier.

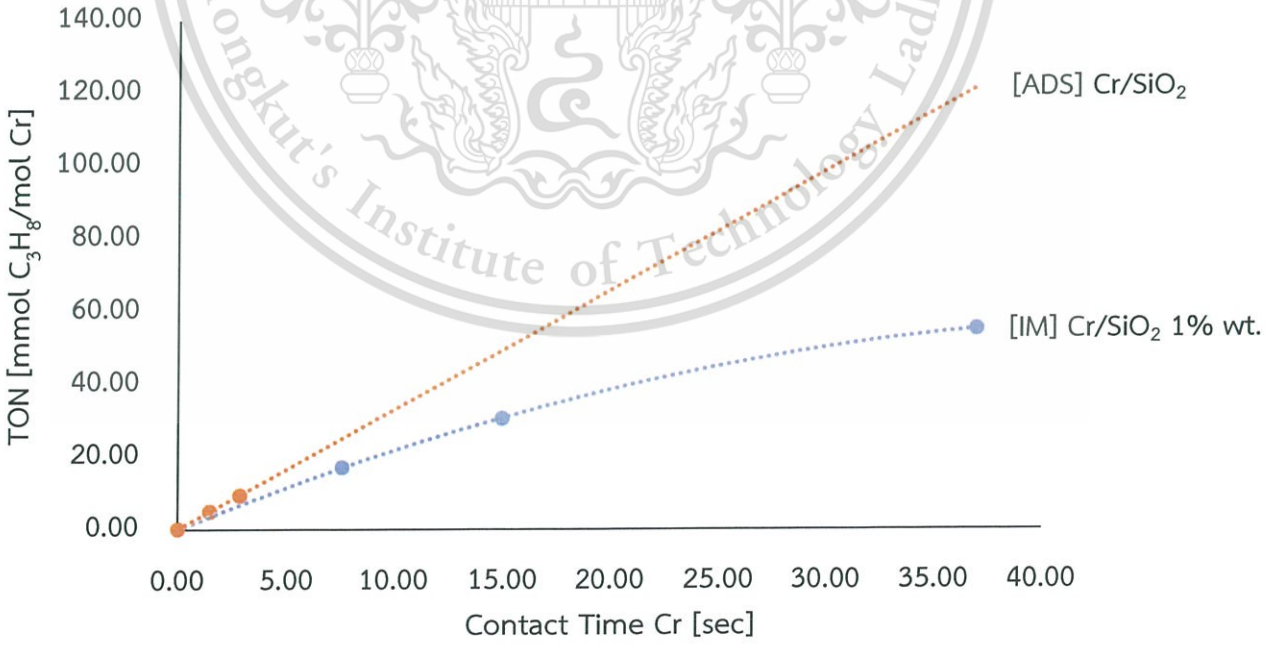

Figure 4.29 Relationship between the turnover number (TON) and contact time.

4.2.7 Comparing chromium single-site and cobalt single-site catalyst

. From the Hu, B., *et al*. reports, the single-site Co^{2+} heterogeneous catalysts on silica support possesses high selectivity of propylene (~90%) [9]. These catalysts have an isolated active site that is believed to provide low coke formation and greater selectivity to the desired products, as compared to those observed over non-single-site heterogeneous catalysts of similar composition. Therefore, it is of interest to compare chromium single-site catalyst prepared in this study with the cobalt single-site catalyst in propane dehydrogenation. The reaction at temperature 550 °C were studied over [ADS] Cr/SiO_2 and [ADS] Co/SiO_2 with same contact time as shown in **Figure 4.30.**

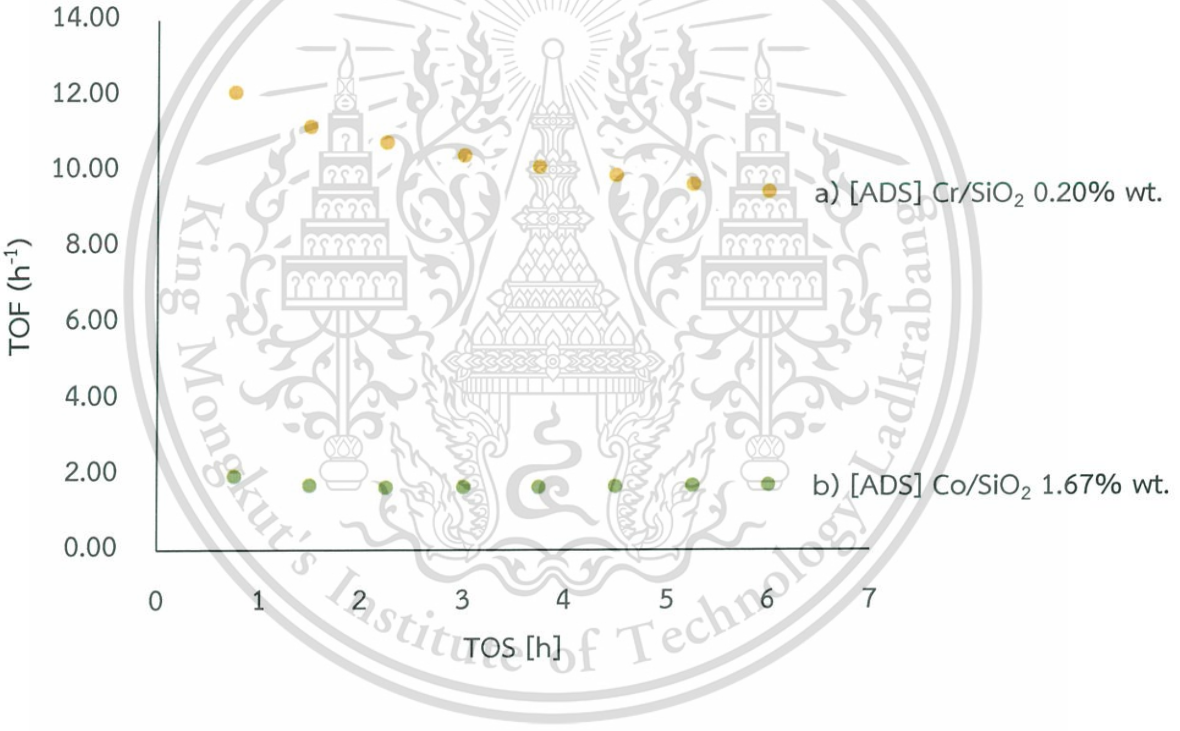

Figure 4.30 Turn over frequency (TOF) for propane dehydrogenation (a) [ADS] Cr/SiO_2 0.2% and (b) [ADS] Co/SiO_2 1.67% wt. catalyst. (Reaction temperature: 550 °C, 0.0258 mol/h of propane (99.95%), and 50 mL/min nitrogen, W/F; 10 g.h/mol,)

From **Figure 4.30**, the [ADS] Cr/SiO_2 0.2% wt. shows notably higher TOF, as compared to the [ADS] Co/SiO_2 1.67% wt. catalyst at the same contact time. This suggests that the [ADS] Cr/SiO_2 possesses activity higher than [ADS] Co/SiO_2 catalyst. This is because Cr^{3+} species in [ADS] Cr/SiO_2 catalyst exhibits stronger Lewis acid character, as compared to Co^{2+} species in [ADS] Co/SiO_2 catalyst [59]. Therefore, C-H bond cleavage can be readily promoted over Cr^{3+} species.

However, the preparation of chromium single-site catalyst with high concentration is somewhat complicated, as compared to the Co^{2+} single-site catalyst. This is due to the nature of chromium oxide that readily form chromium oxide cluster at high concentration [60]. Whereas cobalt complex is stable and can be highly dispersed on silica surface [8]. Therefore, most reports are focused on the cobalt single-site catalysts. Although, chromium single-site catalyst in this study has shown a better activity, a procedure for the preparation of high concentration, uniform chromium single-site need further investigation.

CHAPTER 5
CONCLUSION AND SUGGESTION

5.1 Conclusions

In this thesis, the production of propylene from propane using chromium single-site heterogeneous catalysts on silica support was evaluated. All catalysts were categorized as high surface area material (206-319 m^2/g) with expected metal loading (0.2-10% wt.) as evidence by X-ray fluorescence (XRF) and Inductively coupled plasma mass spectrometry (ICP-MS). The H_2-TPR profiles shows the high reduction temperature (~398 °C) for catalyst species prepared by adsorption method [ADS] and prepared by wetness impregnation [IM] at low chromium loading (<2% wt.). This indicates the present of highly dispersed of monomeric Cr^{6+} in these catalysts. While at high chromium loading, polymeric Cr^{6+} species was observed (~350 °C). In the case of cobalt catalyst, the high reduction temperature (~780 °C) was observed, indicating a highly dispersed Co^{2+} single-site species [36].

For impregnated catalysts, a mixture of octahedral Cr^{3+} and tetrahedral Cr^{6+} species were observed by X-ray absorption spectroscopy near edge structure (XANES). Upon increasing the loading, most of chromium exists as octahedral Cr^{3+} species. The extended X-ray absorption fine structure (EXAFS) indicates that 2-dimensional polymeric chromium oxide sheet on the silica surface is present in the catalysts. DR-UV results confirms that [IM] Cr/SiO_2 1% wt consists of highly dispersed tetrahedral chromium oxide, polymeric chromium oxide and bulk chromium oxide in octahedral coordination. For catalyst prepared by adsorption method, the present of tetrahedral Cr^{6+} species were fulfilled by XANES and EXAFS results. In consistence with DR-UV results, such catalyst only contain highly dispersed, isolated chromium oxide.

Propane dehydrogenation, thermal cracking can be observed over silica supported at >550 °C. When chromium is present, a higher activity was obtained as chromium can promote C-H cracking, rather than C-C cracking. The result shows that the activation of C-H bond cleavage of propane requires at least 500 °C over chromium catalyst. The main product was propylene at all temperatures over 500-650 °C. When the temperature rises, methane and ethylene are observed from the

cracking of propane. While, small amount of ethane is also observed, presumably due to hydrogenation of ethylene. A reaction temperature of 550 °C provide high selectivity of propylene with reasonable propane conversion.

The study on the effect of chromium loading shows that the conversion of propane is not proportionally increased with chromium loading. This is because the chromium single-site are active species for propane dehydrogenation and this chromium single-site species are only found at low chromium concentration (< 2% wt.). The results also show that [ADS] Cr/SiO_2 possesses higher fraction of chromium single-site species, as compare to [IM] Cr/SiO_2 1% wt. catalyst. However, the catalysts are deactivated due to the coke formation. The reaction pathway over [ADS] Cr/SiO_2 is similar to that over [IM] Cr/SiO_2 catalyst; whereby, propane can be mainly dehydrogenated to form propylene and hydrogen. In parallel, thermally cracking to methane and ethylene is evidenced. While some of ethylene can also be hydrogenated to ethane.

Using H_2 as a carrier gas leads to the lower activity compared with using N_2 as a carrier gas. This is due to the hydrogenation of propylene produced in excess H_2. The reduction of Cr^{3+} single-site to Cr^{2+} species at high temperature results in a lower activity. This is because Cr^{2+} possesses a higher electron density, and hence a weaker Lewis acidity, as compared to Cr^{3+} species. It was also observed that [ADS] Cr/SiO_2 shows higher TOF, as compared to [ADS] Co/SiO_2 catalyst. This is due to the stronger Lewis acid character of Cr^{3+}, as compared to Co^{2+}.

5.2 Suggestions

5.2.1) In order to increase high concentration of chromium single-site species, the chromium complexes were should as a precursor for the adsorption technique.

5.2.2) In order to increase the activity, the increase of surface area of the support, such as MCM-41 and silicalite is another promising strategy.

REFERENCES

[1] T. Ren, M. Patel and K. Blok. 2006. "**Olefins from conventional and heavy feedstocks: Energy use in steam cracking and alternative processes.**" *Energy*. 31 : 425–451.

[2] D. Dharia, A. Batachari, P. Naik and C. Bowen. 2004. "**Chapter 8: Catalytic Cracking for Integration of Refinery and Steam Crackers**" Advances in Fluid Catalytic Cracking: Testing Characterization, and Environmental Regulations, CRC Press, pp. 119-126.

[3] X. Zhang, Y. Yue and Z. Gao. 2002. "**Chromium oxide supported on mesoporous SBA-15 as propane dehydrogenation and oxidative dehydrogenation catalysts.**" *Catalyst Letter*. 83 : 19–25.

[4] Z. Rena, Z. Wub, W. Songc, W. Xiaod, Y. Guoa, J. Dingd, S. L. Suiba and P. Gao. 2016. "**Low temperature propane oxidation over Co_3O_4 based nano-array catalysts: Ni dopant effect, reaction mechanism and structural stability.**" *Applied Catalysis B: Environmental*. 180 : 150–160.

[5] X. Ge, H. Zou, J. Wang and J. Shen. 2004. "**Modification of Cr/SiO_2 for the dehydrogenation of propane to propylene in carbon dioxide.**" *Catalyst Letter*. 85 : 253–260.

[6] J. J. H. B. Sattler, J. Ruiz-Martinez, E. Santillan-Jimenez and B. M. Weckhuysen. 2014. "**Catalytic Dehydrogenation of Light Alkanes on Metals and Metal Oxides**" *Chemical Reviews*. 114 : 10613–10653.

[7] M. Larssona, M. Hulténb, E. A. Blekkanc and B. Andersson. 1996. "**The Effect of Reaction Conditions and Time on Stream on the Coke Formed during Propane Dehydrogenation.**" *Journal of Catalysis*. 164 : 44–53.

[8] B. Hu, A. B. Getsoiana, N. M. Schweitzera, U. Dasa, H. Kima, J. Niklasa, O. Poluektova, L. A. Curtissa, P. C. Staira, J. T. Millera and A. S. Hocka, 2015. "**Selective propane dehydrogenation with single-site Co^{II} on SiO_2 by a non-redox mechanism.**" *Journal of Catalysis*. 322 : 24–37.

[9] N. M. Schweitzer, B Hu, U. Das, H. Kim, J. Greeley, L. A. Curtiss, P. C. Stair, J. T. Miller and A. S. Hock. 2014. "**Propylene Hydrogenation and Propane Dehydrogenation by a Single-Site Zn^{2+} on Silica Catalyst**" *ACS Catalysis*. 4 : 1091–1098.

[10] M. P. Conley, M. F. Delley, F. Núñez-Zarur, A. Comas-Vives and C. Copéret. 2015. "**Heterolytic Activation of C-H Bonds on Cr^{III}-O Surface Site Is a Key Step in Catalytic Polymerization of Ethylene and Dehydrogenation of Propane**" *Inorganic Chemistry*. 54 : 5065–5078.

[11] S. Matar and L. F. Hatch. 2000. "**Hydrocarbon Intermediates**" Chemistry of Petrochemical processes, 2.

[12] A. G. Buekens and G. F. Froment. 1968. "**Thermal Cracking of Propane. Kinetics and Product Distributions**" *Ind. Eng. Chem. Process Des. Dev.*, 7(3) : 435-447.

[13] T. A. Petersa, O. Liron, R. Tschentschera, M. Sheintuch, R.Bredesen. 2016. "**Investigation of Pd-based membranes in propane dehydrogenation (PDH) processes**" *Chemical Engineering Journal.*, 305 : 191-200.

[14] A. Tóth, G. Halasi, T. Bánsági and F. Solymosi. 2016. "**Reactions of propane with CO_2 over Au catalysts**" *Journal Catalysis.*, 337 : 57-64.

[15] F. Solymosi, P. Tolmacsov and T. SüliZakar 2005. "**Dry reforming of propane over supported Re catalyst**" *Journal Catalysis.*, 233 : 51-59.

[16] I. Chorkendorff and J. W. Niemantsverdriet. 2003. "**Catalysts Can Be Atoms, Molecules, Enzymes and Solid Surfaces**" Concepts of Modern Catalysis and Kinetics.

[17] E. Farnetti, R. D. Monte and J. Kašpar. 2009. "**Homogeneous and Heterogeneous Catalysis**" Inorganic and Bio-Inorganic Chemistry.

[18] O. Deutschmann, H. Knözinger, K. Kochloefl and T. Turek. 2009. "**Types of Catalysis**" Heterogeneous Catalysis and Solid Catalysts, 2.

[19] C. E. Housecroft and A. G. Sharpe. 2005. "**Homogeneous and heterogeneous catalysis.**" *Catalyst Letter*. 85 : 253–260.

[20] H. Knözinger and K. Kochloefl. 2003. "**Heterogeneous Catalysis and Solid Catalysts**" Inorganic Chemistry, 2.

[21] J. M. Thomas, R. Raja and D. W. Lewis. 2005. "**Single-Site Heterogeneous Catalysts**" *Angew. Chem. Int. Ed.* 44 : 6456–6482.

[22] G. Xiaoguang, F. Guangzong, L. Gang, M. Hao, F. Hongjun, Y. Liang, M. Chao, W. Xing, D. Dehui, W. Mingming, T. Dali, S. Rui, Z. Shuo, L. Jianqi, S. Litao, T. Zichao, P. Xiulian and B. Xinhe. 2014. "**Direct, Nonoxidative Conversion of Methane to Ethylene, Aromatics, and Hydrogen**" *Science*. 344 : 616–619.

[23] C. Copÿret, M. Chabanas, R. P. Saint-Arroman and J. M. Basset . 2003. "**Homogeneous and Heterogeneous Catalysis: Bridging the Gap through Surface Organometallic Chemistry**" *Angew. Chem. Int. Ed*. 42 : 156-181.

[24] K. P. D. Jong and J. R. Regalbuto. 2009. "**Electrostatic Adsorption**" Synthesis of Solid Catalysts. Edited by K.P. de Jong

[25] Y. Liu, L. Luo, Y. Gao and W. Huang. 2016. "**CeO_2 morphology-dependent NbO_x–CeO_2 interaction, structure and catalytic performance of NbO_x/CeO_2 catalysts in oxidative dehydrogenation of propane**" *Applied Catalysis B: Environmental*., 197 : 214-221.

[26] S. A. Al-Ghamdi and H. I. Lasaa. 2014. "**Propylene production via propane oxidative dehydrogenation over VO_x/γ-Al_2O_3 catalyst**" *Fuel*., 128 : 120-140.

[27] J.P. Brunelle. 1978. "**Preparation of Catalysts by Metallic Complex Adsorption on Mineral Oxides**" *Pure Appl. Chem*., 50 : 1211.

[28] V. M. T. Herauville and Frigyes Solymosi., 2005. "**Catalytic Dehydrogenation of Propane Oxidative and Non-Oxidative Dehydrogenation of Propane**" Norwegian University of Science and Technology.

[29] Y. Zhang, Y. Zhou, A. Qiu, Y. Wang, Y. Xu and P. Wu. 2006. "**Effect of Alumina Binder on Catalytic Performance of Pt-Sn-Na/ZSM-5 Catalyst for Propane Dehydrogenation**" *Ind. Eng. Chem. Res*., 45 : 2213-2219.

[30] B. Khanh, V. Myoung, B.Songaln, Y.Ahn, Y. W. Suh, D. J. Suh, J. S. Kim and E. W. Shin 2011. "**Location and structure of coke generated over Pt–Sn/Al2O3 in propane dehydrogenation**" *Journal of Industrial and Engineering Chemistry,* 17 : 71-76.

[31] P. Sabatier. 2004. "**History of Chemistry and Chemical Technology**" *Russian Journal of Applied Chemistry.* 77(11) : 1909-1912.

[32] H. Dyrbeck., 2007. "**Selective Catalytic Oxidation of Hydrogen and Oxygen-assisted Conversion of Propane**" Norwegian University of Science and Technology. 194.

[33] B.M. Weckhuysen, I. E. Wachs and R. A. Schoonheydt. 1996. "**Surface Chemistry and Spectroscopy of Chromium in Inorganic Oxides**" *Chem. Rev.*, 96 : 3327-3349.

[34] S. J. Lippard and J. M. Berg. 1994. "**Principles of Bioinorganic Chemistry**". California : University Science Books.

[35] P. Phichitsurathaworn, S. Ketaniruj and S. Sitthithai 2014. "**Conversion of ethanol to gasoline over metal transition loaded H-ZSM-5 zeolite catalysts**" Bachelor degree of science, Industrial Chemistry, Faculty of Science, King Mongkut's Institute of Technology Ladkrabang.

[36] T. Kurato, S. Kuhatasanadeekul and A. Worathanaseth. 2015. "**The study of cyclohexane cracking using single-site cobalt heterogeneous catalysts**" Bachelor degree of science, Industrial Chemistry, Faculty of Science, King Mongkut's Institute of Technology Ladkrabang.

[37] A. Ausavasukhi. 2002. "**The Production of Gasoline and Aromatics from Ethanol**" Master degree of science, Petrochemical and hydrocarbon chemistry, Faculty of Science, King Mongkut's Institute of Technology Ladkrabang.

[38] J. M. Thomas and P. L. Gai. 2004. "**Electron Microscopy and the Materials Chemistry of Solid Catalysts**" *Advances in Catalysis*, 48 : 171-227.

[39] A. W. Coats and J. P. Redfern. 1963. "**Thermogravimetric Analysis: A Review**" *Analyst*, 88 : 906-924.

[40] P. Fornasiero and M. Cargnello. 2007. "**Characterization of porous solids VII. Studies in surface science and catalysis**" *Elsevier*, 49-56.

[41] D. Gajan and C. Copéret 2011. "**Silica-supported single-site catalysts: to be or not to be? A conjecture on silica surfaces**" *New J. Chem.*, 35 : 2403-2408.

[42] A. Chakrabarti and I. E. Wachs. 2015. "**The Nature of Surface CrO_x Sites on SiO_2 in Different Environments**" *Catal Lett.*, 145 : 985-994.

[43] Y. Jibril. 2004. "**Propane oxidative dehydrogenation over chromium oxide-based catalysts**" *Applied Catalysis A: General*, 264 : 193-202.

[44] H. S. Nalwa 2001. "**Handbook of Surfaces and Interfaces of Materials, Five-Volume Set**" *USA* : Stanford Scientific Corporation.

[45] A. Zecchina, E. Groppo, A. Damin and C. Prestipino. 2005. "**Anatomy of Catalytic Centers in Phillips Ethylene Polymerization Catalyst**" *Top. Organomet. Chem*, 16 : 1-35.

[46] D. Eley, W. Haag and B. Gates 1996. "**Advances in Catalysis**". England : The University Nottingham.

[47] R. Xie, C. Wang, L. Xia, H. Wang, T. Zhao and Y. Sun. 2015. "**Controlled Preparation of Co_3O_4@porous-SiO_2 Nanocomposites for Fischer–Tropsch Synthesis**" *Catal Lett*, 144 : 516-523.

[48] H. Yamashita and M. Anpo. 2004. "**Local structures and photocatalytic reactivities of the titanium oxide and chromium oxide species incorporated within micro- and mesoporous zeolite materials: XAFS and photoluminescence studies**" *Chem. Rev.*, 105 : 115-183.

[49] M. Anpo, T. H. Kim and M. Matsuoka 2009. "**The design of Ti-, V-, Cr-oxide single-site catalysts within zeolite frameworks and their photocatalytic reactivity for the decomposition of undesirable molecules—The role of their excited states and reaction mechanisms**" *Catalysis. Today.*, 142 : 114-124.

[50] H. Yamashita, M. Ariyuki, S. Higashimoto, S. G. Zhang, J. S. Chang, S. E. Park, J. M. Lee, Y. Matsumura and M. Anpo. 1999. "**Characterization and photocatalytic reactivities of Cr-HMS Mesoporous molecular sieves**" *J. Synchrotron Rad.*, 6 : 453-454.

[51] G. Ghiotti, E. Garrone, G. D. Gatta, B. Fubini and E. Giamello. 1983. "**The chemistry of silica-supported chromium ions: Calorimetric and spectroscopic study of nitric oxide adsorption**" *J. Catal.*, 80 : 249-262.

[52] E. Groppo, C. Prestipino, F. Cesano, F. Bonino, S. Bordiga, C. Lamberti, P. C. Thüne, J. W. Niemantsverdriet and A. Zecchinaa. 2004. "**In situ, Cr K-edge XAS study on the Phillips catalyst: activation and ethylene polymerization**" *J. Catal.*, 230 : 98-108.

[53] E. Groppo C. Lamberti, S. Bordiga, G. Spoto and A. Zecchina. 2005. "**The Structure of Active Centers and the Ethylene Polymerization Mechanism on the Cr/SiO_2 Catalyst: A Frontier for the Characterization Methods**" *Chem. Rev.*, 105 : 115-183.

[54] E. L. Lee and I. E. Wachs. 2014. "**In Situ Spectroscopic Investigation of the Molecular and Electronic Structures of SiO_2 Supported Surface Metal Oxides**" *J. Phys. Chem. C.*, 111 : 14110-14425.

[55] J. T. Wright, D. Su, T. V. Buurenc and R. W. Meulenberg. 2014. "**Electronic structure of cobalt doped CdSe quantum dots using soft X-ray spectroscopy**" *J. Mater. Chem. C.*, 2 : 8313-8321.

[56] B. M. Weckhuysen and R. A. Schoonheydt. 1999. "**Alkane dehydrogenation over supported chromium oxide catalysts.**" *Catal. Today.*, 51 : 223-232.

[57] B. M. Weckhuysen and R. A. Schoonheydt. 1999. "**Olefin polymerization over supported chromium oxide catalysts.**" *Catal. Today.*, 51 : 215-221.

[58] J. J. Kay. 1999. "**Application of the Second Law of Thermodynamics and Le Chatelier's Principle to the Developing Ecosystem**". In Muller, F. Handbook of Ecosystem Theories and Management. Environmental & Ecological (Math) Modeling. CRC Press. ISBN 978-1-56670-253-9.

[59] R.G. Pearson. 1963. "**Hard and Soft Acids and Bases**" *Journal of the American Chemical Society*, 85 : 3533-3539.

[60] M. K. Dinker and P. S. Kulkarni. 2015. "**Recent Advances in Silica-Based Materials for Removal of Hexavalent Chromium: A Review**" *Journal of the Chemical & Engineering Data*, 60 : 2521-2540.

APPENDICES

APPENDIX A

CHARACTERIZATION OF CATALYSTS

1. Elemental Analysis and Gas Adsorption

Table A1: Elemental composition of various catalysts

Catalysts	Support calcination temperature (°C)	*S_{BET} (m^2/g)	% Metal loading	**** H_2 consumption (mmol/g)
SiO_2	650	319	-	-
[IM] Cr/SiO_2 1% wt.	650	231	1.05**	0.04
[IM] Cr/SiO_2 2% wt.	650	225	1.83**	0.08
[IM] Cr/SiO_2 5% wt.	650	218	4.89** (5.18)***	0.16
[IM] Cr/SiO_2 10% wt.	650	206	9.58**	0.11
[ADS] Cr/SiO_2	650	263	0.20**	0.12
[ADS] Co/SiO_2	-	206	1.67**	0.27

* Determined by BET ** Determined by ICP-MS *** Determined by XRF **** Determined by H_2-TPR

2. Gas Adsorption Analysis Isotherm

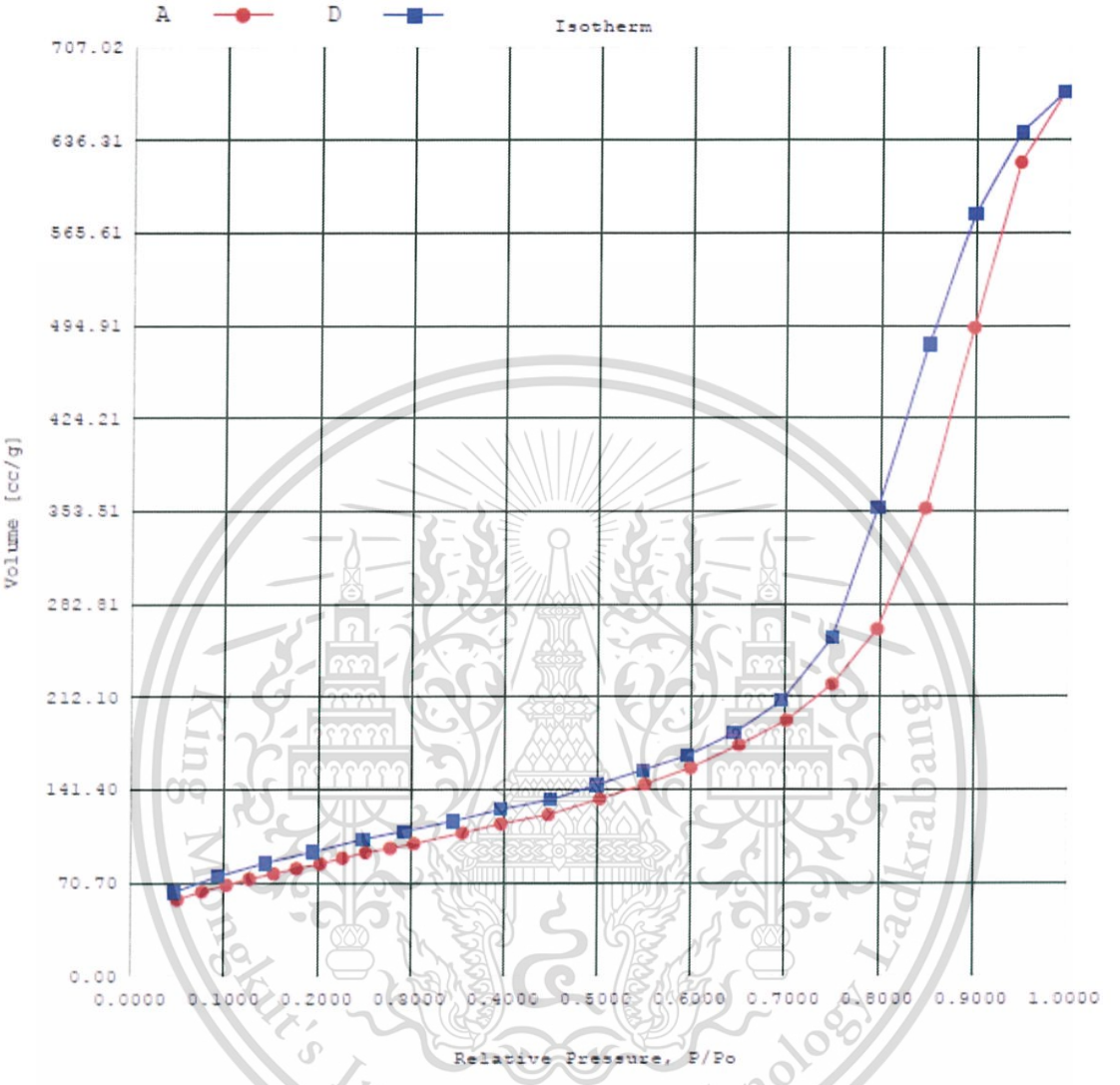

Area 319.05 m²/g

Figure A1 Isotherm of SiO_2

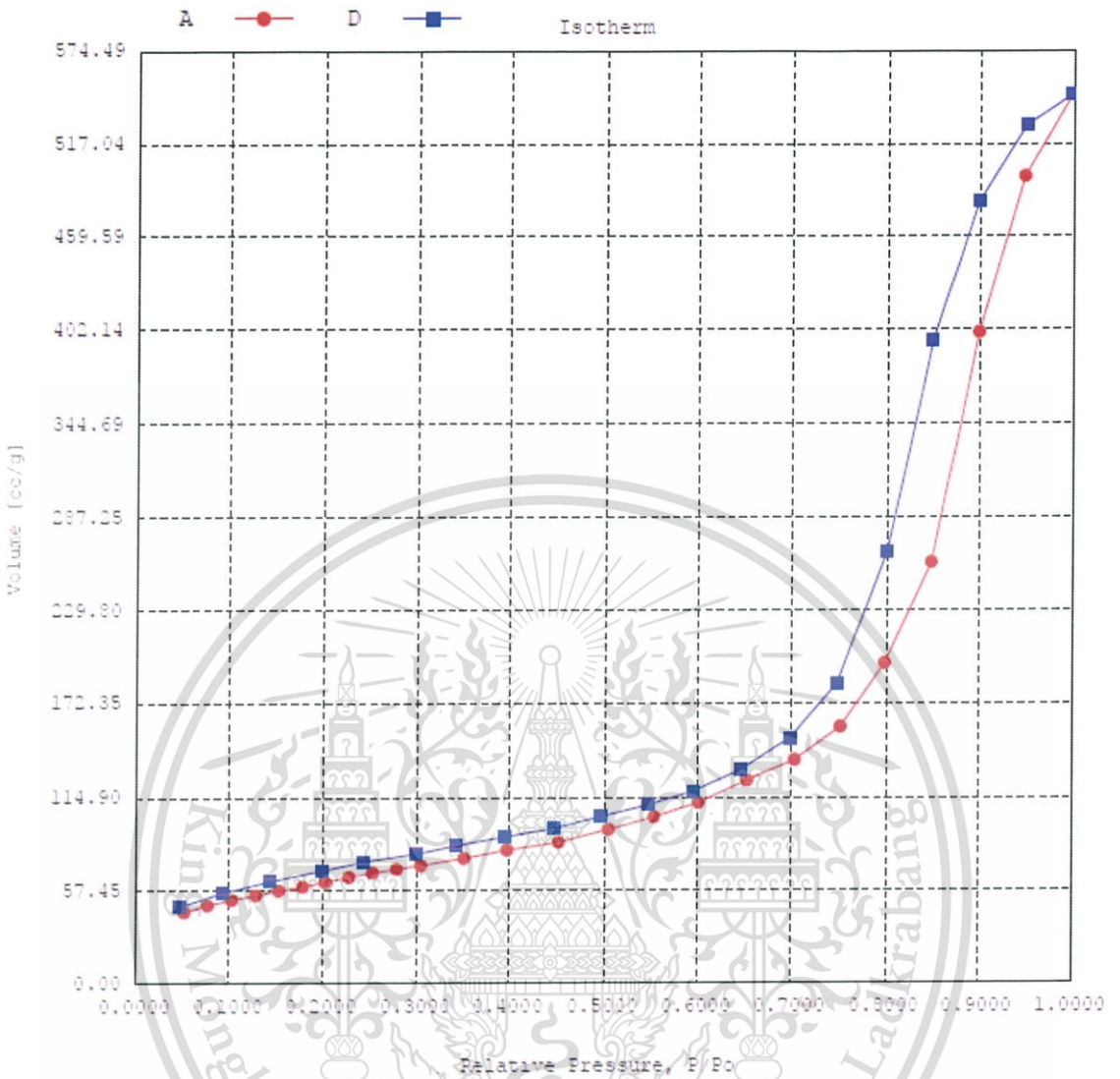

Area 231.18 m²/g

Figure A2 Isotherm of [IM] Cr/SiO_2 1% wt.

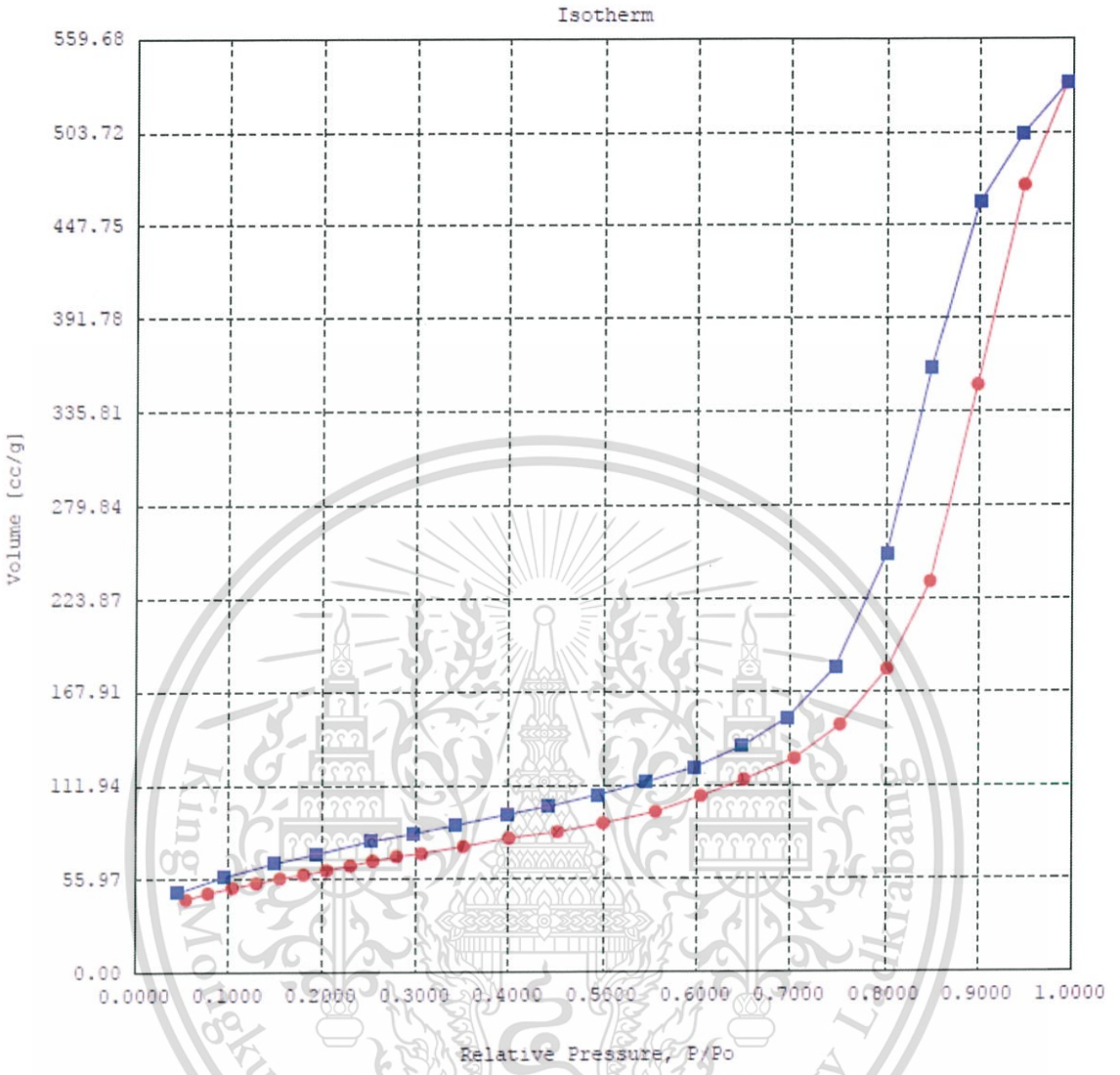

Area 225.11 m²/g

Figure A3 Isotherm of [IM] Cr/SiO_2 2% wt.

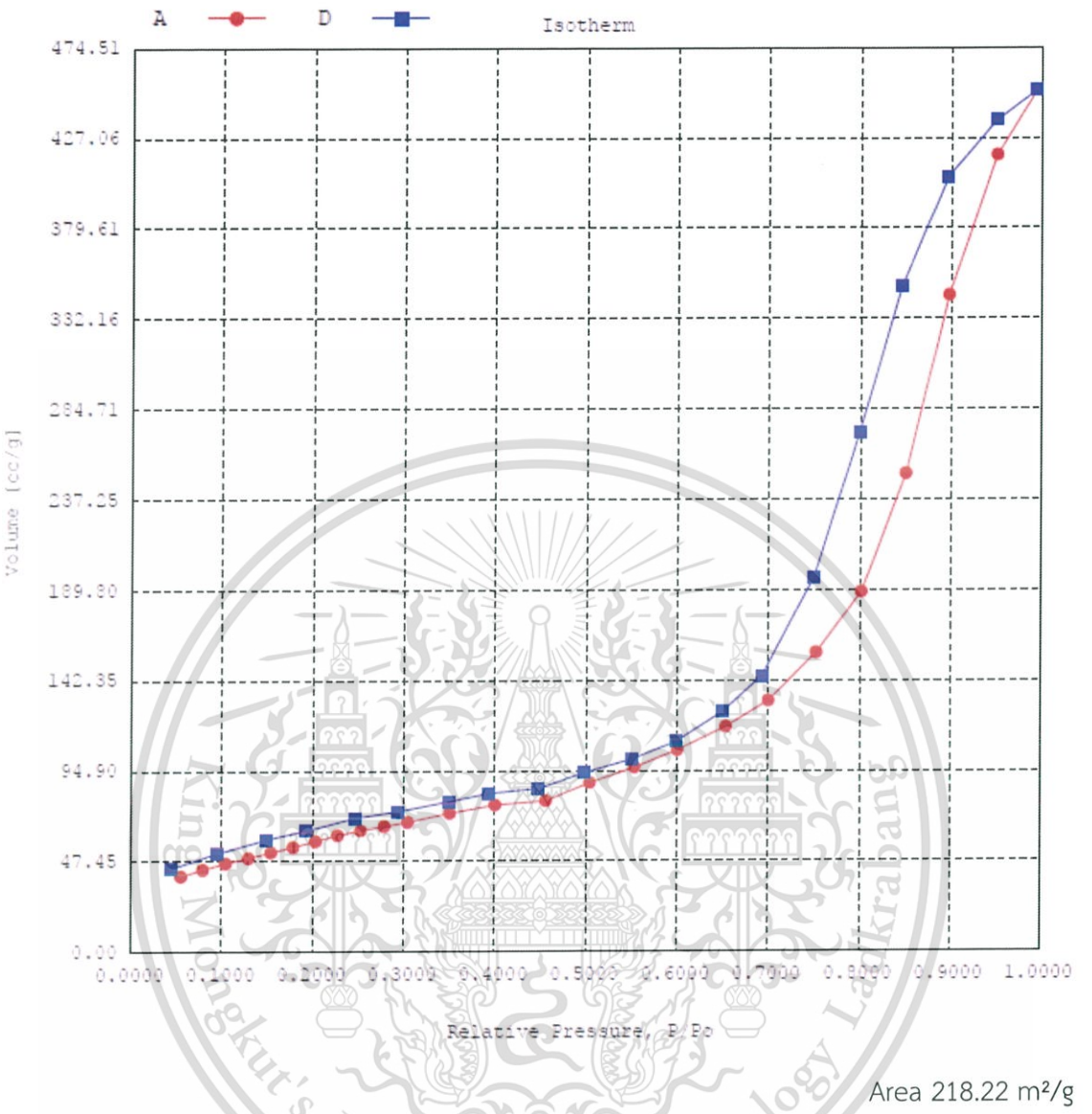

Area 218.22 m²/g

Figure A4 Isotherm of [IM] Cr/SiO_2 5% wt.

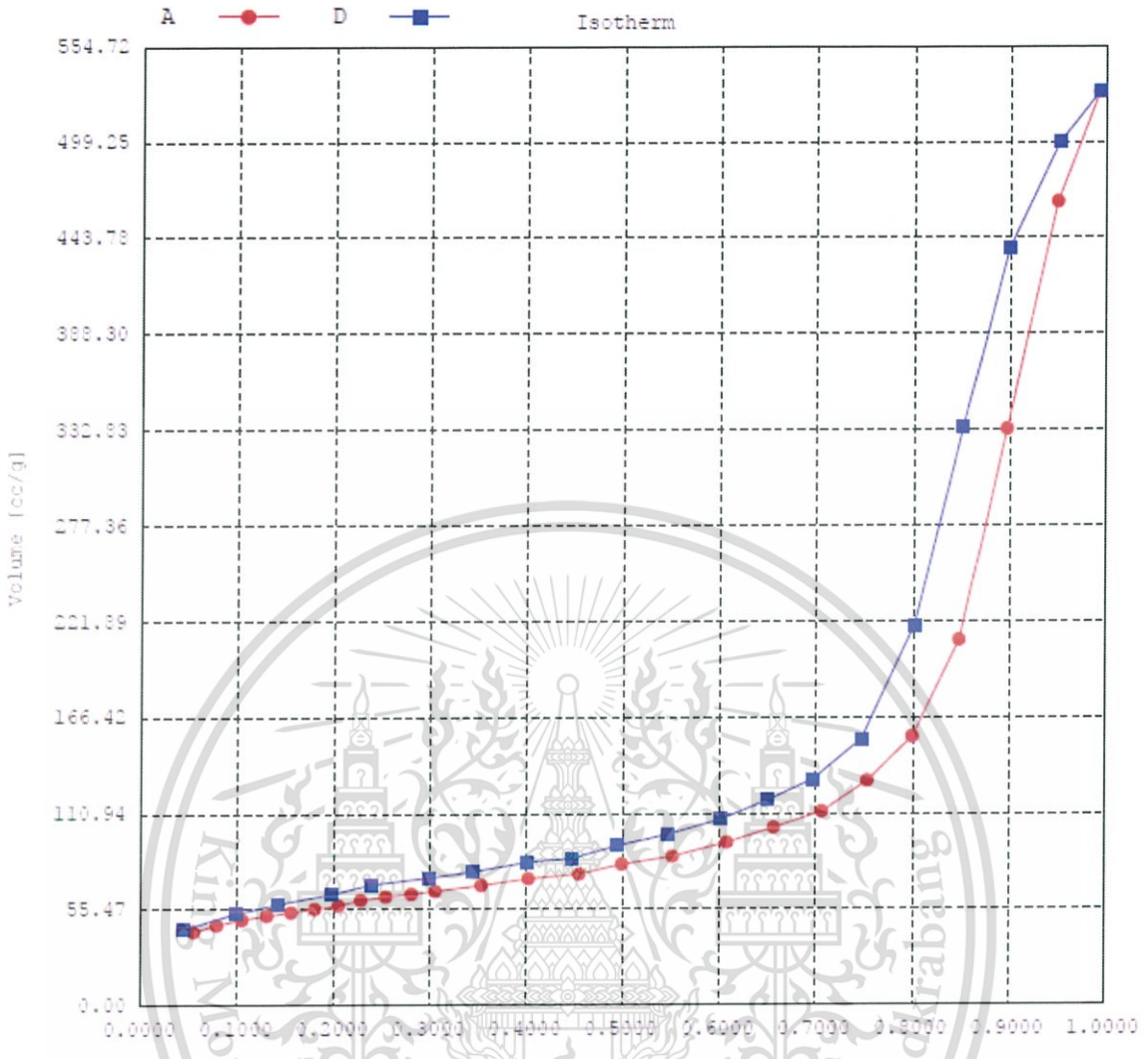

Area 206.36 m²/g

Figure A5 Isotherm of [IM] Cr/SiO_2 10% wt.

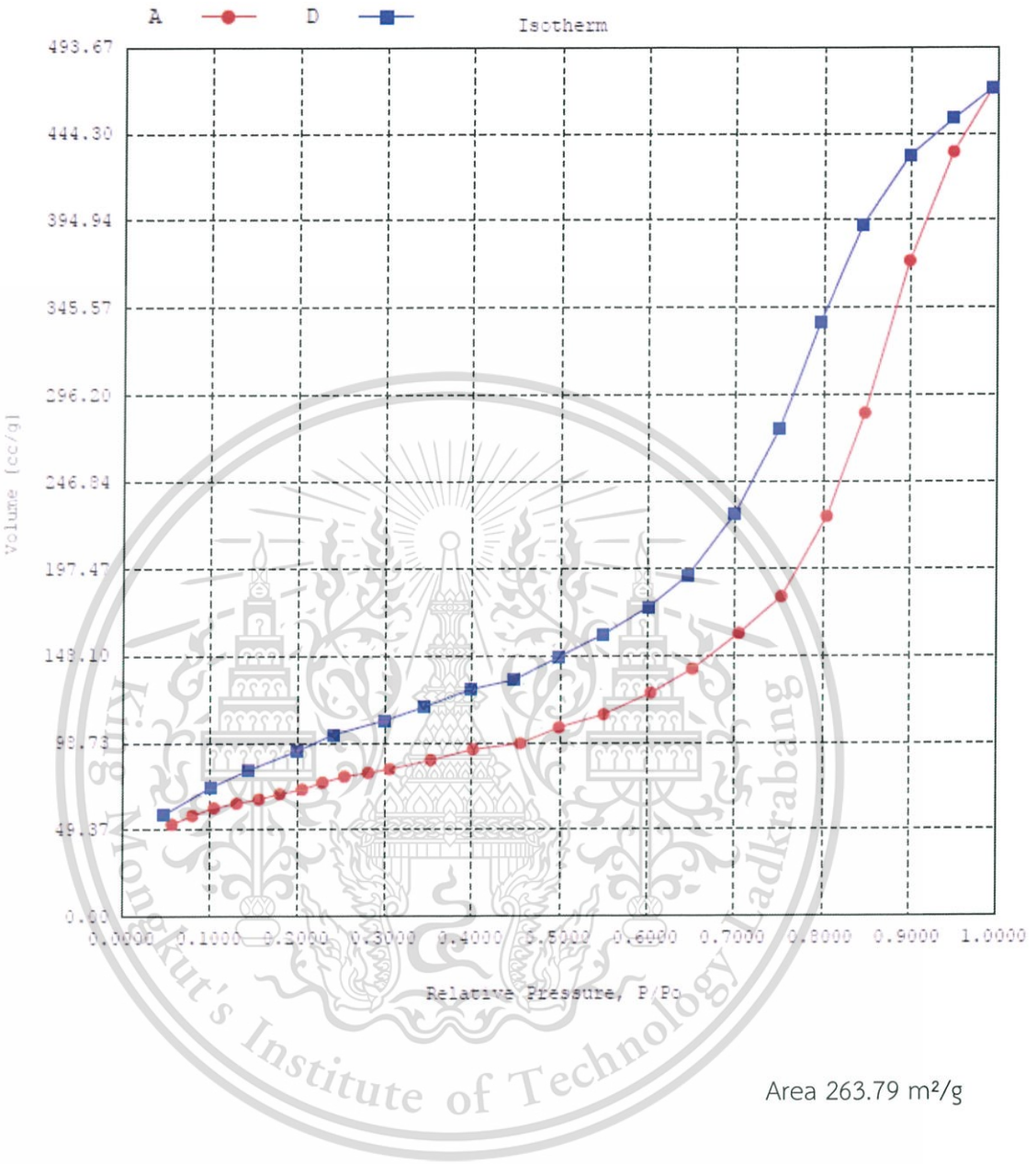

Figure A6 Isotherm of [ADS] Cr/SiO_2

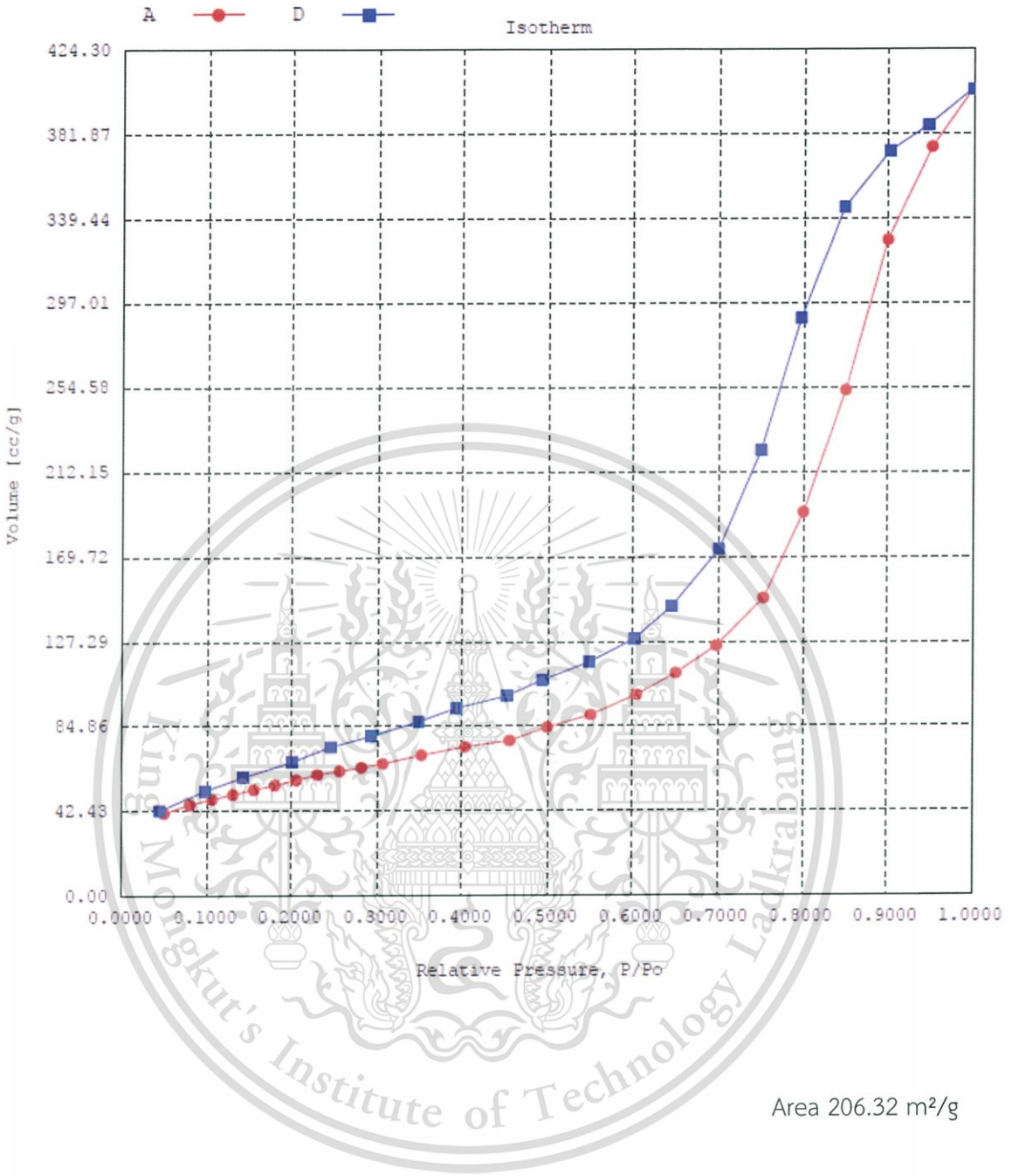

Area 206.32 m²/g

Figure A7 Isotherm of [ADS] Co/SiO_2

3. H_2-Temperature programmed reduction

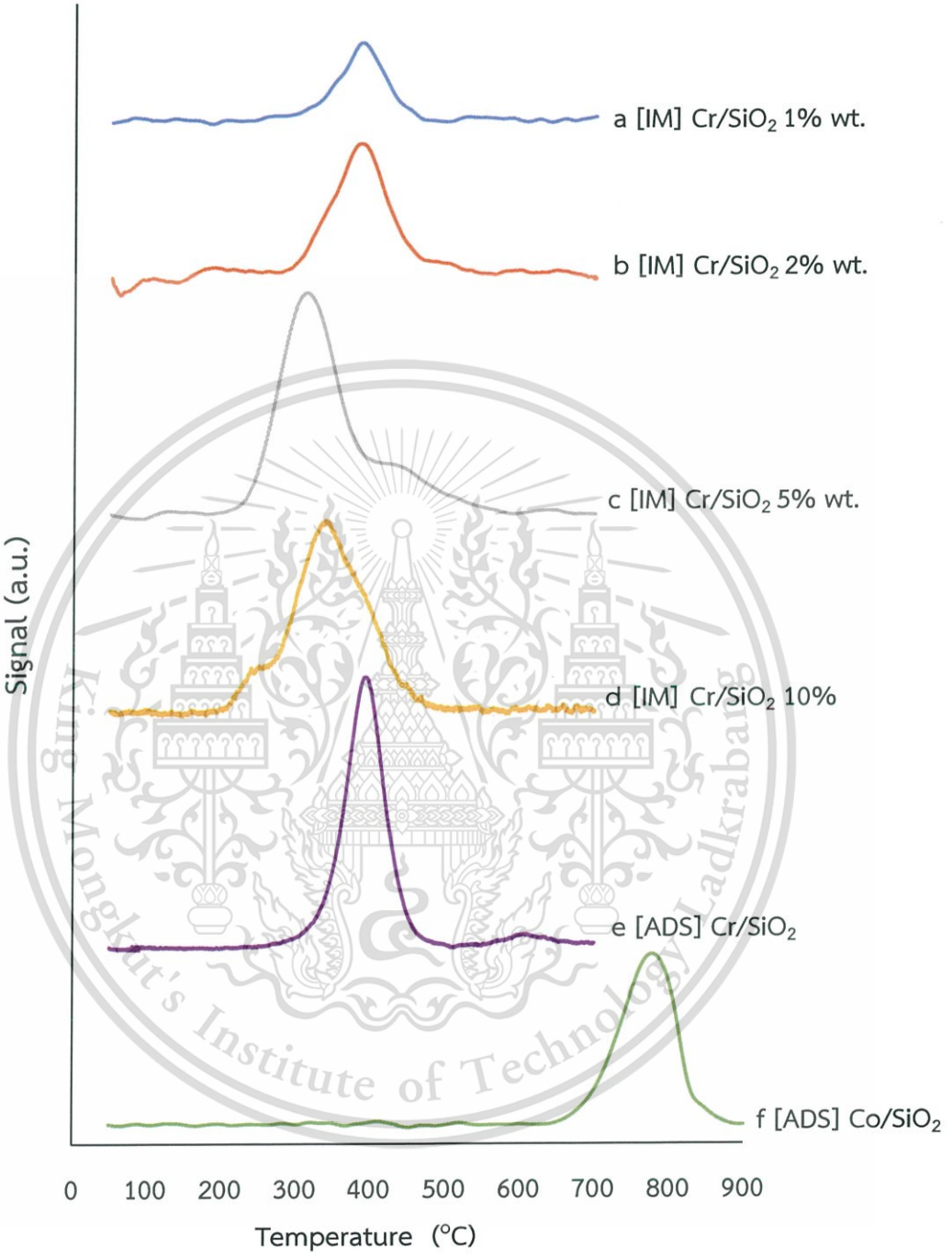

Figure A8 H_2-TPR profiles of those prepared catalysts by wetness impregnation (IM) and strong electrostatic adsorption (ADS) method; (a) [IM] Cr/SiO_2 1% wt, (b) [IM] Cr/SiO_2 2% wt, (c) [IM] Cr/SiO_2 5% wt, (d) [IM] Cr/SiO_2 10% wt, (e) [ADS] Cr/SiO_2, and (f) [ADS] Co/SiO_2.

4. X-Ray Absorption

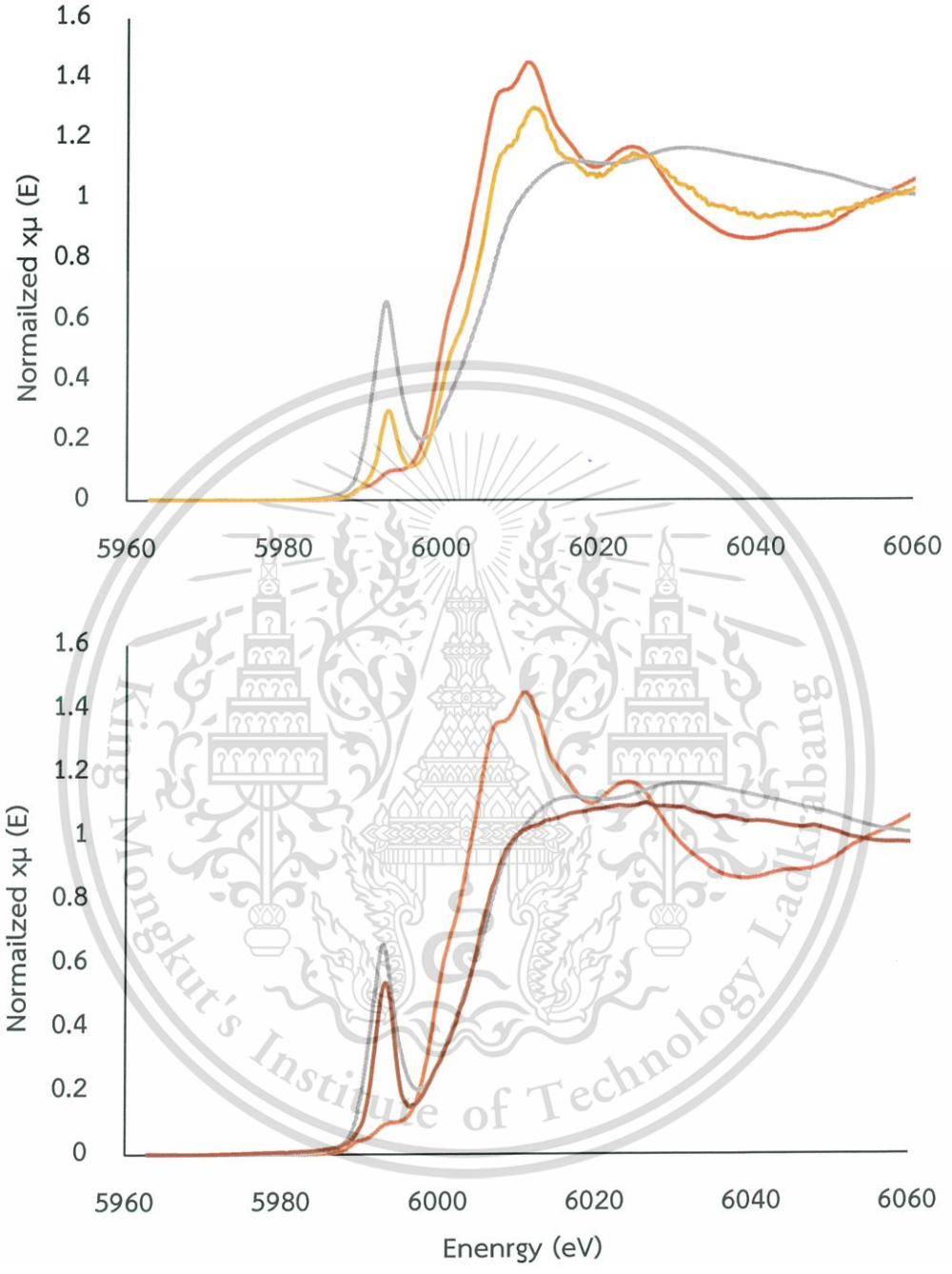

Figure A9 XANES spectra of Cr catalysts: Cr_2O_3 (orange line), CrO_3 (gray line), [IM] 1% wt. Cr/SiO_2 (yellow line) and [ADS] Cr/SiO_2 (brown line) Catalysts

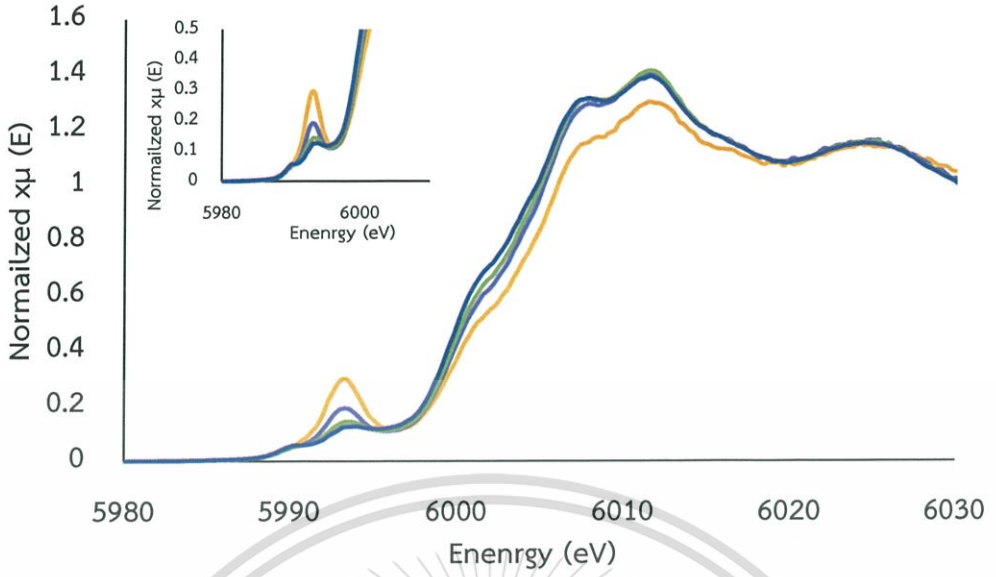

Figure A10 XANES spectra of [IM] Cr catalysts:, [IM] 1% wt Cr/SiO_2 (yellow line), [IM] 2% wt Cr/SiO_2 (blue line), [IM] 5% wt Cr/SiO_2 (green line) and [IM] 10% wt Cr/SiO_2 (dark blue line) catalysts.

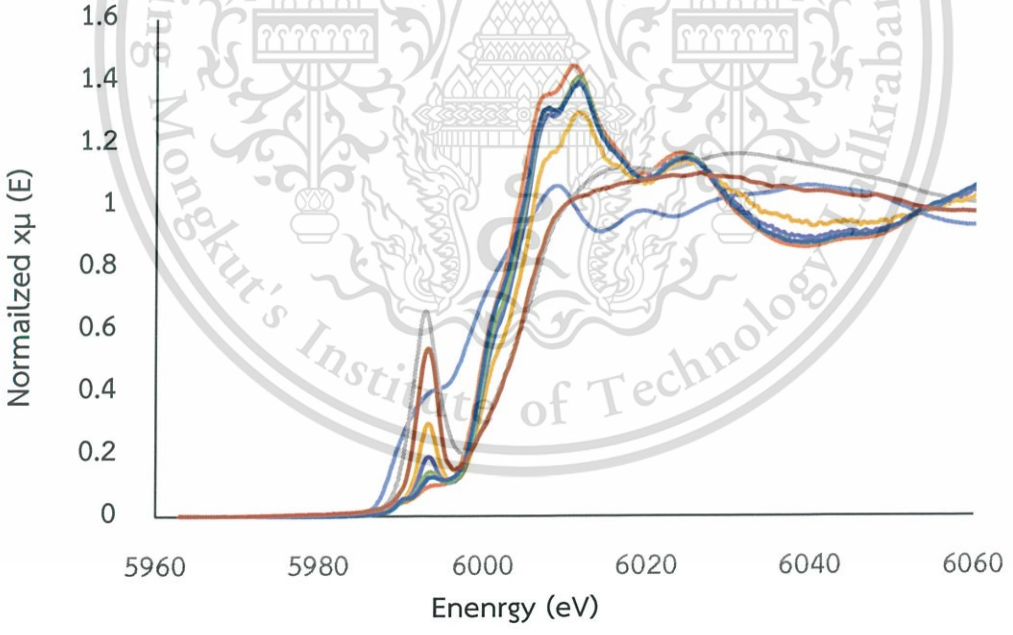

Figure A11 XANES spectra of All Cr catalysts: Cr Foil (light blue line), Cr_2O_3 (orange line), CrO_3 (gray line), [IM] 1% wt. Cr/SiO_2 (yellow line), [IM] 2% wt. Cr/SiO_2 (blue line), [IM] 5% wt. Cr/SiO_2 (green line), [IM] 10% wt. Cr/SiO_2 (dark blue line) and [ADS] Cr/SiO_2 S650 (brown line) Catalysts

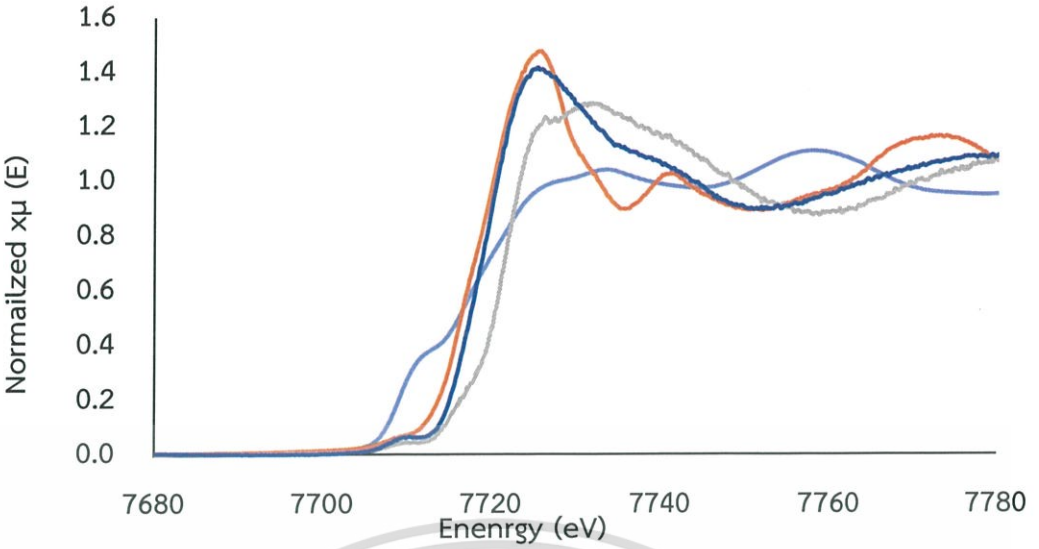

Figure A12 XANES spectra of Co catalysts:, Co Foil (light blue line), CoO standard (orange line), $Co(NH_3)_6Cl_3$ standard (gray line) and [ADS] Co/SiO_2 (dark blue line) catalysts.

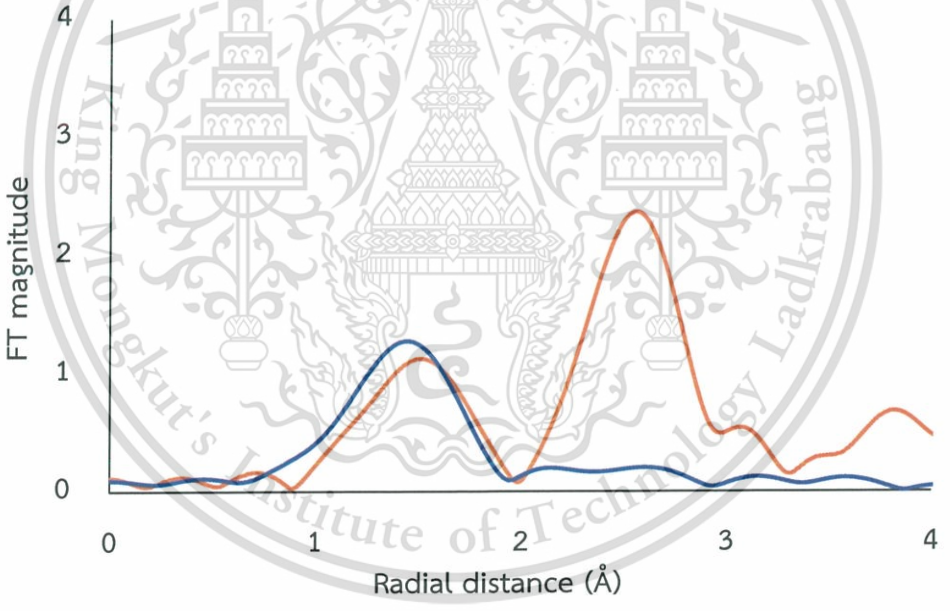

Figure A13 FT-EXAFS spectra of Co catalysts:, CoO standard (orange line) and [ADS] Co/SiO_2 (dark blue line) catalysts.

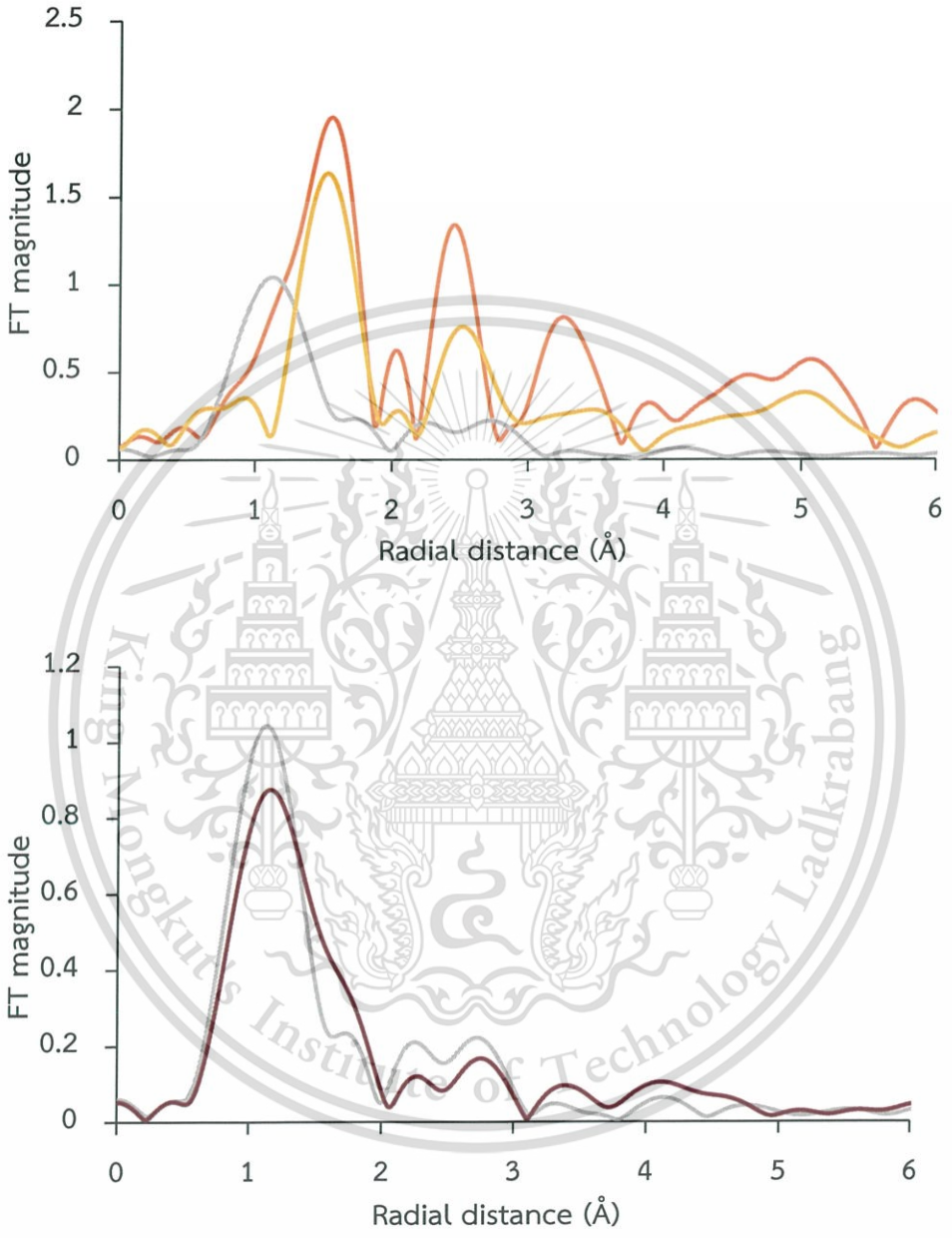

Figure A14 FT-EXAFS spectra of Cr catalysts: Cr_2O_3 (orange line), CrO_3 (gray line), [IM] Cr/SiO_2 1% wt. (yellow line) and [ADS] Cr/SiO_2 S650 (brown line) catalysts.

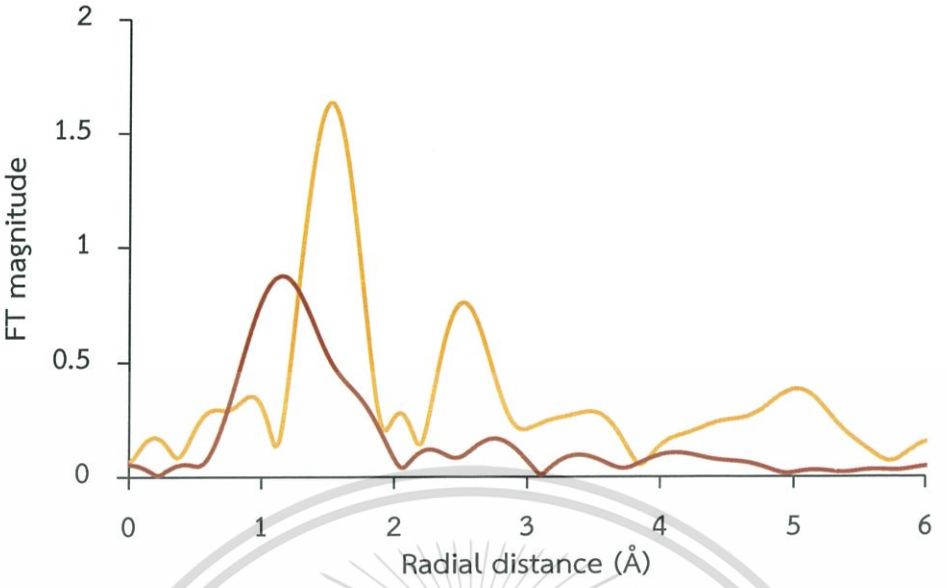

Figure A15 FT-EXAFS spectra of Cr catalysts: [IM] Cr/SiO_2 1% wt. (yellow line), [IM] Cr/SiO_2 and [ADS] Cr/SiO_2 S650 (brown line) catalysts.

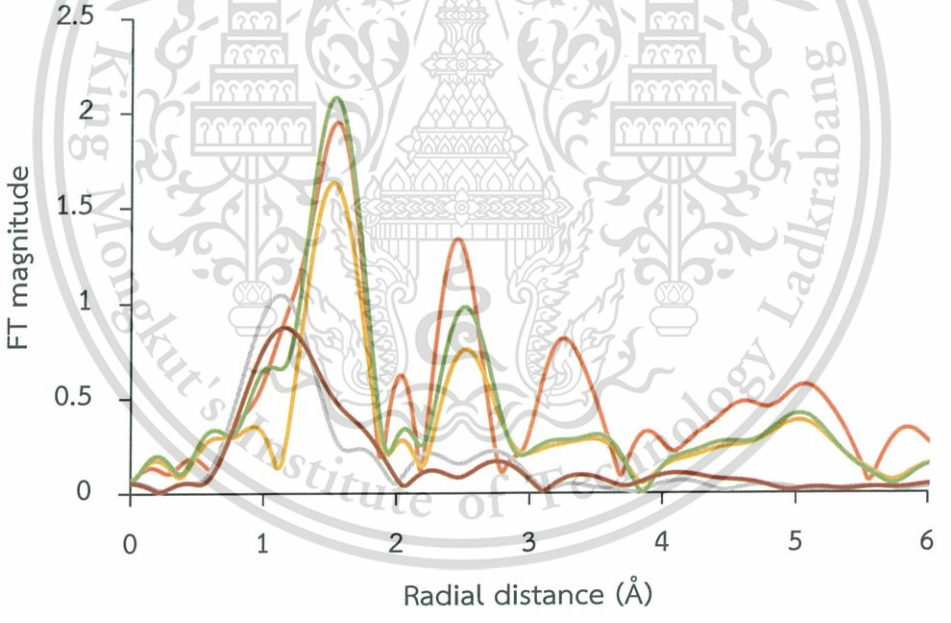

Figure A16 FT-EXAFS spectra of All Cr catalysts: Cr_2O_3 (orange line), CrO_3 (gray line), [IM] Cr/SiO_2 1% wt. (yellow line), [IM] Cr/SiO_2 5% wt. (green line) and [ADS] Cr/SiO_2 S650 (brown line) Catalysts

Table A2: metal formal oxidation state and coordination environment from XANES and EXAFS.

Catalysts	*Edge-adsorption Energy (eV)	*Oxidation State	**Nearest-neighbor distance (Å)					
			Cr=O, Cr-O	Cr-O-Cr	Cr-Cr	Co-O	Co-N	Co-O-Co
Cr Foil	5989.31	(Calibration)	-	-	-	-	-	-
Cr_2O_3	5999.26	+3	1.62	2.45	3.31	-	-	-
CrO_3	6005.21	+6	1.17	-	-	-	-	-
[IM] Cr/SiO_2 1% wt.	5999.64	+3, +6	1.56	2.51	-	-	-	-
[IM] Cr/SiO_2 2% wt.	5999.60	+3, +6	-	-	-	-	-	-
[IM] Cr/SiO_2 5% wt.	5999.57	+3, +6	1.59	2.51	-	-	-	-
[IM] Cr/SiO_2 10% wt.	5999.55	+3, +6	-	-	-	-	-	-
[ADS] Cr/SiO_2	6005.20	+6	1.22	-	-	-	-	-
Co Foil	7709.19	(Calibration)	-	-	-	-	-	-
CoO	7717.95	+2	-	-	-	1.66	-	2.58
$Co(NH_3)_6Cl_3$	7721.01	+3	-	-	-	-	1.47	-
[ADS] Co/SiO_2	7718.43	+2	-	-	-	1.44	-	-

* Determined by XANES

** Determined by FT-EXAFS

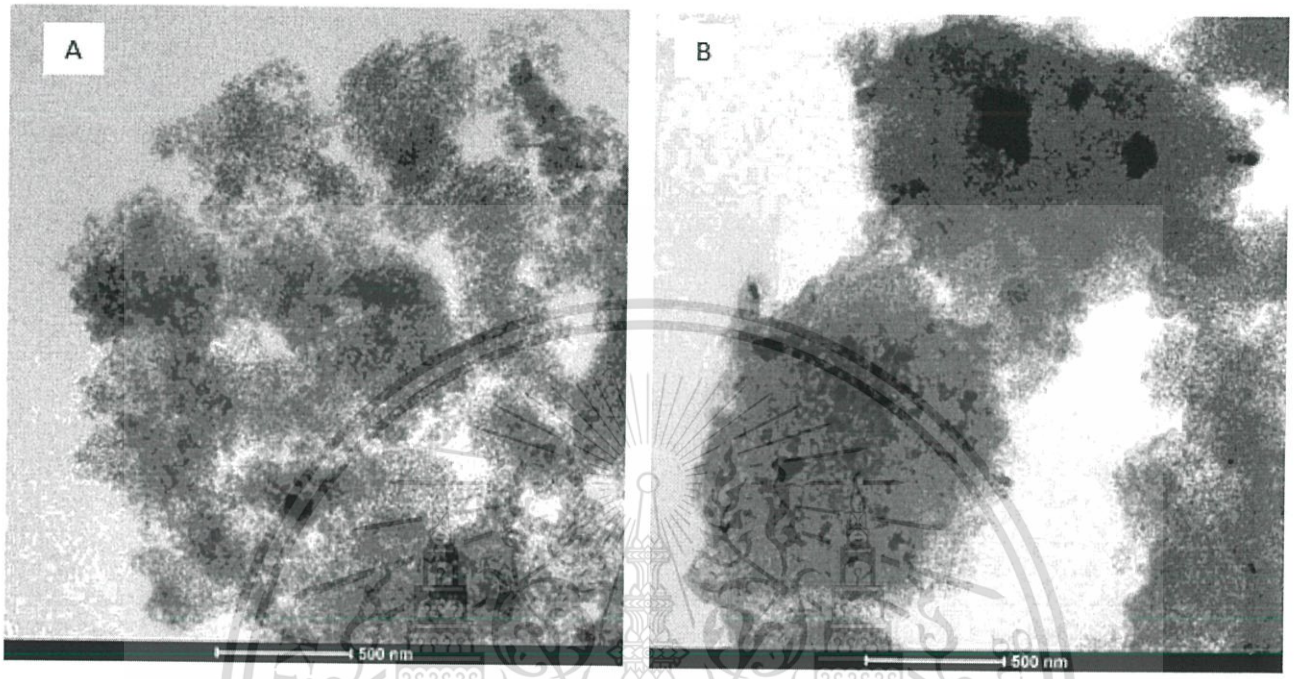

Figure A17 TEM images of fresh catalyst: (A) [IM] Cr/SiO_2 1% wt, (B) [IM] Cr/SiO_2 5% wt

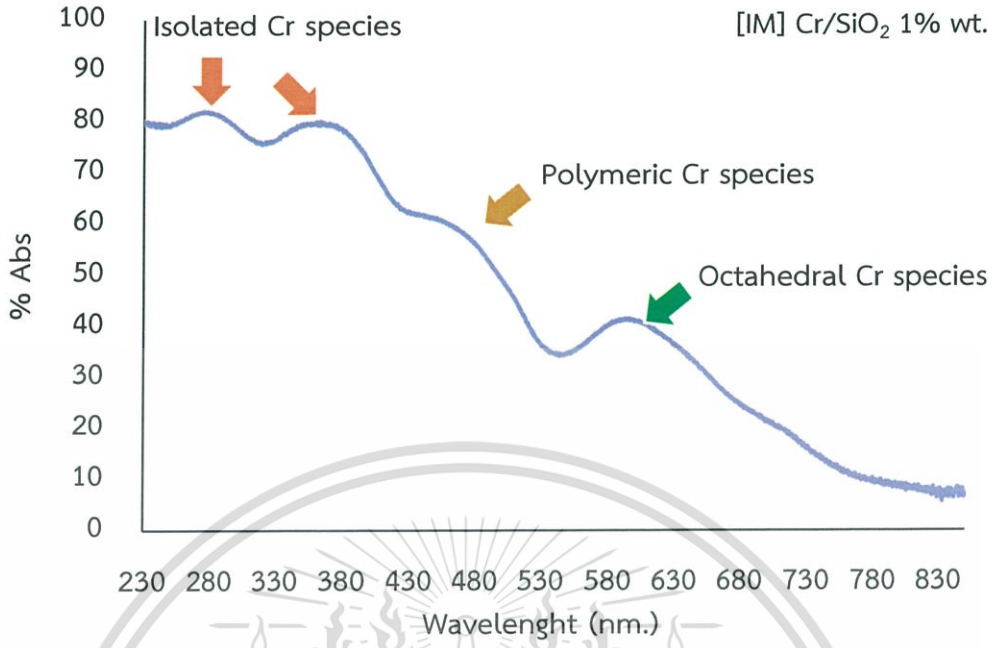

Figure A18 DR-UV reflectance spectra of [IM] Cr/SiO_2 1% wt. catalyst.

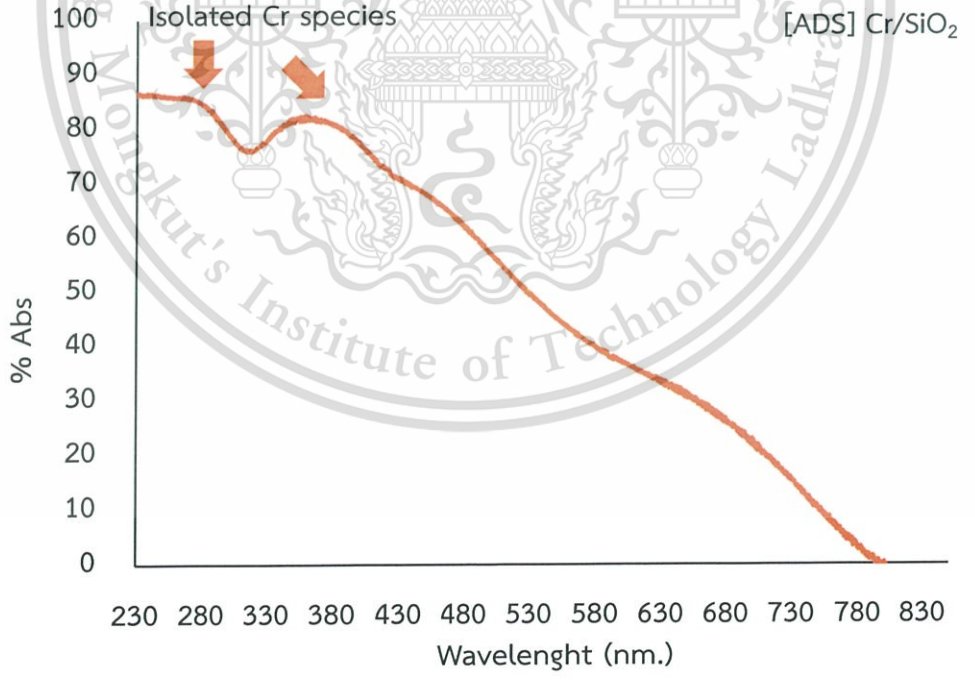

Figure A19 DR-UV reflectance spectra of [ADS] Cr/SiO_2 catalyst.

APPENDIX B

CALCULATION

Example 1: Calculations of catalytic parameters

W/F, conversion, yield and selectivity

Example 2: Calculation of turn over frequency (TOF) and turn over number (TON)

Example 3: Calculations of reducibility

H_2 consumption

B.1 Calculations of catalytic parameters

Contact Time (W/F)

$$W/F = \frac{\text{Weight of catalyst (g)}}{\text{Reactant feed rate (mol/h)}}$$

In the reaction using 0.0257 mol/h of propane in feed and using 0.2675 grams of catalyst, the *W/F* is calculated as follow:

$$W/F = \frac{0.2675\ (g)}{0.0257\ (mol/h)}$$

$$= 10.4144\ g{\cdot}h/mol$$

In a similar manner; *W/F* of catalysts with different catalyst weight and different feed rate are calculated.

Calculation of % yield from gas chromatography

In normalization method, the areas of all eluted peak were computed areas for differences in the detector response to different compound types. The concentration of the analyzed was found from the ratio of its area to the total area of all peaks. The example of the peak area obtained from chromatogram of a mixture reactor outlet is shown in **Table B1**.

Table B1 the example of the peak area for reactor outlet.

Chemicals	Peak area
Methane	14,689
Ethane	5,115
Ethylene	19,566
Propane	21,161,779
Propylene	325,747
C_4	4,491
C_5+	0
Total	21,531,387

Calculate the percent yield of each component in sample as follows:

$$\%\text{Yield in each product} = \frac{\text{peak area of Y} \times 100}{\text{Total corrected area}}$$

When Y is each product.

For example;

$$\%\text{Yield of Propylene} = \frac{325{,}747 \times 100}{21{,}531{,}387}$$

$$= 1.5129$$

The percent yield of each sample which is obtained from above calculation is shown in Table B2.

Table B2 % yield derived by normalization method.

Chemicals	%Yield of sample
Methane	0.07
Ethane	0.02
Ethylene	0.09
Propylene	1.51
C_4	0.02
C_5+	0.00
Total yield	1.72

Selectivity

%Selectivity can be obtained from the following equation.

$$\%\text{Selectivity in each product} = \frac{\%\text{ Yield in each product}}{\%\text{ total yield}} \times 100$$

For example;

$$\%\text{Selectivity of Propylene} = \frac{1.51}{1.72} \times 100$$

$$= 87.8$$

B.2 Calculations of turn over frequency (TOF) and ture over number (TON)

In order to calculate TOF, 0.2675 grams of [IM] Cr/SiO_2 1% wt must be transformed to molar unit (0.0540 mmol).

TOF for the conversion of propane 1.1302 g/h equivalent to 25.6856 mmol/h, was expressed by :

Thus, from conversion 1.72 %, the propane was equal to:

$$\text{Mole conversion} = \frac{1.72 \times 25.68565 \text{ mmol/h}}{100}$$

$$= 0.4409 \text{ mmol/h.}$$

Divide by mole of the catalysts.

$$\text{TOF} = \frac{0.4409 \text{ mmol/h.}}{0.0540 \text{ mmol}}$$

$$= 8.1624 \text{ h}^{-1}$$

Transverse to turn over number (TON)

$$\text{TON} = \text{TOF } (h^{-1}) \times \text{Contact Time based on chromium (h)}$$

$$= 8.1624 \times 0.0021$$

$$= 0.0172 \text{ mol } C_3H_8/\text{mol Cr}$$

$$= 17.1660 \text{ mmol } C_3H_8/\text{mol Cr}$$

B.4 Calculations of reducibility

The electronic signal from the TCD detector during TPR analysis is converted to mmol H_2, employing copper (II) oxide (CuO) as a standard. Therefore, CuO is used because it is a highly-reducible metal with clean and well-known reduction giving Cu metal as a final product following the equation;

$$CuO\ (s) + H_2\ (g) \rightarrow Cu\ (s) + H_2O\ (g)$$

An example of TPR profile of CuO is shown in **Figure B1.**

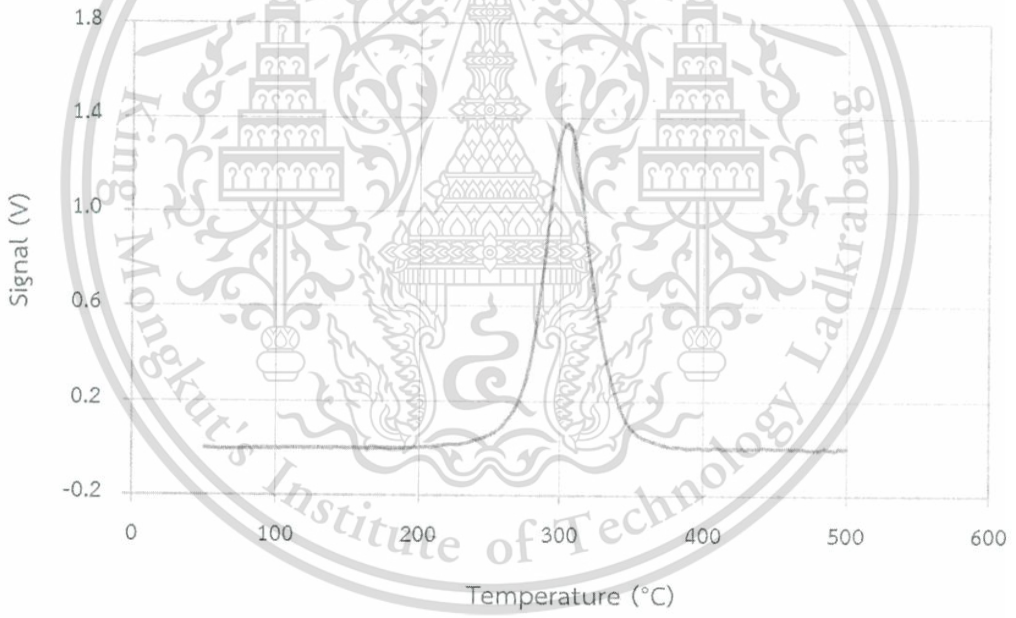

Figure B1 TPR profile of CuO

A few runs were performed by variation of the mass of CuO. Then, the peak area (integrated with **Origin Pro 8.0**) in the range T = 50-500 °C is plotted against the mole of CuO. The resulting plot (**Figure B2**) serves as a calibration curve where the mmol H_2 of any sample could be calculated from the peak area as shown below.

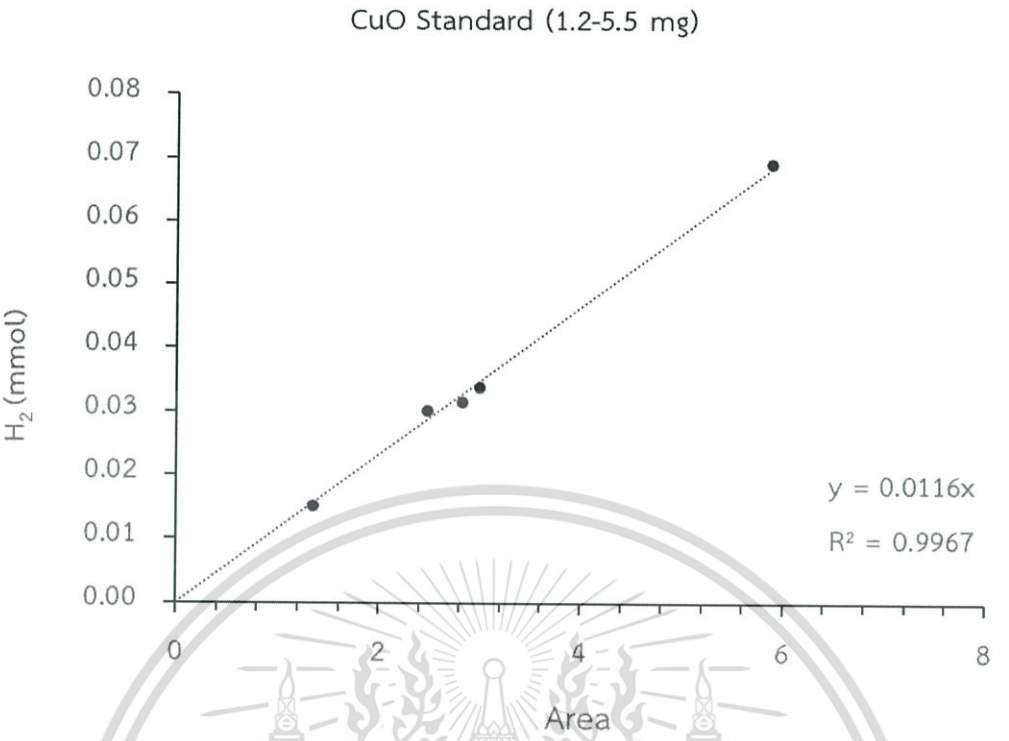

Figure A2 Standard curve of CuO; peak area *vs* the mole number of CuO

From TPR results, the [ADS] Cr/SiO_2 S650 (0.3121 g) sample gives the peak area of 4.9654. Substituting this number into the equation in **Figure A2** gives;

$$y = 0.0117x$$

$$y = (0.0117 \times 4.9654) / 0.3121$$

$$y = 0.1862 \text{ mmol/g}$$

As the mole ratio of Cr_2O_3 to H_2 is 2:3, the number of mmol of H_2 consumed by [ADS] Cr/SiO_2 equals 0.1862 mmol/g as well. So, the reducibility of [ADS] Cr/SiO_2 is;

$$0.1862 \text{ mmol/g} \times (2/3) = 0.1241 \text{ mmol/g of } CrO_3$$

The H_2 consumption of various catalysts are shown in **TableA1**.

APPENDIX C

GAS CHROMATOGRAM

Analysis gas product from gas chromatography

Prior analysis, GC-MS (gas chromatography with mass spectrometer detector) was used to identify the structure of products in the sample and the GC-FID (gas chromatography with flam ionization detector) was used to determine the quantitative of the product with the condition expressed in **Table C1.**

Table C1: The GC Condition for Quantitative Analysis

Column	Rt®-Q-BOND (30 m x 0.53 mm x 0.20 um)
Temperature program	30°C (7 min hold) to 85°C (4 min hold) at 20°/min after than ramp to 140°C (3 min hold) at 20°/min and ramp to 225°C (6.83 min hold) at 15°/min
Split Ratio	100
GC Carrier gas	Nitrogen gas, flow rate 5.19 ml/min
Injector temperature	250 °C
Detector temperature	FID at 250 °C

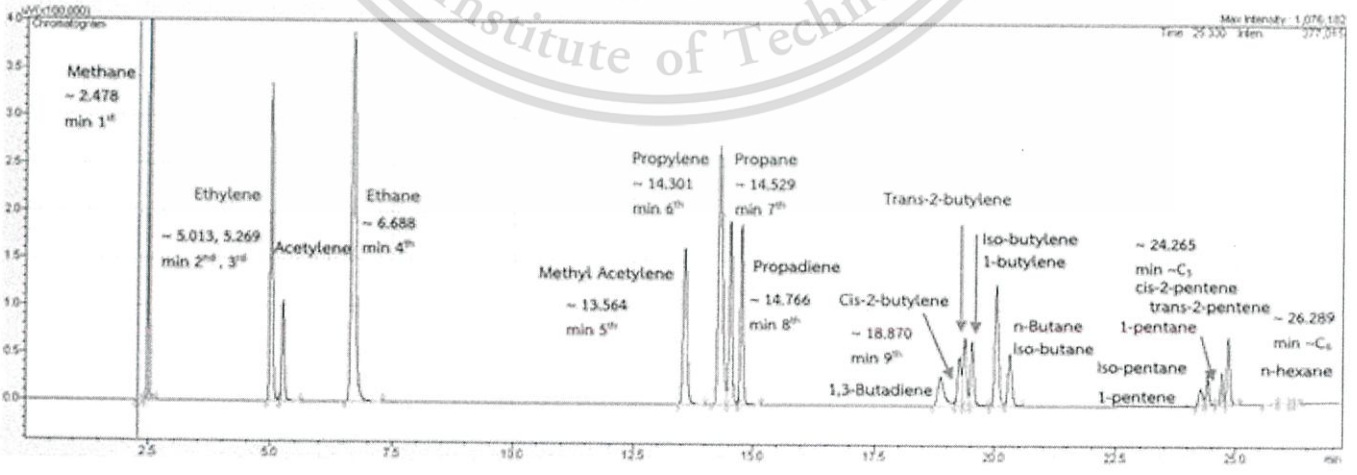

Figure C1 Chromatogram of Hydrocarbon Gas Standard

APPENDIX D

REACTION DATA

D1: Temperature Scan for Propane Conversion.

Table D1.1: The Area of Propane Dehydrogenation at 450-650 °C

Catalyst	Temperature (°C)	Area						Total Area
		Methane	Ethane	Ethylene	Propane	Propylene	C_4	
SiO_2	450	0	0	0	12062207	0	0	12062207
	500	0	0	0	14382247	3335	0	14385582
	550	2871	0	5172	14450203	12371	0	14470617
	600	12416	0	23067	14076446	54112	0	14166041
	650	70044	2160	128195	13672453	247659	0	14120511
[IM] Cr/SiO_2 2% wt.	450	0	0	0	14530685	4445	0	14535130
	500	0	0	0	14185275	34297	0	14219572
	550	4324	1417	6446	14504192	125407	3835	14645621
	600	11759	0	20164	14114597	191028	3021	14340569
	650	59311	1800	106339	12824685	372592	2618	13367345

(Reaction temperature: 450 – 650 °C, 0.0258 mol/h of propane (99.95%), and 50 mL/min nitrogen, W/F: (SiO_2) 7.1869 g.h/mol, ([IM] Cr/SiO_2 2% wt.) 7.1129 g.h/mol)

Table D1.2: Product selectivity of Propane Dehydrogenation at 450-650 °C

Catalyst	Temperature (°C)	% Conversion	% Selectivity				
			Methane	Ethane	Ethylene	Propylene	C_4
SiO_2	450	0.00	0.0	0.0	0.0	0.00	0.0
	500	0.04	0.0	0.0	0.0	100.0	0.0
	550	0.16	14.1	0.0	25.3	60.6	0.0
	600	0.65	13.9	0.0	25.7	60.4	0.0
	650	3.14	15.6	0.5	28.6	55.3	0.0
[IM] Cr/SiO_2 2% wt.	450	0.04	0.0	0.0	0.0	100.0	0.0
	500	0.24	0.0	0.0	0.0	100.0	0.0
	550	0.97	3.0	1.0	4.6	88.7	2.7
	600	1.58	5.2	0.0	9.0	84.5	1.3
	650	4.06	10.9	0.3	19.6	68.7	0.5

(Reaction temperature: 450 – 650 °C, 0.0258 mol/h of propane (99.95%), and 50 mL/min nitrogen, W/F; (SiO_2) 7.1869 g.h/mol, ([IM] Cr/SiO_2 2% wt.) 7.1129 g.h/mol)

D2: Propane Dehydrogenation over SiO_2 catalyst.

Table D2.1: The Area of Propane Dehydrogenation at 550 °C

Time on steam (h)	Area						Total Area
	Methane	Ethane	Ethylene	Propane	Propylene	C_4	
0.75	6899	0	12748	19550146	21181	0	19590974
1.5	6618	0	12148	20202276	20339	0	20241381
2.25	6650	0	12041	20184703	20481	0	20223875
3	6654	0	12179	20194588	20603	0	20234024
3.75	6890	0	12399	19560006	21233	0	19600528
4.5	6857	0	12680	19537177	20621	0	19577335
5.25	6586	0	11986	20195483	20261	0	20234316
6	6636	0	12041	20175471	19982	0	20214130

(Reaction temperature: 550 °C, 0.0258 mol/h of propane (99.95%), and 50 mL/min nitrogen, W/F; 10.2003 g.h/mol, Time on stream; 6 hours)

Table D2.2: Product selectivity of Propane Dehydrogenation at 550 *°C*

Time on steam (h)	% Conversion	% Selectivity				
		Methane	Ethane	Ethylene	Propylene	C_4
0.75	0.21	16.9	0.0	31.2	51.9	0.0
1.5	0.19	16.9	0.0	31.1	52.0	0.0
2.25	0.19	17.0	0.0	30.7	52.3	0.0
3	0.19	16.9	0.0	30.9	52.2	0.0
3.75	0.21	17.0	0.0	30.6	52.4	0.0
4.5	0.21	17.1	0.0	31.6	51.3	0.0
5.25	0.19	17.0	0.0	30.9	52.2	0.0
6	0.19	17.2	0.0	31.1	51.7	0.0

(Reaction temperature: 550 °C, 0.0258 mol/h of propane (99.95%), and 50 mL/min nitrogen, W/F; 10.2003 g.h/mol, Time on stream; 6 hours)

D3: Propane Dehydrogenation over [IM] Cr/SiO_2 1% wt. catalyst.

Table D3.1: The Area of Propane Dehydrogenation at 550 °C

Time on steam (h)	Area						Total Area
	Methane	Ethane	Ethylene	Propane	Propylene	C_4	
0.75	14689	5115	19566	21161779	325747	4491	21531387
1.5	11189	4312	15223	21481580	316045	4026	21832375
2.25	10341	3677	14467	21267115	297247	4449	21597296
3	9949	3341	14040	21102566	279718	3953	21413567
3.75	9722	3182	14018	21164304	272254	3491	21466971
4.5	9806	3232	14468	21183075	238599	2708	21451888
5.25	8393	2926	12453	21047136	235654	3170	21309732
6	8413	2828	12510	21051656	236042	0	21311449

(Reaction temperature: 550 °C, 0.0258 mol/h of propane (99.95%), and 50 mL/min nitrogen, W/F; 10.4144 g.h/mol, Time on stream; 6 hours)

Table D3.2: Product selectivity of Propane Dehydrogenation at 550 °C

Time on steam (h)	TOF (h^{-1})	% Conversion	% Selectivity				
			Methane	Ethane	Ethylene	Propylene	C_4
0.75	8.16	1.72	4.0	1.4	5.3	88.1	1.2
1.5	7.64	1.61	3.2	1.2	4.3	90.1	1.1
2.25	7.27	1.53	3.1	1.1	4.4	90.0	1.3
3	6.91	1.45	3.2	1.1	4.5	89.9	1.3
3.75	6.70	1.41	3.2	1.1	4.6	90.0	1.2
4.5	5.96	1.25	3.6	1.2	5.4	88.8	1.0
5.25	5.86	1.23	3.2	1.1	4.7	89.7	1.2
6	5.86	1.23	3.2	1.1	4.8	90.9	0.0

(Reaction temperature: 550 °C, 0.0258 mol/h of propane (99.95%), and 50 mL/min nitrogen, W/F; 10.4144 g.h/mol, Time on stream; 6 hours)

D4: Propane Dehydrogenation over [IM] Cr/SiO_2 2% wt. catalyst.

Table D4.1: The Area of Propane Dehydrogenation at 550 °C

Time on steam (h)	Area						Total Area
	Methane	Ethane	Ethylene	Propane	Propylene	C_4	
0.75	7789	3150	10792	17304468	283653	4901	17614753
1.5	4162	2001	5067	18586009	198419	5832	18801490
2.25	3855	1729	4770	18467605	183685	4142	18665786
3	3529	1520	4716	18345685	161253	3648	18520351
3.75	3186	1200	4197	18136224	154067	5069	18303943
4.5	3498	1371	4993	18280338	140885	0	18431085
5.25	3992	1721	5385	18121055	128167	0	18260320
6	3053	1134	4177	17853654	127365	1503	17990886

(Reaction temperature: 550 °C, 0.0258 mol/h of propane (99.95%), and 50 mL/min nitrogen, W/F; 10.5273 g.h/mol, Time on stream; 6 hours)

Table D3.2: Product selectivity of Propane Dehydrogenation at 550 °C

Time on steam (h)	TOF (h^{-1})	% Conversion	% Selectivity				
			Methane	Ethane	Ethylene	Propylene	C_4
0.75	4.75	1.76	2.5	1.0	3.5	91.4	1.6
1.5	3.09	1.15	1.9	0.9	2.4	92.1	2.7
2.25	2.87	1.06	1.9	0.9	2.4	92.7	2.1
3	2.55	0.94	2.0	0.9	2.7	92.3	2.1
3.75	2.47	0.92	1.9	0.7	2.5	91.9	3.0
4.5	2.21	0.82	2.3	0.9	3.3	93.5	0.0
5.25	2.06	0.76	2.9	1.2	3.9	92.0	0.0
6	2.06	0.76	2.2	0.8	3.0	92.8	1.1

(Reaction temperature: 550 °C, 0.0258 mol/h of propane (99.95%), and 50 mL/min nitrogen, W/F; 10.5273 g.h/mol, Time on stream; 6 hours)

D4: Propane Dehydrogenation over [IM] Cr/SiO_2 5% wt. catalyst.

Table D4.1: The Area of Propane Dehydrogenation at 550 °C

Time on steam (h)	Area						Total Area
	Methane	Ethane	Ethylene	Propane	Propylene	C_4	
0.75	10864	5012	15035	21058186	358305	0	21447402
1.5	10498	4128	14578	21313836	331231	0	21674271
2.25	10433	3313	14747	21351778	313166	0	21693437
3	9959	3419	14340	21476080	282812	0	21786610
3.75	9414	3285	13948	21327629	258038	0	21612314
4.5	9018	2851	13461	21280994	239637	0	21545961
5.25	8698	2682	13109	21429530	230282	0	21684301
6	8457	2535	12985	21152066	218654	0	21394697

(Reaction temperature: 550 °C, 0.0258 mol/h of propane (99.95%), and 50 mL/min nitrogen, W/F; 10.5585 g.h/mol, Time on stream; 6 hours)

Table D4.2: Product selectivity of Propane Dehydrogenation at 550 °C

Time on steam (h)	TOF (h^{-1})	% Conversion	% Selectivity				
			Methane	Ethane	Ethylene	Propylene	C_4
0.75	1.83	1.81	2.8	1.3	3.9	92.1	0.0
1.5	1.67	1.66	2.9	1.1	4.0	91.9	0.0
2.25	1.59	1.57	3.1	1.0	4.3	91.7	0.0
3	1.44	1.43	3.2	1.1	4.6	91.1	0.0
3.75	1.33	1.32	3.3	1.2	4.9	90.6	0.0
4.5	1.24	1.23	3.4	1.1	5.1	90.4	0.0
5.25	1.18	1.17	3.4	1.1	5.1	90.4	0.0
6	1.14	1.13	3.5	1.0	5.4	90.1	0.0

(Reaction temperature: 550 °C, 0.0258 mol/h of propane (99.95%), and 50 mL/min nitrogen, W/F; 10.5585 g.h/mol, Time on stream; 6 hours)

D5: Propane Dehydrogenation over [IM] Cr/SiO_2 10% wt. catalyst.

Table D5.1: The Area of Propane Dehydrogenation at 550 °C

Time on steam (h)	Area						Total Area
	Methane	Ethane	Ethylene	Propane	Propylene	C_4	
0.75	18073	6402	25583	20750382	393585	0	21194025
1.5	14634	4446	21785	21124252	305178	0	21470295
2.25	12371	3061	18707	20559037	252816	0	20845992
3	11052	2703	16999	21020502	234784	0	21286040
3.75	10273	2249	16052	21200079	219166	0	21447819
4.5	9959	2158	15827	21164434	200374	0	21392752
5.25	9405	1681	14832	21333110	186981	0	21546009
6	8409	0	13574	20897143	171234	0	21090360

(Reaction temperature: 550 °C, 0.0258 mol/h of propane (99.95%), and 50 mL/min nitrogen, W/F; 10.3833 g.h/mol, Time on stream; 6 hours)

Table D5.2: Product selectivity of Propane Dehydrogenation at 550 °C

Time on steam (h)	TOF (h^{-1})	% Conversion	% Selectivity				
			Methane	Ethane	Ethylene	Propylene	C_4
0.75	1.09	2.09	4.1	1.4	5.8	88.7	0.0
1.5	0.84	1.61	4.2	1.3	6.3	88.2	0.0
2.25	0.72	1.38	4.3	1.1	6.5	88.1	0.0
3	0.65	1.25	4.2	1.0	6.4	88.4	0.0
3.75	0.60	1.16	4.1	0.9	6.5	88.5	0.0
4.5	0.56	1.07	4.4	0.9	6.9	87.8	0.0
5.25	0.52	0.99	4.4	0.8	7.0	87.8	0.0
6	0.48	0.92	4.4	0.0	7.0	88.6	0.0

(Reaction temperature: 550 °C, 0.0258 mol/h of propane (99.95%), and 50 mL/min nitrogen, W/F; 10.3833 g.h/mol, Time on stream; 6 hours)

D6: Propane Dehydrogenation over [ADS] Cr/SiO_2 0.2% wt catalyst.

Table D6.1: The Area of Propane Dehydrogenation at 550 °C

Time on steam (h)	Area						Total Area
	Methane	Ethane	Ethylene	Propane	Propylene	C_4	
0.75	5299	1731	9255	20739467	84295	0	20840047
1.5	5674	1473	9498	20832943	76692	0	20926280
2.25	5857	1374	9969	20747444	72311	0	20836955
3	5962	1397	10128	20831760	69501	0	20918748
3.75	5896	1201	10175	20643893	66351	0	20727516
4.5	5710	1160	9769	19909458	62254	0	19988351
5.25	5957	1059	10289	20879437	63403	0	20960145
6	5915	0	10351	20488988	61346	0	20566600

(Reaction temperature: 550 °C, 0.0258 mol/h of propane (99.95%), and 50 mL/min nitrogen, W/F; 10.3910 g.h/mol, Time on stream; 6 hours)

Table D6.2: Product selectivity of Propane Dehydrogenation at 550 °C

Time on steam (h)	TOF (h^{-1})	% Conversion	% Selectivity				
			Methane	Ethane	Ethylene	Propylene	C_4
0.75	11.90	0.48	5.3	1.7	9.2	83.8	0.0
1.5	10.99	0.45	6.1	1.6	10.2	82.2	0.0
2.25	10.59	0.43	6.5	1.5	11.1	80.8	0.0
3	10.25	0.42	6.9	1.6	11.6	79.9	0.0
3.75	9.94	0.40	7.1	1.4	12.2	79.3	0.0
4.5	9.73	0.39	7.2	1.5	12.4	78.9	0.0
5.25	9.49	0.39	7.4	1.3	12.7	78.6	0.0
6	9.30	0.38	7.6	0.0	13.3	79.0	0.0

(Reaction temperature: 550 °C, 0.0258 mol/h of propane (99.95%), and 50 mL/min nitrogen, W/F; 10.3910 g.h/mol, Time on stream; 6 hours)

D7: Propane Dehydrogenation over [ADS] Co/SiO_2 1.67% wt catalyst.

Table D7.1: The Area of Propane Dehydrogenation at 550 °C

Time on steam (h)	Area						Total Area
	Methane	Ethane	Ethylene	Propane	Propylene	C_4	
0.75	6139	1713	11721	22675578	114360	0	22809511
1.5	6439	0	12096	22808954	99586	0	22927075
2.25	6110	0	11472	21934991	91951	0	22044524
3	6229	0	11470	21946035	92539	0	22056273
3.75	6327	0	11906	22067927	92539	0	22178699
4.5	6516	0	12055	22689068	96295	0	22803934
5.25	6457	0	11902	22418783	97125	0	22534267
6	6094	0	11203	21995683	96907	0	22109887

(Reaction temperature: 550 °C, 0.0258 mol/h of propane (99.95%), and 50 mL/min nitrogen, W/F; 10.6130 g.h/mol, Time on stream; 6 hours)

Table D7.2: Product selectivity of Propane Dehydrogenation at 550 °C

Time on steam (h)	TOF (h^{-1})	% Conversion	% Selectivity				
			Methane	Ethane	Ethylene	Propylene	C_4
0.75	1.95	0.59	4.6	1.3	8.8	85.4	0.0
1.5	1.71	0.52	5.5	0.0	10.2	84.3	0.0
2.25	1.65	0.50	5.6	0.0	10.5	83.9	0.0
3	1.66	0.50	5.7	0.0	10.4	83.9	0.0
3.75	1.66	0.50	5.7	0.0	10.7	83.5	0.0
4.5	1.67	0.50	5.7	0.0	10.5	83.8	0.0
5.25	1.70	0.51	5.6	0.0	10.3	84.1	0.0
6	1.72	0.52	5.3	0.0	9.8	84.9	0.0

(Reaction temperature: 550 °C, 0.0258 mol/h of propane (99.95%), and 50 mL/min nitrogen, W/F; 10.6130 g.h/mol, Time on stream; 6 hours)

D8: The Effect of Contact Time over [IM] Cr/SiO_2 1% wt. catalyst.

Table D8.1: The Area of Propane Dehydrogenation at 550 °C

Time on steam (h)	Area						Total Area
	Methane	Ethane	Ethylene	Propane	Propylene	C_4	
0.75	14689	5115	19566	21161779	325747	4491	21531387
1.5	11189	4312	15223	21481580	316045	4026	21832375
2.25	10341	3677	14467	21267115	297247	4449	21597296
3	9949	3341	14040	21102566	279718	3953	21413567
3.75	9722	3182	14018	21164304	272254	3491	21466971
4.5	9806	3232	14468	21183075	238599	2708	21451888
5.25	8393	2926	12453	21047136	235654	3170	21309732
6	8413	2828	12510	21051656	236042	0	21311449

(Reaction temperature: 550 °C, 0.0258 mol/h of propane (99.95%), and 50 mL/min nitrogen, W/F; 10.4144 g.h/mol, Time on stream; 6 hours)

Table D8.2: Product selectivity of Propane Dehydrogenation at 550 °C

Time on steam (h)	TOF (h^{-1})	% Conversion	% Selectivity				
			Methane	Ethane	Ethylene	Propylene	C_4
0.75	8.16	1.72	4.0	1.4	5.3	88.1	1.2
1.5	7.64	1.61	3.2	1.2	4.3	90.1	1.1
2.25	7.27	1.53	3.1	1.1	4.4	90.0	1.3
3	6.91	1.45	3.2	1.1	4.5	89.9	1.3
3.75	6.70	1.41	3.2	1.1	4.6	90.0	1.2
4.5	5.96	1.25	3.6	1.2	5.4	88.8	1.0
5.25	5.86	1.23	3.2	1.1	4.7	89.7	1.2
6	5.86	1.23	3.2	1.1	4.8	90.9	0.0

(Reaction temperature: 550 °C, 0.0258 mol/h of propane (99.95%), and 50 mL/min nitrogen, W/F; 10.4144 g.h/mol, Time on stream; 6 hours)

Table D8.3: Turn over number of Propane Dehydrogenation at 550 °C

Contact Time of Cr (h)	TOF (h^{-1})	TON (mmol C_3H_8.mol Cr^{-1})	TON (mmol C_3H_8.mol Cr^{-1})				
			Methane	Ethane	Ethylene	Propylene	C_4
0.0021	8.16	17.17	0.68	0.24	0.91	15.13	0.21
	7.64	16.07	0.51	0.20	0.70	14.48	0.18
	7.27	15.29	0.48	0.17	0.67	13.76	0.21
	6.91	14.52	0.46	0.16	0.66	13.06	0.18
	6.70	14.10	0.45	0.15	0.65	12.68	0.16
	5.96	12.53	0.46	0.15	0.67	11.12	0.13
	5.86	12.32	0.39	0.14	0.58	11.06	0.15
	5.86	12.32	0.39	0.13	0.59	11.08	0.00

(Reaction temperature: 550 °C, 0.0258 mol/h of propane (99.95%), and 50 mL/min nitrogen, W/F: 10.4144 g.h/mol, Time on stream; 6 hours)

D9: The Effect of Contact Time over [IM] Cr/SiO_2 1% wt. catalyst.

Table D9.1: The Area of Propane Dehydrogenation at 550 °C

Time on steam (h)	Area						Total Area
	Methane	Ethane	Ethylene	Propane	Propylene	C_4	
0.75	15593	6116	21432	17877168	522889	0	18443198
1.5	12298	4362	17305	16554268	434870	0	17023103
2.25	12003	4208	17032	17404400	430910	0	17868553
3	10716	3586	15533	16908669	401054	0	17339558
3.75	10571	3500	15453	17248409	390913	0	17668846
4.5	10185	3142	14865	16978361	361141	0	17367694
5.25	10068	3373	14924	17493192	350380	0	17871937
6	9636	3215	14100	17473960	332319	0	17833230

(Reaction temperature: 550 °C, 0.0258 mol/h of propane (99.95%), and 50 mL/min nitrogen, W/F; 20.5368 g.h/mol, Time on stream; 6 hours)

Table D9.2: Product selectivity of Propane Dehydrogenation at 550 °C

Time on steam (h)	TOF (h^{-1})	% Conversion	% Selectivity				
			Methane	Ethane	Ethylene	Propylene	C_4
0.75	7.40	3.07	2.8	1.1	3.8	92.4	0.0
1.5	6.64	2.75	2.6	0.9	3.7	92.8	0.0
2.25	6.26	2.60	2.6	0.9	3.7	92.8	0.0
3	5.99	2.49	2.5	0.8	3.6	93.1	0.0
3.75	5.74	2.38	2.5	0.8	3.7	93.0	0.0
4.5	5.41	2.24	2.6	0.8	3.8	92.8	0.0
5.25	5.11	2.12	2.7	0.9	3.9	92.5	0.0
6	4.86	2.01	2.7	0.9	3.9	92.5	0.0

(Reaction temperature: 550 °C, 0.0258 mol/h of propane (99.95%), and 50 mL/min nitrogen, W/F; 20.5368 g.h/mol, Time on stream; 6 hours)

Table D9.3: Turn over number of Propane Dehydrogenation at 550 *°C*

Contact Time of Cr (h)	TOF (h^{-1})	TON (mmol C_3H_8.mol Cr^{-1})	TON (mmol C_3H_8.mol Cr^{-1})				
			Methane	Ethane	Ethylene	Propylene	C_4
0.0041	7.40	30.69	0.85	0.33	1.16	28.35	0.00
	6.64	27.54	0.72	0.26	1.02	25.55	0.00
	6.26	25.98	0.67	0.24	0.95	24.12	0.00
	5.99	24.85	0.62	0.21	0.90	23.13	0.00
	5.74	23.80	0.60	0.20	0.87	22.12	0.00
	5.41	22.42	0.59	0.18	0.86	20.79	0.00
	5.11	21.19	0.56	0.19	0.84	19.61	0.00
	4.86	20.15	0.54	0.18	0.79	18.63	0.00

(Reaction temperature: 550 °C, 0.0258 mol/h of propane (99.95%), and 50 mL/min nitrogen, W/F; 20.5368 g.h/mol, Time on stream; 6 hours)

D10: The Effect of Contact Time over [IM] Cr/SiO_2 1% wt. catalyst.

Table D10.1: The Area of Propane Dehydrogenation at 550 °C

Time on steam (h)	Area						Total Area
	Methane	Ethane	Ethylene	Propane	Propylene	C_4	
0.75	23907	10491	31022	19848082	1098414	0	21013832
1.5	22076	9347	29462	19679625	1034748	0	20777688
2.25	20908	8533	28359	19972702	1002644	0	21034296
3	20237	8380	27710	19999823	962298	0	21018448
3.75	18946	7382	26279	20128027	915957	0	21096591
4.5	17891	6728	25235	19946849	878583	0	20875286
5.25	16796	6013	24229	19811210	844910	0	20703158
6	16058	5827	23109	19611345	806384	0	20462723

(Reaction temperature: 550 °C, 0.0258 mol/h of propane (99.95%), and 50 mL/min nitrogen, W/F; 50.8028 g.h/mol, Time on stream; 6 hours)

Table D10.2: Product selectivity of Propane Dehydrogenation at 550 °C

Time on steam (h)	TOF (h^{-1})	% Conversion	% Selectivity				
			Methane	Ethane	Ethylene	Propylene	C_4
0.75	5.41	5.55	2.1	0.9	2.7	94.2	0.0
1.5	5.15	5.28	2.0	0.9	2.7	94.2	0.0
2.25	4.92	5.05	2.0	0.8	2.7	94.4	0.0
3	4.72	4.85	2.0	0.8	2.7	94.5	0.0
3.75	4.48	4.59	2.0	0.8	2.7	94.6	0.0
4.5	4.34	4.45	1.9	0.7	2.7	94.6	0.0
5.25	4.20	4.31	1.9	0.7	2.7	94.7	0.0
6	4.06	4.16	1.9	0.7	2.7	94.7	0.0

(Reaction temperature: 550 °C, 0.0258 mol/h of propane (99.95%), and 50 mL/min nitrogen, W/F; 50.8028 g.h/mol, Time on stream; 6 hours)

Table D10.3: Turn over number of Propane Dehydrogenation at 550 *°C*

Contact Time of Cr (h)	TOF (h^{-1})	TON (mmol C_3H_8.mol Cr^{-1})	TON (mmol C_3H_8.mol Cr^{-1})				
			Methane	Ethane	Ethylene	Propylene	C_4
0.0103	5.41	55.48	1.14	0.50	1.48	52.27	0.00
	5.15	52.85	1.06	0.45	1.42	49.80	0.00
	4.92	50.47	0.99	0.41	1.35	47.67	0.00
	4.72	48.46	0.96	0.40	1.32	45.78	0.00
	4.48	45.91	0.90	0.35	1.25	43.42	0.00
	4.34	44.48	0.86	0.32	1.21	42.09	0.00
	4.20	43.08	0.81	0.29	1.17	40.81	0.00
	4.06	41.61	0.78	0.28	1.13	39.41	0.00

(Reaction temperature: 550 °C, 0.0258 mol/h of propane (99.95%), and 50 mL/min nitrogen, W/F; 50.8028 g.h/mol, Time on stream; 6 hours)

D11: The Effect of Contact Time over [ADS] Cr/SiO_2 0.2% wt. catalyst.

Table D11.1: The Area of Propane Dehydrogenation at 550 °C

Time on steam (h)	Area						Total Area
	Methane	Ethane	Ethylene	Propane	Propylene	C_4	
0.75	5299	1731	9255	20739467	84295	0	20840047
1.5	5674	1473	9498	20832943	76692	0	20926280
2.25	5857	1374	9969	20747444	72311	0	20836955
3	5962	1397	10128	20831760	69501	0	20918748
3.75	5896	1201	10175	20643893	66351	0	20727516
4.5	5710	1160	9769	19909458	62254	0	19988351
5.25	5957	1059	10289	20879437	63403	0	20960145
6	5915	0	10351	20488988	61346	0	20566600

(Reaction temperature: 550 °C, 0.0258 mol/h of propane (99.95%), and 50 mL/min nitrogen, W/F; 10.5468 g.h/mol, Time on stream; 6 hours)

Table D11.2: Product selectivity of Propane Dehydrogenation at 550 °C

Time on steam (h)	TOF (h^{-1})	% Conversion	% Selectivity				
			Methane	Ethane	Ethylene	Propylene	C_4
0.75	11.90	0.48	5.3	1.7	9.2	83.8	0.0
1.5	10.99	0.45	6.1	1.6	10.2	82.2	0.0
2.25	10.59	0.43	6.5	1.5	11.1	80.8	0.0
3	10.25	0.42	6.9	1.6	11.6	79.9	0.0
3.75	9.94	0.40	7.1	1.4	12.2	79.3	0.0
4.5	9.73	0.39	7.2	1.5	12.4	78.9	0.0
5.25	9.49	0.39	7.4	1.3	12.7	78.6	0.0
6	9.30	0.38	7.6	0.0	13.3	79.0	0.0

(Reaction temperature: 550 °C, 0.0258 mol/h of propane (99.95%), and 50 mL/min nitrogen, W/F; 10.5468 g.h/mol, Time on stream; 6 hours)

Table D11.3: Turn over number of Propane Dehydrogenation at 550 °C

Contact Time of Cr (h)	TOF (h^{-1})	TON (mmol C_3H_8.mol Cr^{-1})	TON (mmol C_3H_8.mol Cr^{-1})				
			Methane	Ethane	Ethylene	Propylene	C_4
0.0004	11.90	4.83	0.25	0.08	0.44	4.04	0.00
	10.99	4.46	0.27	0.07	0.45	3.66	0.00
	10.59	4.30	0.28	0.07	0.48	3.47	0.00
	10.25	4.16	0.29	0.07	0.48	3.32	0.00
	9.94	4.03	0.28	0.06	0.49	3.20	0.00
	9.73	3.95	0.29	0.06	0.49	3.11	0.00
	9.49	3.85	0.28	0.05	0.49	3.02	0.00
	9.30	3.77	0.29	0.00	0.50	2.98	0.00

(Reaction temperature: 550 °C, 0.0258 mol/h of propane (99.95%), and 50 mL/min nitrogen, W/F; 10.5468 g.h/mol, Time on stream; 6 hours)

D12: The Effect of Contact Time over [ADS] Cr/SiO_2 0.2% wt. catalyst.

Table D12.1: The Area of Propane Dehydrogenation at 550 °C

Time on steam (h)	Area						Total Area
	Methane	Ethane	Ethylene	Propane	Propylene	C_4	
0.75	11966	3345	18776	20610198	159288	0.00	20803573
1.5	11470	2809	17982	21597455	169443	0.00	21799159
2.25	11383	2620	17996	21352460	164083	0.00	21548542
3	11227	0	18496	21697588	157901	0.00	21885212
3.75	10288	2132	16605	21129399	147317	0.00	21305741
4.5	12093	2988	16288	21355254	143192	0.00	21529815
5.25	9849	0	15881	21779654	140517	0.00	21945901
6	11894	0	15657	21450333	137144	0.00	21615028

(Reaction temperature: 550 °C, 0.0258 mol/h of propane (99.95%), and 50 mL/min nitrogen, W/F; 20.4200 g.h/mol, Time on stream; 6 hours)

Table D12.2: Product selectivity of Propane Dehydrogenation at 550 °C

Time on steam (h)	TOF (h^{-1})	% Conversion	% Selectivity				
			Methane	Ethane	Ethylene	Propylene	C_4
0.75	11.83	0.93	6.2	1.7	9.7	82.4	0.0
1.5	11.78	0.93	5.7	1.4	8.9	84.0	0.0
2.25	11.59	0.91	5.8	1.3	9.2	83.7	0.0
3	10.91	0.86	6.0	0.0	9.9	84.2	0.0
3.75	10.54	0.83	5.8	1.2	9.4	83.5	0.0
4.5	10.32	0.81	6.9	1.7	9.3	82.0	0.0
5.25	9.64	0.76	5.9	0.0	9.6	84.5	0.0
6	9.70	0.76	7.2	0.0	9.5	83.3	0.0

(Reaction temperature: 550 °C, 0.0258 mol/h of propane (99.95%), and 50 mL/min nitrogen, W/F; 20.4200 g.h/mol, Time on stream; 6 hours)

Table D12.3: Turn over number of Propane Dehydrogenation at 550 *°C*

Contact Time of Cr (h)	TOF (h^{-1})	TON (mmol C_3H_8.mol Cr^{-1})	TON (mmol C_3H_8.mol Cr^{-1})				
			Methane	Ethane	Ethylene	Propylene	C_4
0.0008	11.83	9.30	0.58	0.16	0.90	7.66	0.00
	11.78	9.25	0.53	0.13	0.82	7.77	0.00
	11.59	9.10	0.53	0.12	0.84	7.61	0.00
	10.91	8.57	0.51	0.00	0.85	7.21	0.00
	10.54	8.28	0.48	0.10	0.78	6.91	0.00
	10.32	8.11	0.56	0.14	0.76	6.65	0.00
	9.64	7.58	0.45	0.00	0.72	6.40	0.00
	9.70	7.62	0.55	0.00	0.72	6.34	0.00

(Reaction temperature: 550 °C, 0.0258 mol/h of propane (99.95%), and 50 mL/min nitrogen, W/F; 20.4200 g.h/mol, Time on stream; 6 hours)

D13: The Effect of Contact Time over [ADS] Cr/SiO_2 0.2% wt. catalyst.

Table D13.1: The Area of Propane Dehydrogenation at 550 °C

Time on steam (h)	Area						Total Area
	Methane	Ethane	Ethylene	Propane	Propylene	C_4	
0.75	12882	4594	20063	22261999	212500	0	22512038.00
1.5	12151	3583	19178	22074920	196781	0	22306613.00
2.25	11702	3192	18492	22021940	190642	0	22245968.00
3	11368	2829	18053	22285543	184612	0	22502405.00
3.75	10622	2336	17241	21737668	174574	0	21942441.00
4.5	10003	2344	16181	21944167	168832	0	22141527.00
5.25	9399	2035	15260	21739278	162815	0	21928787.00
6	9237	2032	15058	21736393	162843	0	21925563.00

(Reaction temperature: 550 °C, 0.0258 mol/h of propane (99.95%), and 50 mL/min nitrogen, W/F; 30.3828 g.h/mol, Time on stream; 6 hours)

Table D13.2: Product selectivity of Propane Dehydrogenation at 550 *°C*

Time on steam (h)	TOF (h^{-1})	% Conversion	% Selectivity				
			Methane	Ethane	Ethylene	Propylene	C_4
0.75	9.50	1.11	5.2	1.8	8.0	85.0	0.0
1.5	8.89	1.04	5.2	1.5	8.3	84.9	0.0
2.25	8.62	1.01	5.2	1.4	8.3	85.1	0.0
3	8.25	0.96	5.2	1.3	8.3	85.1	0.0
3.75	7.99	0.93	5.2	1.1	8.4	85.3	0.0
4.5	7.63	0.89	5.1	1.2	8.2	85.5	0.0
5.25	7.39	0.86	5.0	1.1	8.1	85.9	0.0
6	7.38	0.86	4.9	1.1	8.0	86.1	0.0

(Reaction temperature: 550 °C, 0.0258 mol/h of propane (99.95%), and 50 mL/min nitrogen, W/F; 30.3828 g.h/mol, Time on stream; 6 hours)

Table D13.3: Turn over number of Propane Dehydrogenation at 550 *°C*

Contact Time of Cr (h)	TOF (h^{-1})	TON (mmol C_3H_8.mol Cr^{-1})	TON (mmol C_3H_8.mol Cr^{-1})				
			Methane	Ethane	Ethylene	Propylene	C_4
0.0012	9.50	11.11	0.57	0.20	0.89	9.44	0.00
	8.89	10.39	0.54	0.16	0.86	8.82	0.00
	8.62	10.07	0.53	0.14	0.83	8.57	0.00
	8.25	9.64	0.51	0.13	0.80	8.20	0.00
	7.99	9.33	0.48	0.11	0.79	7.96	0.00
	7.63	8.91	0.45	0.11	0.73	7.63	0.00
	7.39	8.64	0.43	0.09	0.70	7.42	0.00
	7.38	8.63	0.42	0.09	0.69	7.43	0.00

(Reaction temperature: 550 °C, 0.0258 mol/h of propane (99.95%), and 50 mL/min nitrogen, W/F; 30.3828 g.h/mol, Time on stream; 6 hours)

D14: The Effect of Carrier Gas over [ADS] Cr/SiO_2 0.2% wt catalyst.

Table D14.1: The Area of Propane Dehydrogenation at 550 °C

Carrier gas	Time on steam (h)	Area						Total Area
		Methane	Ethane	Ethylene	Propane	Propylene	C_4	
H_2	0.75	2560	0	4201	17089324	17512	0	17113597
	1.5	1488	0	2878	17001640	13619	0	17019625
	2.25	1717	0	2860	17107041	14080	0	17125698
	3	1511	0	2729	16996919	13497	0	17014656
	3.75	1488	0	2878	17001640	13619	0	17019625
N_2	4.5	3605	0	6238	21847454	42905	0	21900202
	5.25	5664	0	9671	19913445	61567	0	19990347
	6	5903	0	9927	20647141	66453	0	20729424

(Reaction temperature: 550 °C, 0.0258 mol/h of propane (99.95%), and 50 mL/min hydrogen, W/F; 10.5117 g.h/mol, Time on stream; 0.75-3.45 hours, 0.0258 mol/h of propane (99.95%), and 50 mL/min nitrogen, W/F; 10.5117 g.h/mol, Time on stream; 4.5-6 hours)

Table D14.2: Product selectivity of Propane Dehydrogenation at 550 °C

Carrier gas	Time on steam (h)	TOF (h^{-1})	% Conversion	% Selectivity				
				Methane	Ethane	Ethylene	Propylene	C_4
H_2	0.75	3.51	0.14	10.5	0.0	17.3	72.1	0.0
	1.5	2.61	0.11	8.3	0.0	16.0	75.7	0.0
	2.25	2.69	0.11	9.2	0.0	15.3	75.5	0.0
	3	2.58	0.10	8.5	0.0	15.4	76.1	0.0
	3.75	2.61	0.11	8.3	0.0	16.0	75.7	0.0
N_2	4.5	5.96	0.24	6.8	0.0	11.8	81.3	0.0
	5.25	9.51	0.38	7.4	0.0	12.6	80.1	0.0
	6	9.82	0.40	7.2	0.0	12.1	80.8	0.0

(Reaction temperature: 550 °C, 0.0258 mol/h of propane (99.95%), and 50 mL/min hydrogen, W/F; 10.5117 g.h/mol, Time on stream; 0.75-3.45 hours, 0.0258 mol/h of propane (99.95%), and 50 mL/min nitrogen, W/F; 10.5117 g.h/mol, Time on stream; 4.5-6 hours)

D15: The Effect of Reduction Temperature over [ADS] Cr/SiO_2 0.2% wt catalyst.

Table D15.1: The Area of Propane Dehydrogenation at 550 °C

Reduction Temperature (°C)	Time on steam (h)	Area						Total Area
		Methane	Ethane	Ethylene	Propane	Propylene	C_4	
450[a]	0.75	5299	1731	9255	20739467	84295	0	20840047
	1.5	5674	1473	9498	20832943	76692	0	20926280
	2.25	5857	1374	9969	20747444	72311	0	20836955
	3	5962	1397	10128	20831760	69501	0	20918748
	3.75	5896	1201	10175	20643893	66351	0	20727516
	4.5	5710	1160	9769	19909458	62254	0	19988351
	5.25	5957	1059	10289	20879437	63403	0	20960145
	6	5915	0	10351	20488988	61346	0	20566600
650[b]	0.75	5476	1418	10476	20831947	25497	0	20874814
	1.5	5589	0	10462	21094320	25656	0	21136027
	2.25	6347	0	10788	21067804	25890	0	21110829
	3	5273	0	9708	19446007	23726	0	19484714
	3.75	5194	0	9670	18787235	23185	0	18825284
	4.5	5021	0	9209	18803514	26241	0	18843985
	5.25	5934	0	10905	21708367	26241	0	21751447
	6	5217	0	9868	19450341	24031	0	19489457

[a) Reaction temperature: 550 °C, 0.0258 mol/h of propane (99.95%), and 50 mL/min nitrogen, W/F; 10.3910 g.h/mol, Time on stream; 6 hours]

[b) Reaction temperature: 550 °C, 0.0258 mol/h of propane (99.95%), and 50 mL/min nitrogen, W/F; 10.5117 g.h/mol, Time on stream; 6 hours]

Table D15.2: Product selectivity of Propane Dehydrogenation at 550 °C

Reduction Temperature (°C)	Time on steam (h)	TOF (h^{-1})	% Conversion	% Selectivity				
				Methane	Ethane	Ethylene	Propylene	C_4
450[a]	0.75	11.90	0.48	5.3	1.7	9.2	83.8	0.0
	1.5	10.99	0.45	6.1	1.6	10.2	82.2	0.0
	2.25	10.59	0.43	6.5	1.5	11.1	80.8	0.0
	3	10.25	0.42	6.9	1.6	11.6	79.9	0.0
	3.75	9.94	0.40	7.1	1.4	12.2	79.3	0.0
	4.5	9.73	0.39	7.2	1.5	12.4	78.9	0.0
	5.25	9.49	0.39	7.4	1.3	12.7	78.6	0.0
	6	9.30	0.38	7.6	0.0	13.3	79.0	0.0
650[b]	0.75	5.16	0.21	12.8	3.3	24.4	59.5	0.0
	1.5	4.96	0.20	13.4	0.0	25.1	61.5	0.0
	2.25	5.12	0.20	14.8	0.0	25.1	60.2	0.0
	3	4.99	0.20	13.6	0.0	25.1	61.3	0.0
	3.75	5.08	0.20	13.7	0.0	25.4	60.9	0.0
	4.5	5.40	0.21	12.4	0.0	22.8	64.8	0.0
	5.25	4.98	0.20	13.8	0.0	25.3	60.9	0.0
	6	5.05	0.20	13.3	0.0	25.2	61.4	0.0

[a) Reaction temperature: 550 °C, 0.0258 mol/h of propane (99.95%), and 50 mL/min nitrogen, W/F; 10.3910 g.h/mol, Time on stream; 6 hours]

[b) Reaction temperature: 550 °C, 0.0258 mol/h of propane (99.95%), and 50 mL/min nitrogen, W/F; 10.5117 g.h/mol, Time on stream; 6 hours]

D16: The Effect of Reduction Temperature over [IM] Cr/SiO_2 1% wt catalyst.

Table D16.1: The Area of Propane Dehydrogenation at 550 °C

Reduction Temperature (°C)	Time on steam (h)	Area						Total Area
		Methane	Ethane	Ethylene	Propane	Propylene	C_4	
450[a]	0.75	14689	5115	19566	21161779	325747	4491	21531387
	1.5	11189	4312	15223	21481580	316045	4026	21832375
	2.25	10341	3677	14467	21267115	297247	4449	21597296
	3	9949	3341	14040	21102566	279718	3953	21413567
	3.75	9722	3182	14018	21164304	272254	3491	21466971
	4.5	9806	3232	14468	21183075	238599	2708	21451888
	5.25	8393	2926	12453	21047136	235654	3170	21309732
	6	8413	2828	12510	21051656	236042	0	21311449
650[b]	0.75	9647	1516	16254	20389360	115002	0	20531779
	1.5	8199	1024	14019	19148517	91022	0	19262781
	2.25	8403	1127	14448	20438831	88676	0	20551485
	3	8217	0	14148	20380000	83162	0	20485527
	3.75	7508	0	12864	19744543	75743	0	19840658
	4.5	6995	0	12239	19385766	70020	0	19475020
	5.25	6617	0	11493	18861234	65643	0	18944987
	6	6664	0	11525	18863651	65415	0	18947255

[a) Reaction temperature: 550 °C, 0.0258 mol/h of propane (99.95%), and 50 mL/min nitrogen, W/F; 10.4144 g.h/mol, Time on stream; 6 hours]

[b) Reaction temperature: 550 °C, 0.0258 mol/h of propane (99.95%), and 50 mL/min nitrogen, W/F; 10.3599 g.h/mol, Time on stream; 6 hours]

Table D16.2: Product selectivity of Propane Dehydrogenation at 550 °C

Reduction Temperature (°C)	Time on steam (h)	TOF (h^{-1})	% Conversion	% Selectivity				
				Methane	Ethane	Ethylene	Propylene	C_4
450[a]	0.75	8.16	1.72	4.0	1.4	5.3	88.1	1.2
	1.5	7.64	1.61	3.2	1.2	4.3	90.1	1.1
	2.25	7.27	1.53	3.1	1.1	4.4	90.0	1.3
	3	6.91	1.45	3.2	1.1	4.5	89.9	1.3
	3.75	6.70	1.41	3.2	1.1	4.6	90.0	1.2
	4.5	5.96	1.25	3.6	1.2	5.4	88.8	1.0
	5.25	5.86	1.23	3.2	1.1	4.7	89.7	1.2
	6	5.86	1.23	3.2	1.1	4.8	90.9	0.0
650[b]	0.75	3.32	0.69	6.8	1.1	11.4	80.7	0.0
	1.5	2.84	0.59	7.2	0.9	12.3	79.7	0.0
	2.25	2.62	0.55	7.5	1.0	12.8	78.7	0.0
	3	2.46	0.52	7.8	0.0	13.4	78.8	0.0
	3.75	2.32	0.48	7.8	0.0	13.4	78.8	0.0
	4.5	2.19	0.46	7.8	0.0	13.7	78.5	0.0
	5.25	2.11	0.44	7.9	0.0	13.7	78.4	0.0
	6	2.11	0.44	8.0	0.0	13.8	78.2	0.0

[a) Reaction temperature: 550 °C, 0.0258 mol/h of propane (99.95%), and 50 mL/min nitrogen, W/F; 10.4144 g.h/mol, Time on stream; 6 hours]

[b) Reaction temperature: 550 °C, 0.0258 mol/h of propane (99.95%), and 50 mL/min nitrogen, W/F; 10.3599 g.h/mol, Time on stream; 6 hours]

AUTHOR BIOGRAPHY

Mr. Supanut Ketanirut was born on November 7, 1991 in Bangkok. He graduated a Senior High school form Triamudomsuksa School and B.Sc. in Industrial Chemical Science from King Mongkut's Institute of Technology Ladkrabang in 2015. He has been a graduate student in Petrochemical and Hydrocarbon Chemistry program of Faculty of Science, King Mongkut's Institute of Technology Ladkrabang since 2015.

Work experiences:

Mar – Apr 2014	Internship at PTT Global Chemical Company Limited.
(Jun) 2015 – (Sep) 2017	Teacher Assistant, King Mongkut's Institute of Technology Ladkrabang.
(Oct) 2015 - (Jun) 2017	Co-project Researcher, Project: Heterolytic C-H activation of Methane using single-site heterogeneous catalysts (Phase 1), SCG Chemical Company Limited and Catalytic Chemistry Research Unit, Department of Chemistry, Faculty of Science, King Mongkut's Institute of Technology Ladkrabang, Bangkok, Thailand.

Scholarship:

2015-2017 M.Sc.'s scholarship	SCG Chemical scholarship program 2015 (2)

Conferences:

(Jul) 2016 The 2nd Internal meeting of SCG Catalysis conference, "Brand New Catalytic Reaction-II for Methane to Ethylene", Oral presentation, 13 – 15 July, 2016, Cape Dara Resort, Pattaya, Thailand.

(Feb) 2017 **Supanut Ketanirut**, Kittisak Choojun, and Tawan Sooknai, "Heterolytic C-H Activation of Propane using Chromium Single-Site Heterogeneous Catalyst", Poster Presentation, Pure and Applied Chemistry International Conference 2017 (PACCON 2017), February 2-3 2017, Centra Government Complex Hotel & Convention Centre Bangkok, Thailand.

Publication:

2017 **Supanut Ketanirut**, Kittisak Choojun, and Tawan Sooknai, 2017. "Heterolytic C-H Activation of Propane using Chromium Single-Site Heterogeneous Catalyst", PACCON 2017 Conference Proceedings. : 1321-1326